Fabrication of μ-pH Biosensor for Implantable Medical Devices and Applications in Detecting Post-Operative Complications

by

Youssef Helwa

A thesis

presented to the University of Waterloo

in fulfillment of the

thesis requirements for the degree of

Masters of Applied Science

In

Electrical and Computer Engineering (Nanotechnology)

Waterloo, Ontario, Canada, 2017

Authors Declaration:

I hereby declare that I am the sole author of this thesis. This is a true copy of the thesis, including any required final revisions, as accepted by my examiners.

I understand that my thesis may be made electronically available to the public.

Abstract

The monitoring of the pH milieu inside the body is critical to the functions associated with implantable medical devices. By monitoring the variation of pH in real-time inside the body, we are capable of identifying the body's response to the implant, the probability of infection, calibrating sensors and monitoring complications such as internal bleeding or anastomotic leakage.

In this work, a pH sensor is presented consisting of a working electrode, a counter electrode and reference Ag/AgCl fabricated to allow the signals to be collected and compared to a reference value. For the working electrode, we chose Polyaniline (PANI) as the sensing material. Upon exposure to different pH solutions, PANI (the active sensing material) acts as an ion-selective membrane, the concentration gradient of ions across the membrane generates a potential difference that can be measured.

We first fabricate microscale interdigitated electrodes by photolithography, e-beam deposition, etching, and liftoff. Then we coated a conducting hydronium-sensitive layer of PANI or PU by electropolymerization onto the active electrode. Then we placed the second electrode into a solution of KCl to apply a thin layer of AgCl on the Ag electrode, creating the Ag/AgCl reference electrode. The potential for the polymerization to provide the most stable active layer and the Nernstian potential was optimized. Moreover, the porosity of the active layers has been modified to allow the highest concentration of hydronium ions to diffuse to the electrodes, maximizing the signal stability. This bio-compatible electrodeposited polymer layer also protects the electrode from cellular attacks and biofouling.

The fabricated device was used to monitor changes in pH in biological fluids such as gastric juice, simulated blood, and peritoneal fluid. The device was capable of monitoring changes in pH with a Nernstian potential of 68mV/pH. In addition, the active layer demonstrated an active lifetime of five weeks where the electrodes were capable of collecting data continuously during the active period.

Acknowledgements

To begin with, I would like to take this chance to express my great gratitude and thanks to my mentor, Professor Bo Cui. It is such a great honor to be part of his group and to learn directly from him. Dr. Cui is one of the most knowledgeable people I have ever met and will meet, and I am so glad that I had the chance to learn under him directly. Dr. Cui taught me as a student during my time as an undergraduate at the University of Waterloo, and I had the chance to do it all over again with him as my mentor in my graduate studies. I would also like to mention that he stood by me in my entrepreneurial endeavors for all over four years of full support and thus I have no words to express my gratitude and my happiness to be one of his students.

The second person I would like to mention is Dr. Juewen Liu. He gave me the first research assistant position even though I was not qualified for the position by any means. Yet he took the time to teach me himself the basics of how to operate in the lab up to advanced topics in polymer chemistry allowing me to publish three of my four publications!

I would also love to extend my gratitude to Dr. Guo-Xing Miao. As my professor in undergraduate, he taught me a lot of things, but I also had the opportunity to work with him directly when he first came to the University of Waterloo. He granted me access to great opportunities allowing me to access clean-room facilities even though at the time I was the first person to access the facility. Not only that, but he also granted me the opportunity to work at the National Institute of Standards and Technology. I am very grateful for his support.

The next person to mention is Dr. Dmitry Pushin. Dr. Pushin was one of the people who taught me that I could do more than what I think I am capable of. He was truly a great friend and I was so honored to get the opportunity to be trained directly by him in different fields. Oh and Dusan Sarenac is truly one of the best people I got to know, he is very nice, talented and a great squash partner (I was very short when I stood next to the both of you)

Table of Contents

List of Figures

List of Tables

1.0 Introduction

In this section, a background will be provided covering the medical background identifying the post-operative complications that will be addressed. The theory behind pH sensing will be provided, and the state of the art technology currently used in the market will be addressed. In addition, the biochip platform where the pH sensor will be utilized will be introduced.

1.1 Laparoscopic Surgery

Laparoscopy is a type of surgical procedure that allows a surgeon to access the inside of the abdomen (tummy) and pelvis without having to make large incisions in the skin. This procedure is also known as keyhole surgery or minimally invasive surgery. Large incisions can be avoided during laparoscopy because the surgeon uses an instrument called a laparoscope. An example of the typical setup used when performing laparoscopic surgery can be seen in Figure 1. This is a small tube that has a light source and a camera, that relays images from the interior of the abdomen or pelvis to an external television monitor. General surgeons, gastroenterologists, urologists, bariatric surgeons and gynecologists are practicing many laparoscopic abdominal and pelvic surgeries that are superior to open surgeries. Laparoscopic procedures cause less post-operative pain and discomfort. Studies have shown that patients undergoing laparoscopic procedures report less pain and require smaller doses of pain relievers versus open surgeries. MIS procedures require a smaller incision – which means small, less noticeable scars. The other benefits of MIS include less blood loss, decreased need for blood transfusions, shorter hospitals stay, early resumption of regular diet, quick recovery and return to normal activities [1]. Complications related to those procedures are numerous and often include internal bleeding, anastomotic leakage, organ injury, septic shocks, peritonitis and local inflammation [2]. This section will go into some details in addressing some of these complications, their causes, risk factors, means of diagnosis and treatment.
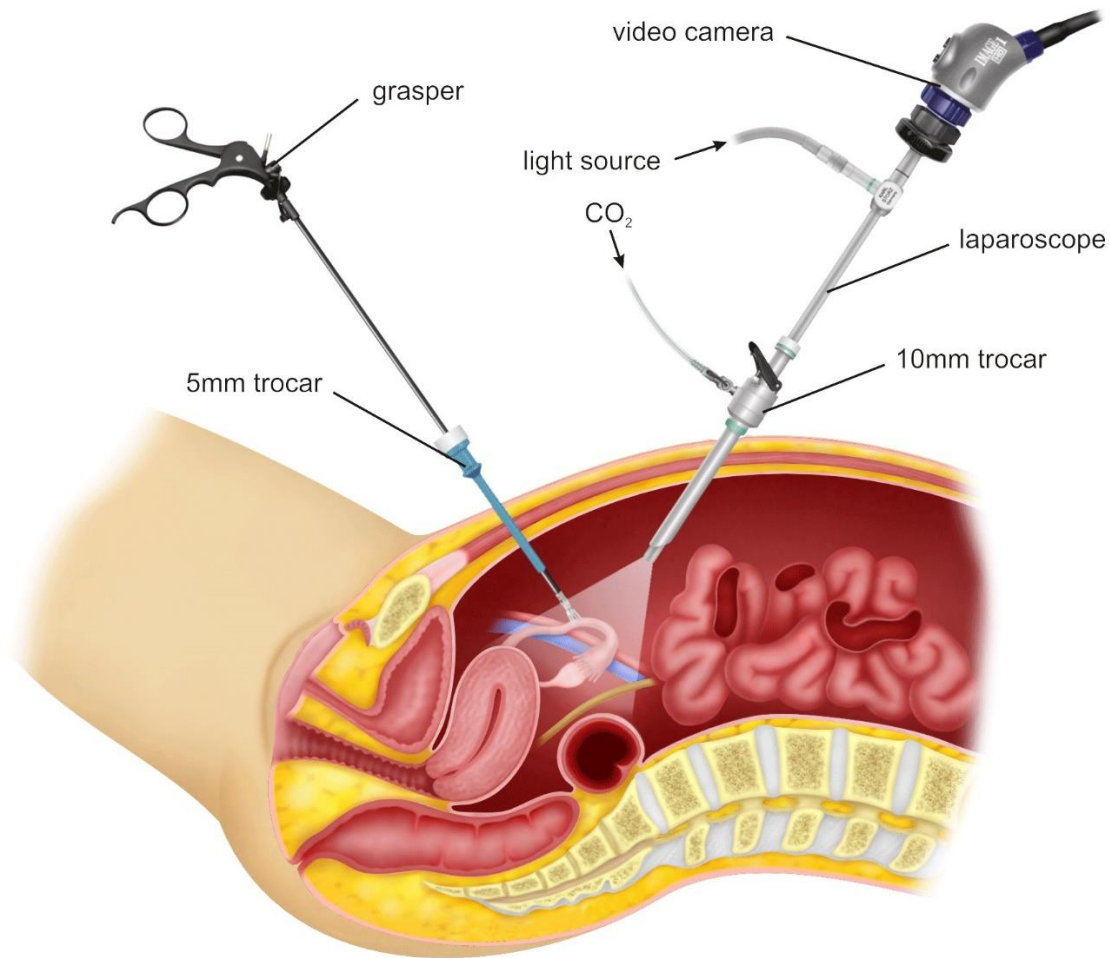
Figure 1. The typical setup used when performing minimally invasive surgery. Copyright © Dr.Ravi Chander Veligeti.

1.1.1 Anastomotic Leakage

Leakage of gastric fluids and blood within the first 72 hours after surgery is one of the serious complications related to upper gastrointestinal tract injury with a high incidence of critical morbidity and mortality rates. Patients have a leakage risk up to three weeks post-operatively (Figure 2) [3]. This could occur due to improper stapling, stitching of major arteries, accidental cuts made by surgical tools and pressure build up in the stomach after the surgery [4]. If left unattended, this complication may lead to peritonitis and can quickly turn fatal [5]. The incidence rate for anastomotic leakage is reported to be

between 1% to 30%. The large variance is due to heavy influence of the risk factors such as male gender, older age, poor nutritional status and advanced tumor stage, and technical factors, including local ischemia, anastomotic tension, local sepsis and the presence of distal obstruction [6,7]. The risk also varies with the site of the anastomosis with those placed < 5 cm from the anal verge being particularly vulnerable [8].
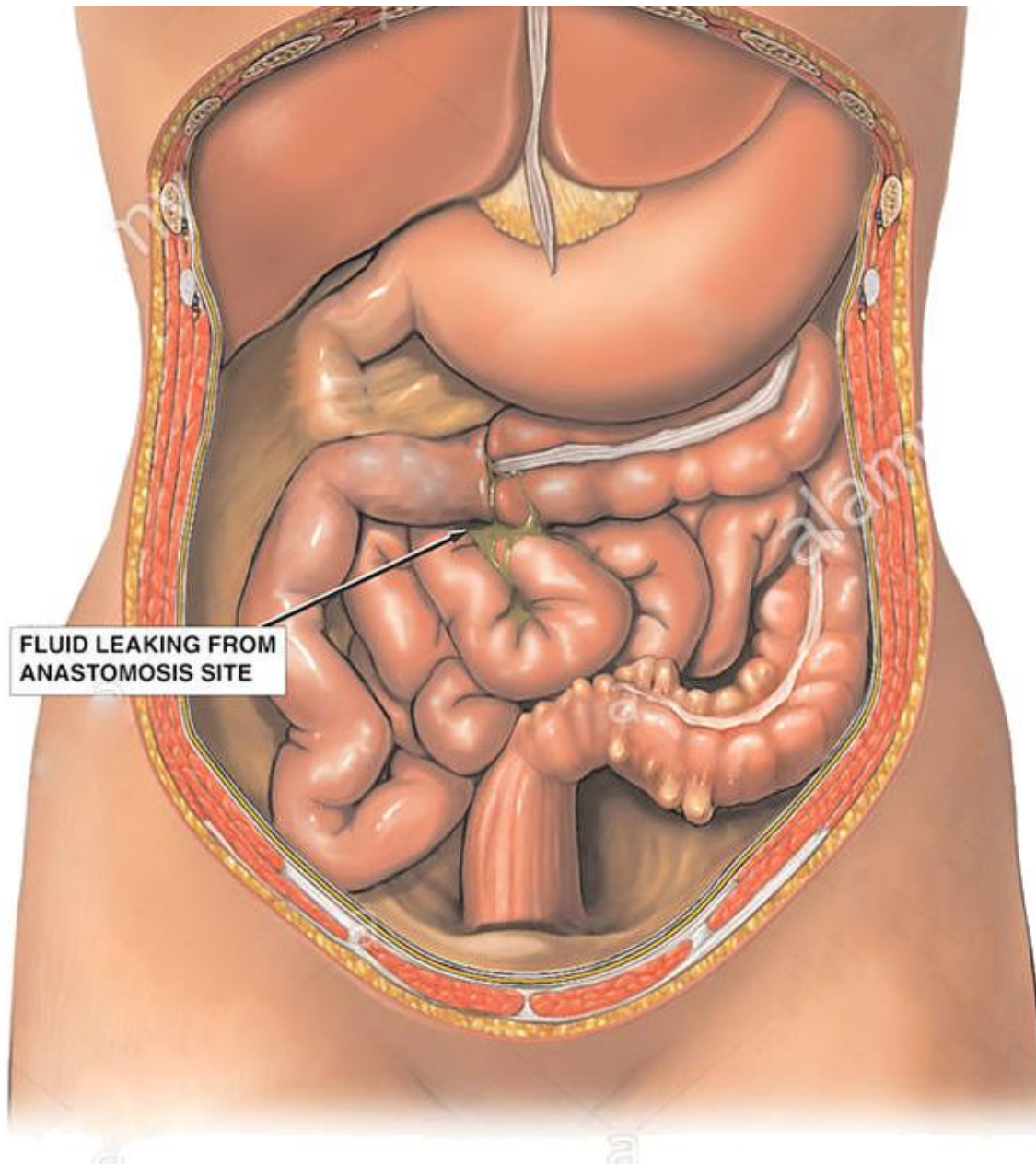
Figure 2. An example of an anastomotic leakage from the ileum. Copyright © Alamy (ADW7G9)

Early diagnosis and management of anastomotic leakage are critical to minimizing morbidity and mortality with a positive correlation between the timing of intervention and septic complications [9]. In one study, it has been reported that a delay of 2.5 days to re-operation or definitive intervention for anastomotic leakage was associated with an increase in mortality from 24% to 39% [10]. Timely diagnosis of anastomotic leakage is therefore, of utmost importance, yet there is no consensus as to the 'best' diagnostic test. Practice varies among institutions and, because of the acute nature of the condition, there is a paucity of data comparing the sensitivity and specificity of the various modalities. Anastomotic leakage may also present in varying guises, ranging from the sudden onset of fulminant sepsis with multi-organ failure to a more insidious presentation with ileus and failure to progress in the postoperative period, or it may even be subclinical.

Current technologies able to detect leaked fluids are nonspecific, time-consuming and expensive systems that are unable to monitor real-time leakage post-operation. These systems include upper gastrointestinal (UGI) radiography (e.g. barium fluoroscopy), Computerized Tomography (CT) scans, ultrasonography, peritoneal drains and other nonspecific interventional methods that require many skilled personnel and availability of well-equipped hospital facility [3]. Thus, there has been a need for small, cost-effective, and a real-time method of monitoring for gastric perforation or leaks that might be anastomotic, ischemic or accidentally injured during the surgery or post-operative.

1.1.2 Peritoneal Infections (Peritonitis)

Another type of postoperative complication that could develop following abdominal surgery is the introduction of infectious bacteria into the region [11]. With several studies identifying a variety of bacteria that are commonly identified in the peritoneum such as *Staphylococcus aureus*, the development of such infection, if not identified and treated would lead to Peritonitis. Peritonitis is the inflammation and irritation of the thin layer of tissue that covers the wall of the abdomen (peritoneal cavity) and most of its organs. Peritonitis is a serious condition that needs immediate medical attention (Figure 3). The prompt

interventions usually with intravenous antimicrobials are needed to treat the infection and guard against more complications. Surgery is sometimes necessary to remove infected tissue. The infection can spread and become life-threatening if it is not treated promptly. The bacterial contamination that leads to the infection can be introduced through various means such as the surgical equipment utilized during and following the surgery (peritoneal drains), failure of the anastomotic integrity, ulcer, kidney, and liver failure, etc. [12].
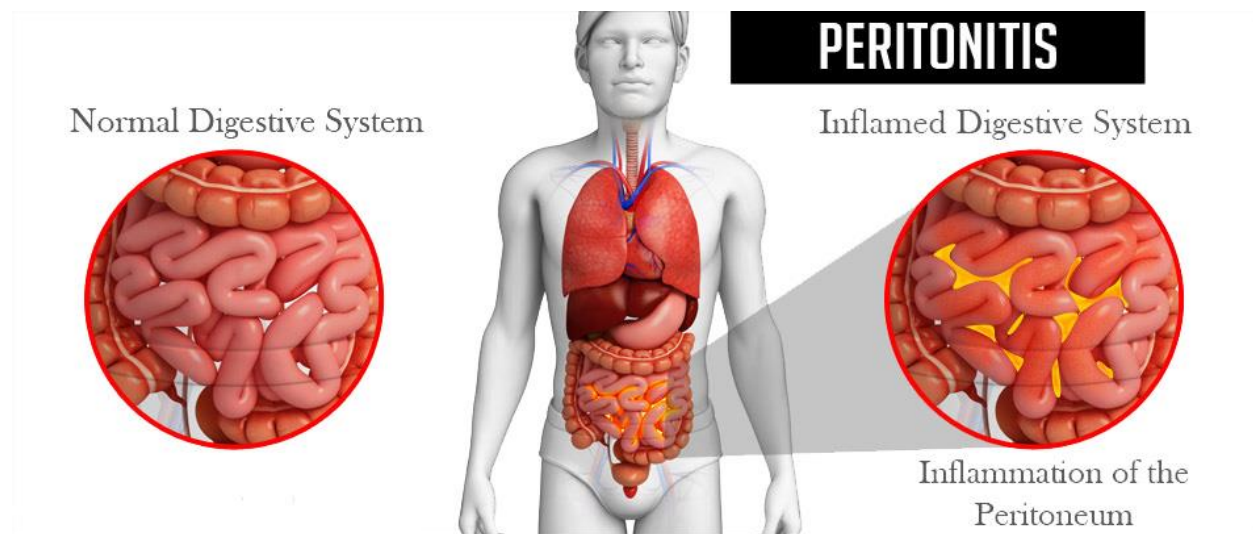
Figure 3. A comparison between a normal digestive system and an inflamed digestive system due to peritonitis. Copyright © www.medindia.net.

There are numerous methods that are used to help identify if the patient is suffering from peritonitis. Surprisingly, the most common method of diagnosing peritonitis is by monitoring the patient's vital signs. Another common method is to perform laboratory tests (blood tests) called a complete blood count (CBC) that can measure your white blood cell count, and C-reactive protein (CRP) which is a marker for inflammation in the body. A high white blood cell count and CRP usually signal the process of ongoing inflammation or infection. A blood culture can help to identify the bacteria causing the infection or inflammation. In addition, analysis of the peritoneal fluid can help identify bacterial development; the doctor can use a needle to remove some and send it to a laboratory for fluid analysis. Culturing the fluid

5

can also help identify bacteria. The same method can be applied if the patient is using a peritoneal drain, although in this case a color change can also be observed where the fluid collected can be observed to be cloudy. Imaging tests, such as CT scans and X-rays, can also show any perforations or holes in the peritoneum.

Similar to anastomotic leakage, early detection is critical to proper treatment. The early phase in treating peritonitis is defining and determining its underlying cause. Treatment usually involves antibiotics to fight infection and medication for pain. If the patient has infected bowels, an abscess (a collection of pus), or an inflamed appendix, the patient may need surgery to remove the infected tissue. If the patient is on kidney dialysis and has peritonitis, the patient may have to wait until the infection clears up to receive more dialysis. If the infection continues, you might need to switch to a different type of dialysis. The treatment must begin promptly to avoid serious and potentially fatal complications [13]. It has been noted that each hour of delay in administration of antibiotics from the onset of septic shock was associated with a decrease in survival of 7.6% [10].

1.1.3 Wound Healing Monitoring

One of the most sensitive areas following surgery is the incision point; this is the port that the doctor would use to perform the surgery. A variety of complications could develop around the incision area, ranging from infection, disruption (wound reopening), ulcers, incisional hernia, sinus, granuloma, etc. Thus monitoring the wound healing as it progresses is essential for the health of the patient. Current medical facilities rely mainly on visual examination and physical examination of the wound to make sure the wound is healing normally. The wound healing process includes four phases, which are overlapping – hemostasis, inflammation, proliferation, and remodeling.

In the last century, there have only been a handful of technical advances that have contributed to changes in the discipline of wound management. One of the most important was in the 1960s when it was found

that keeping a wound moist accelerates the healing processes. The time taken from the initial presentation of a wound to the commencement of a wound management plan may be lengthy and require multiple appointments with a clinician, as any laboratory tests ordered can take hours or days to complete. Once treatment has commenced the patient would then be re-evaluated at subsequent appointments which can be days to months apart. These cumulative delays and follow-up appointments stall the administration of appropriate treatment and lead to increased cost. This is critical in terms of chronic wound management, where it has been shown that the longer the delay in treatment, the more difficult a wound is to heal [14]. As such, the use of rapid, specific and quantitative assessments, that can be completed during a standard medical consultation, would be better suited to wound management [15].

1.2 pH General Review

In this section, the basics of how pH is measured will be explored. This will include the relationship between the hydrogen and the hydroxide ion in aqueous solutions. What is pH, and how is it detected?

1.2.1 Water autoionization

Water is the most common substance known to man and is the most important as well. In vapor, liquid or solid form, water covers more than seventy percent of the Earth's surface and is a major component of the atmosphere. Water molecules are in continuous motion, even at lower temperatures. When two water molecules collide, a hydrogen ion is transferred from one molecule to the other. The water molecule that loses the hydrogen ion becomes a negatively charged hydroxide ion. The water molecule that gains the hydrogen ion becomes a positively charged hydronium ion. This process is commonly referred to as the self-ionization of water.

Figure 4. Self-ionization of water. Copyright © www.khanacademy.org.

This reaction can be written as a simple dissociation. At 25° C in pure water, each concentration of hydrogen ions and hydroxide ions is only $1 \times 10^{-7} M$. It is important to note that the number of hydrogen and hydroxide ions produced from this reaction is equal. This is why pure water is often described as a neutral solution.

In all other aqueous solutions, the relative concentrations of each of these ions is unequal. When more of one ion is added to the solution, the concentration of the other decreases. Equation 1 describes this relationship.

$$[H^+][OH^-] = 1 \times 10^{-14} \left(\frac{mol}{L}\right)^2 = K_w \qquad (1)$$

K_w is the autoionization constant. Aqueous solutions that have a hydrogen ion concentration greater than the hydroxide ion concentration are called acidic solutions. When the hydroxide ion concentration is greater than the hydrogen ion concentration, the solution is called basic or alkaline.

1.2.2 What is pH?

pH is the measurement of the hydrogen ion concentration, [H+]. Every aqueous solution can be assessed to determine its pH value. This value ranges from 0 to 14 pH for the wide majority of aqueous solutions. Values below 7 pH exhibit acidic properties. Values above 7 pH exhibit basic (also known as caustic or

alkaline) properties. pH was originally defined as the negative logarithm of the hydrogen ion concentration in 1909 by the Danish biochemist, Soren Peter Lauritz Sorensen [16] as seen in equation 2.

$$pH = -\log[H^+] \tag{2}$$

This definition was later changed, as the concentration n of the hydrogen ion is not the only factor influencing the pH of a solution. The concentration of other chemicals in the solution, or the *ionic strength* of the solution, is also a major influence on the pH measurement. The term "ionic strength" describes the amount of ionic species in a solution, as well as the magnitude of charge on those species. This effect can be seen in equation 3.

$$pH = -\log[H^+] \times f \tag{3}$$

Where f is the activity coefficient (The value of f can be obtained from standard tables [17]). In solutions where the ionic strength is very low, the activity coefficient is 1.00, making the activity of hydrogen ion equal to its concentration. As the ionic strength of a solution increases, the activity coefficient decreases. This has the effect of lowering the activity of hydrogen ion, which is seen as an increase in pH.

1.2.3 Common pH measurement Techniques

There are a variety of ways to measure pH. The most traditional ways of measuring pH is to use pH indicators. pH indicators are halochromic chemical compounds (Typically weak acids) that indicate the concentration of H_3O^+ via a color change. The color of a wetted sample (solution or strip) is matched to a color on a color chart to infer a pH value. The accuracy of the pH paper are usually in the range of ± 1pH with the range of the measurement being between 1.0 to 11.0pH for most color indicators. pH paper is typically used for preliminary and small volume measuring. It cannot be used for continuous monitoring of a process. Though pH paper is inexpensive, it can be attacked by process solutions, which may interfere

with the color change [18]. Colorimeter another form of indicators uses a vial filled with an appropriate volume of sample to which the indicator is added. As the halochromic chemical compounds is added, a color change takes place. The color of this solution is then compared to a color wheel or spectral standard to interpolate the pH value.

The most accurate and common way of measuring pH is to use pH meter. As for most application, they have the advantage of being precise and continuous forms of sensing. In the upcoming section, we will be looking at these components and how a pH meter works.

1.2.4 pH Meter

A pH Meter is a scientific device that can measure the level of hydrogen-ion motion in water-based solutions, representing its acidity or alkalinity expressed as pH. The pH meter measures the difference in electrical potential between a pH electrode and a reference (standard) electrode, and accordingly the pH meter is occasionally known as a "potentiometric pH meter". The difference in electrical potential relates to the acidity or pH of the solution. The pH electrode is sometimes called the glass electrode, and is also referred to as a membrane measuring or active electrode (Figure 5).
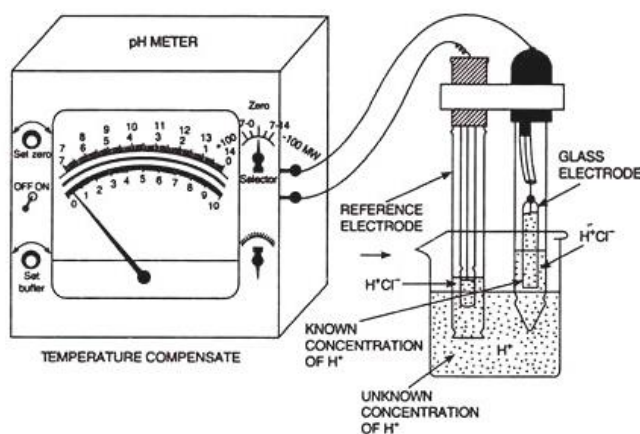
Figure 5. pH meter demonstrating the glass and reference electrodes Copyright ©

http://www.biologydiscussion.com

10

1.2.4.1 Nernst Equation

To understand how pH meters work it is important to understand mathematically how each of the electrodes work. This is well defined in the Nernst equation as seen in equation 4

$$E = E_o - \frac{2.3RT}{nf} \log a_i \qquad (4)$$

Where E is the total potential between the electrodes E_o is the standard potential of the ion, R is the universal gas constant $\left(\frac{J}{mol \cdot K}\right)$ T is the absolute temperature (K), n is the ion charge, F is faraday's constant $\left(\frac{C}{mol}\right)$ and a_i is the activity of the ion. The term $\frac{2.3RT}{nf}$ is usually defined as the Nernst factor. This term provides the amount of change in total potential for every ten-fold change in ion concentration.

For H_3O^+ ion activity, the Nernst factor is 59.16 mV for every ten-fold change in activity at 25°C. This means that for every pH unit change, the total potential will change 59.16 mV. The following general equation (Equation 5) may be stated for any temperature

$$E = E_o + (1.98 \times 10^{-4})T_k \times pH \qquad (5)$$

It is important to know that the Nernst factor will change as the temperature changes. At 25° C the slope of the pH electrode is 59.16 mV/pH unit. At 0° C the slope value is approximately 54 mV/pH, and at 100° C the slope value is approximately 74 mV/pH. The millivolt output of the glass pH electrode will change with temperature in accordance with the Nernst equation. As the temperature increases, so does the millivolt output. Specifically, the slope of the electrode is what changes.

The second electrode utilized in our measurement is the standard reference electrode. A standard reference electrode is an electrode which has a stable and well-known electrode potential. The high stability of the electrode potential is usually reached by employing a redox system with constant (buffered or saturated) concentrations of each participant of the redox reaction. The standard hydrogen electrode (SHE) is the basis on which all other electrodes are compared (E=0.0V). The SHE consists of a platinum electrode immersed

in a solution with a hydrogen ion concentration of 1.00M. The platinum electrode is made of a small square of platinum foil, which is platinized with a finely divided layer of platinum (known as platinum black). Hydrogen gas, at a pressure of 1 atmosphere, is bubbled around the platinum electrode. The platinum black serves as a large surface area for the reaction to take place, and the stream of hydrogen keeps the solution saturated at the electrode site with respect to the gas.

1.2.4.2 Electrode System

The pH measurement is comprised of two half-cell, or electrode, potentials. One half-cell is the pH sensitive glass measuring electrode, and the other is the reference electrode. Just as the two half-cell potentials of a battery are required to complete a circuit so does a pH sensor. Since voltage-measuring devices only determine differences in potentials, there is no method for determining the potential of a single electrode. A galvanic measurement circuit is formed by connecting the measuring electrode (half-cell potential) and the reference electrode (half-cell potential) to the signal input of the measuring device. At the reference electrode, there is a solid/solution interface, where a chemical reaction takes place. This enables an electrical current to flow through the measuring device, the pH meter, which allows the reading to be made. Since the current that passes through the half-cells and the solution being measured is extremely small, the pH meter must have a high internal impedance, so it does not "drag down" the millivolt potential produced by the electrodes. This low current flow ensures that the chemical characteristics of the solution being measured remain unaltered.

The galvanic voltage output produced by a measuring electrode will depend on the ionic activity of the species of ions which the electrode was designed to measure. In the case of pH electrodes, it is the hydrogen ion activity. The active part of a pH measuring electrode is the probe tip. The probe tip is constructed from a special composition glass which senses the hydrogen ion concentration. This glass is mostly amorphous silicon dioxide (SiO_2), with embedded oxides of alkali metals, mainly Na. It is made to be as thin as possible, about 0.1 mm thick. When the surface of the glass is exposed to water, the alkali metal ions of the

glass and the hydrogen ions (H_3O^+) in the solution undergo an ion exchange reaction. A thin, about 10 nm, hydrated gel layer forms on the outer surface of the glass, the so-called glass membrane. Such a hydrated gel layer arises also on the inside of the glass tip, which is in contact with a buffer solution, usually 0.1M HCl, with a constant pH value. This phenomena is demonstrated in figure 6
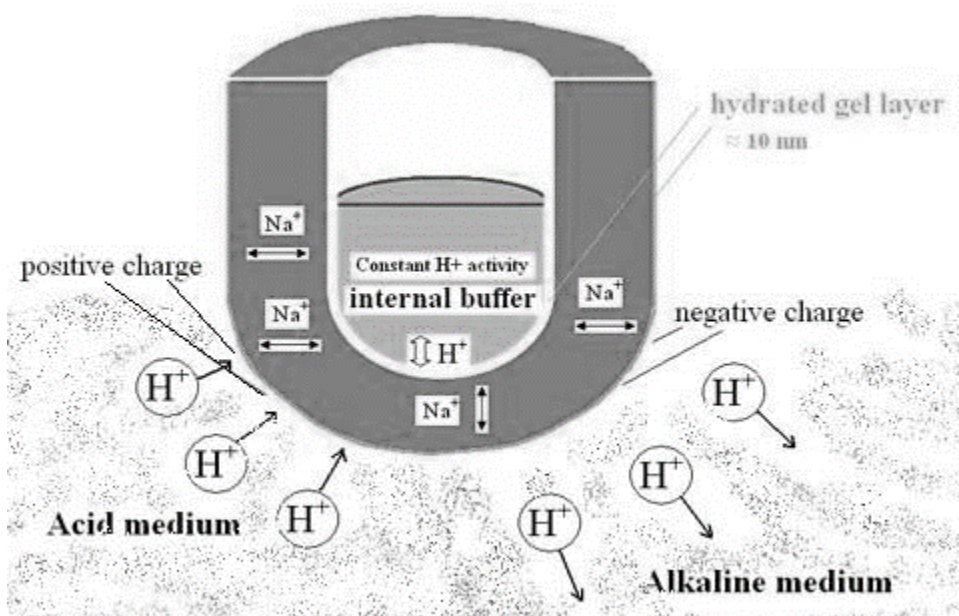
Figure 6. Glass Electrode Probe Tip. Copyright © all-about-pH.com

Depending on the pH of the solution being measured, hydrogen ions (H_3O^+) will migrate into or out of the gel layer. In an alkaline solution, hydrogen ions migrate out of the gel layer and a negative charge is developed on the outer gel layer. Hydrogen ion does not cross through the glass membrane, it is the Na^+ which crosses and allows for a change in free energy.

The reference electrode consists of a silver wire coated with silver chloride that is immersed in an electrolyte solution. This wire must be electrically connected with the solution being measured. This is accomplished through a porous junction, commonly called a salt bridge, which physically isolates the electrolyte and wire from the solution being measured. The electrolyte solution must have a high ionic strength to minimize resistance and not affect the solution being measured, and must remain stable over large temperature swings. Potassium chloride (KCl) solutions that are 3.0 molar, 3.5 molar, or saturated have been used

successfully for many years. This reference wire and electrolyte combination is the silver/silver chloride reference system. Other types of reference systems are also manufactured for specific measurement needs. These alternate reference systems consist of calomel, thalomid or mercury.

1.2.4.3 Sources of Error

It is important to determine the possible sources of error for the pH meter and to account for them when developing and researching new systems. A list of the possible sources of error has been outlined in table 1.

Table 1. Sources of Error in pH meters

Error Source	Description of Error
Asymmetry Potential	When a pH electrode is immersed in a solution with the same pH as its internal fill solution, there should not be a measurable potential across the glass membrane. If such a potential exists, it is known as an asymmetry potential
Sodium Ion Error	Sodium ion error, also referred to as alkaline error, is the result of alkali ions, particularly sodium ions, penetrating the glass electrode silicon-oxygen molecular structure and creating a potential difference between the outer and inner surfaces of the electrode. Hydrogen ions are replaced with sodium ions, decreasing the hydrogen ion activity, thereby artificially suppressing the true pH value.
Acid Error	Acid error affects the low end of the pH measuring scale. As pH decreases and the acid error begins, water activity is reduced due to higher concentrations of acid displacing water molecules. The thickness of the

14

	hydrated gel layer becomes thinner due to acid stripping. This effect has a negative influence on the mV output, thereby causing the measured pH value to remain higher than the theoretical pH value.
Temperature Effects	Temperature affects the pH measurement in two ways. The first is a change in pH due to changes in dissociation constants of the ions in the solution being measured. This implies that as solution's temperature changes, the pH value also changes. The second reason temperature affects the pH measurement, is glass electrode resistance. Since the glass measuring electrode is an ionic conductor, it stands to reason that the resistance of the glass will change as the solution temperature changes. As temperature rises, resistance across the glass bulb decreases.
Reference Junction	The reference junction (salt bridge) is located at the measuring end of the reference electrode (or reference electrode assembly for a differential pH sensor). There are times when the solution being measured does penetrate the junction and contaminate the reference system. Due to junction contamination, junction plugging, electrolyte dilution, and chemical attack of the silver/silver chloride wire, the resistance is always changing, as is the chemical composition of the whole reference electrode.

1.3 pH Technology Platform

The biochip platform in which the pH sensor will be integrated aims to save lives, reduce the risks that are associated with surgeries by monitoring a patient's health after a surgical procedure and decrease the number of unnecessary follow-ups that the medical facility has to perform. By placing the biochip close to the surgical site, the biochip oversees and assesses the body's natural biomarkers, identifying the kind of

complication taking place and sends feedback to the caregiver according to the changes happening inside the body. With the aim to detect complications at earlier stages and prevent the development of any further complications thus eliminating the stress that physicians and patients go through due to post-operative complications.

The chip is a post-surgical implantable biochip, consisting of multiple arrays of biosensors. The chip is placed inside the body at the end of the operation before closure. The biochip will be utilized in general, obstetrical and gynecological surgeries such as operations in the urinary and digestive systems, laparoscopies, laparotomies, intestinal surgeries, and bariatric surgeries. The biochip is small (1 cm x 2 cm), provides real-time feedback and is made entirely out of biocompatible materials making it completely harmless to the body. The solution is considered to be the first of its kind in the field of detecting postoperative complications in real-time. The ability to provide real-time information to the physicians adds a new dimension of detection that would allow the caregivers to react appropriately to deal with the complication at hand. The current solutions for detecting postoperative complications (imaging techniques and routine blood investigations) rely on the patient showing symptoms of illness initially before taking the necessary measures to try to identify the complication.
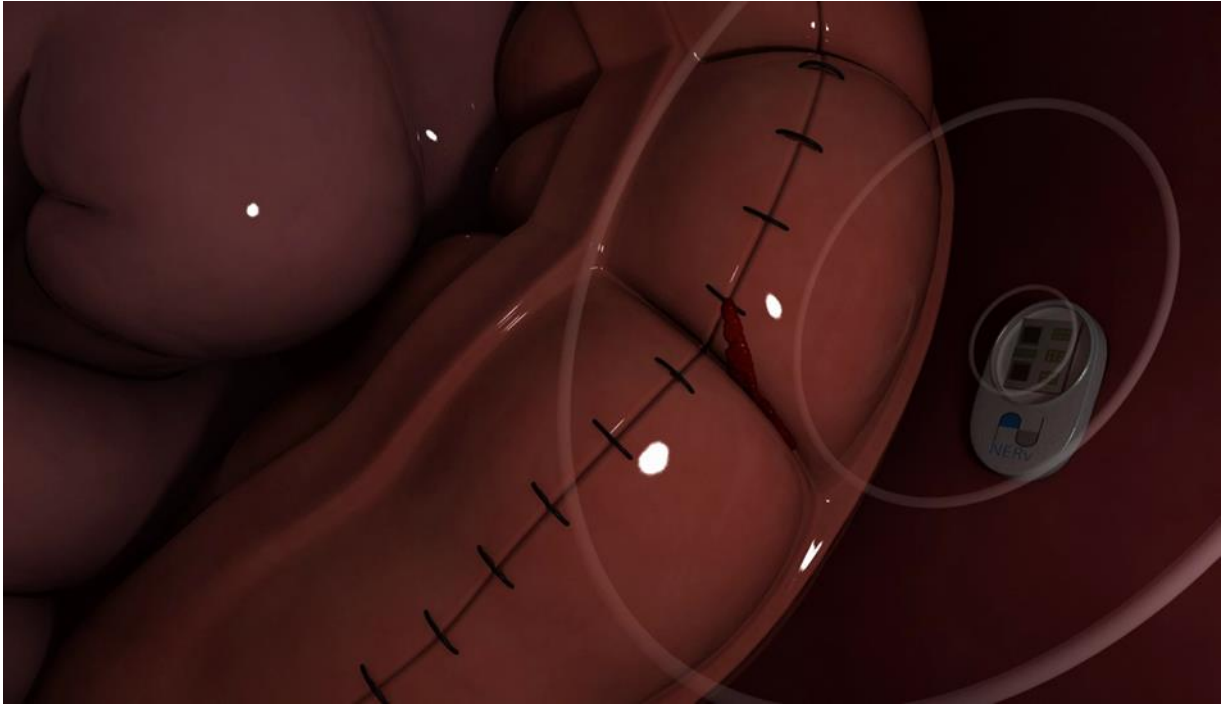
Figure 7. The pH Sensor chip communicating the development of anastomotic leakage Copyright © ne-

rv.com

The biochip consists of biosensors, a polymeric substrate, and power & wireless communication modules. The biochip is implanted into the body at the end of surgical procedures using a bioadhesive to ensure the biochip remains close to where the surgical site is. It then assesses many of the biomarkers, the trends in these biomarkers & other vital signs in the body to identify if a complication is developing. If there is a sign or potential that a complication could develop, the biochip sends a signal to the physician with detailed information about the nature, location, & type of complication that is happening. The biochip sends out the wireless transmission to a receiver located in the trans-dermal patch outside of the body. The receiver then sends out that communication via the cloud to both the physician & the patient in terms of readable data. The physician receives information about the biological changes in the body, including the patient's vital signs, changes in the biomarkers' levels, & the general status of the patient to identify the kind of complication and eliminate any ambiguity. The patient gets a more simplified message that informs them of the need to seek medical assistance.

The solution has the potential to reduce the costs associated with detecting postoperative complications and monitoring patients after surgery. Currently, each patient costs the healthcare system on average over $15K in post-operative check-ups. Using such solution, costs associated with keeping patients inside hospitals for an extended period can be reduced as patients can be monitored from the comfort of their homes. Additional routine investigations could be avoided by determining if a complication is occurring. Finally, the solution is real-time, reducing the costs associated with the late detection of complications.

One of the major parts of the biochip platform is the utilization of sensors to identify biomedical complications. In this thesis, I will explore and design a pH sensor that can monitor the pH milieu of the area of implantation (The peritoneal cavity).

2.0 Analysis, Constraints and Requirements

In this section, an analysis would be performed to identify the correlation between pH and the medical complications we have previously identified. Based on the data collected the device constraints and requirements will be identified.

2.1 pH and Post-Operative Complications

It is important to determine if pH is a good biomarker to target given the previously addressed complications demonstrated in section 1.1. To address this issue, in the following section the effect of the complications on the milieu of the pH in the region will be studied.

2.1.1 Anastomotic Leakage pH Change

The peritoneal cavity is covered with peritoneal fluid. Peritoneal fluid is a liquid made in the abdominal cavity which lubricates the surface of the tissue that lines the abdominal wall and pelvic cavity. It covers most of the organs in the abdomen. If a leak is to happen, it will mix with the peritoneal fluid altering and changing its pH. By looking at the composition of the peritoneal fluid and analysis of its pH, we know that the pH of the peritoneal fluid at normal circumstances would range from 7.60 to 7.64 [19]. To cause a pH change the fluid that would need to leak would have to have a pH value different from that of the peritoneal fluid. To do so, we will analyze the different surgeries that could happen along the gastrointestinal (GI) tract. By looking over the GI tract as seen in Figure 8. We realize that across the GI tract the natural pH is different from that of the peritoneal fluid [7].
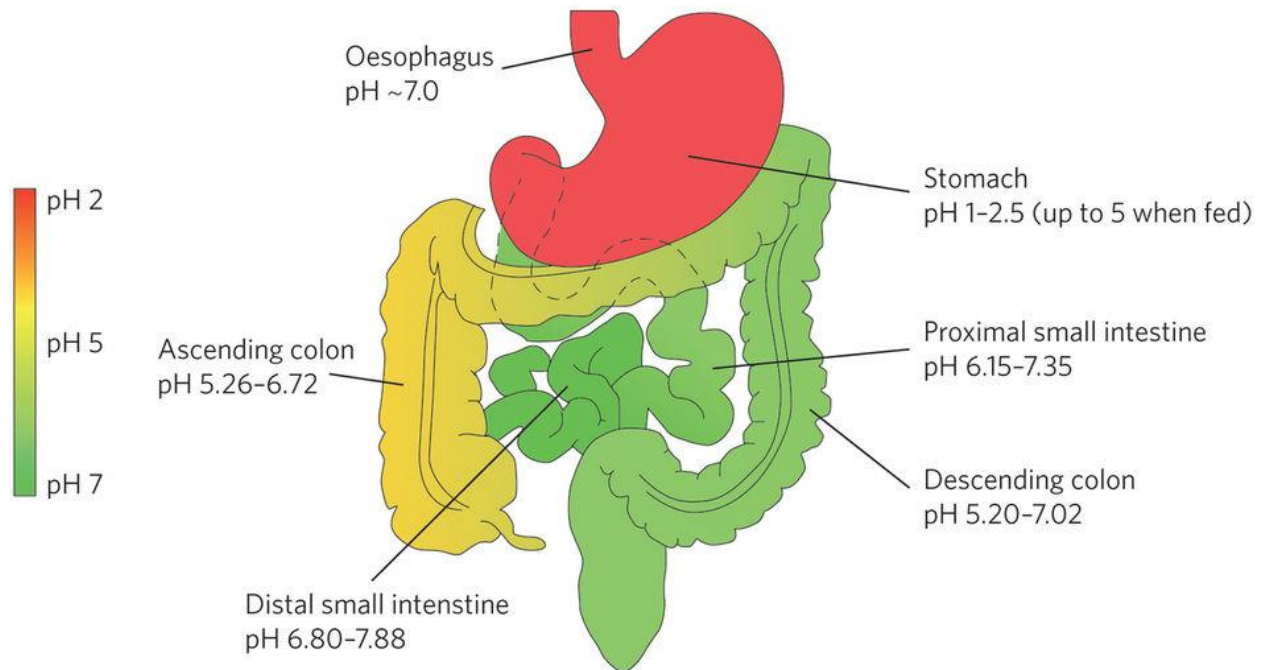
Figure 8. Gastrointestinal tract pH values [20]

This means that surgeries such as gastric bypass or gastric sleeve, where the main target is the stomach, if a leak is to develop the sudden pH drop could be clearly measured because of the mixing between the gastric juices and the peritoneal fluid [21]. The same can be observed across different parts of the GI tract such as the colon and the intestines [5]. By analyzing the data, we can see that the pH of the peritoneal fluid would change according to the graph seen in figure 9. As soon as the leak starts, a large change in pH is observed in the peritoneal fluid. It is to be noted that the leak demonstrated in figure 8 is considered a major leak. Minor leaks tend to be the most deadly as they can go undetected for up to a couple of days following the surgery, in which the patient may have already been discharged from the hospital. Even in the case where a minor leak does develop, a pH change will be observed in the peritoneal fluid. One thing to note as well, is one of the main causes of anastomotic leakage, is ischemia. Ischaemia is a restriction in blood supply to tissues, causing a shortage of oxygen and glucose needed for cellular metabolism (to keep tissue alive). If ischemia does develop the tissues, move from aerobic metabolism to anaerobic causing a release of lactic acid which causes a local drop in pH. If leakage does develop due to cell death from ischemia, a small drop in pH is to be observed followed by a steep pH drop.
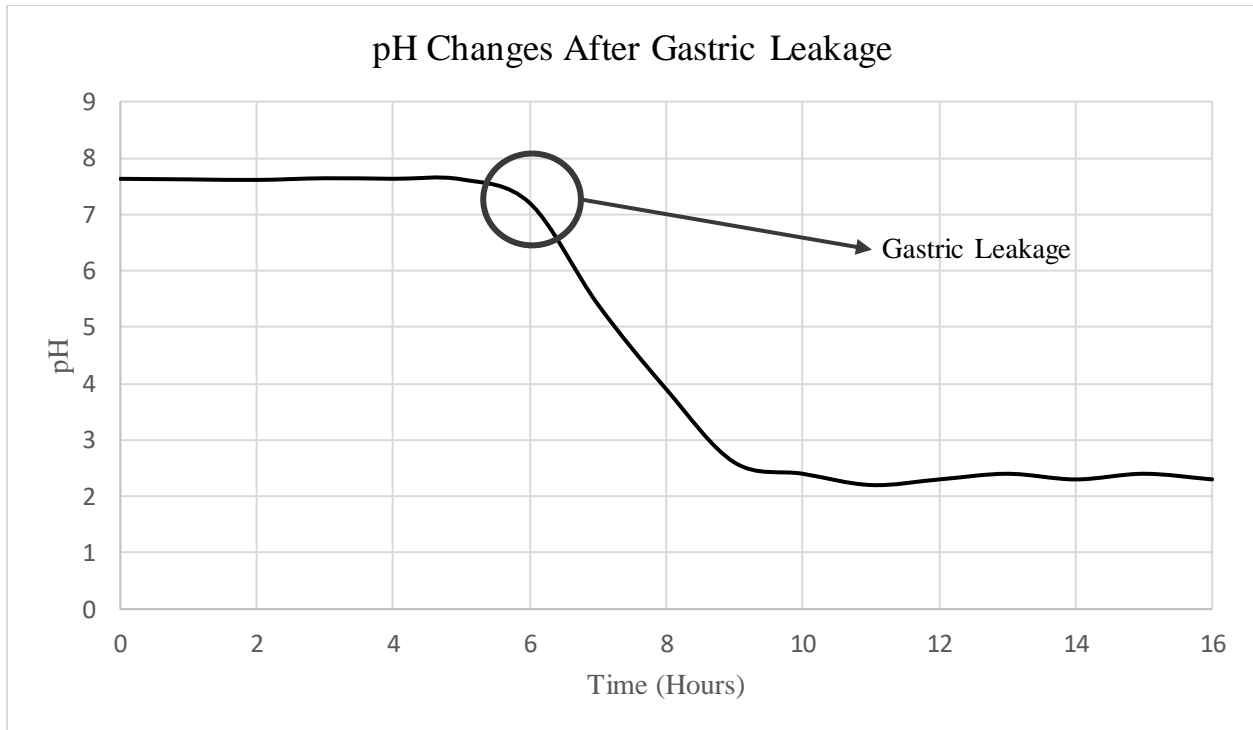
Figure 9. pH changes following an anastomotic leak of gastric juice into the peritoneum

2.1.2 Peritonitis and pH changes

Another complication where monitoring the pH milieu of the peritoneal fluid can provide a major indication of it developing is peritonitis. Bacterial development in the peritoneal cavity is the main cause of peritonitis, as it develops into a sepsis, which in turn may lead to a septic shock (One of the lead causes in morbidity and mortality following surgeries) [11]. Based on this information an analysis has been performed to determine the link between bacterial development in the peritoneum and variations in pH.

We will look over the three main stages of bacterial development in the peritoneum as demonstrated in figure 10. The first stage is when bacteria are introduced to the region. Bacteria start to use the resources available (glucose), and they start producing toxins. When analyzing the pH changes as bacteria start to grow and produce their toxins it is observed that the pH of the area increases to be in the range between 8.1-8.3 pH [22-23]. This period typically lasts from 0 Hours (The time of the infection) and can last 12-24 hours.
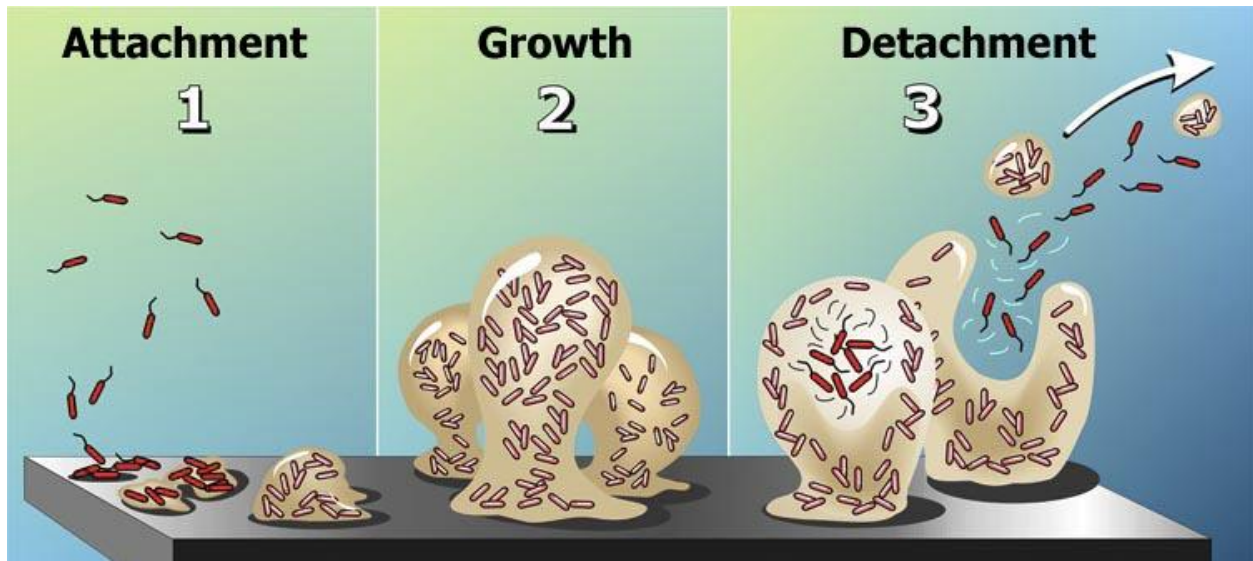
Figure 10. Bacterial Development Cycles in the peritoneum Copyright © Center for Biofilm Engineering at MSU-Bozeman P.Dirckx

The second stage is the growth stage (aggregation). At this stage, bacterial colonies have developed, and what is further observed in this region is that bacteria start competing for glucose (energy) due to their metabolic activities. Which leads the bacterial colonies to transfer from aerobic respiration to anaerobic respiration. This leads to the release of lactic acid in most common bacteria observed in the peritoneum [24]. This leads to a drop in the pH observed in the peritoneal fluid. As a matter of fact, during peritoneal dialysis, the pH variation has been directly correlated and utilized in the medical field to identify peritonitis in 95% of the cases [25]. Not only is that true, but it has been further studied and observed that by monitoring the rate of these pH changes the medical facility can identify specific infectious strains of bacteria [26]. In general, the pH would drop to be in the range between 5.8-7.1pH is a strong indication that an infection might be developing in the region. The timeline for this stage can typically start anywhere from 12 hours following the infection and can last for 24-36 hours.

The last stage, detachment (dispersion), is when the bacteria start dispersing into different parts of the body infecting different regions and the cycle starts over again. It is therefore of great importance to identify infection at its onset and provide the best treatment option as soon as possible. It has been proved in research

that early identification is key to help save the patient [27]. This is one of the great advantages of monitoring pH changes and correlating them with the different the different cycles (stages) observed in peritonitis. By monitoring the rate of pH change, the medical facility can identify if an infection happens first of all. It can then determine if the body's natural defense system is capable of neutralizing the infection. This can then be followed by an antibiotic treatment, while still monitoring the progression of the infection. If it is still observed that the bacterial infection is developing a follow-up surgery may be required to intervene and help save the patient [28]. The pH changes of a bacterial cycle monitored at the infection site is expected to follow a trend similar to the trend shown in figure 11.
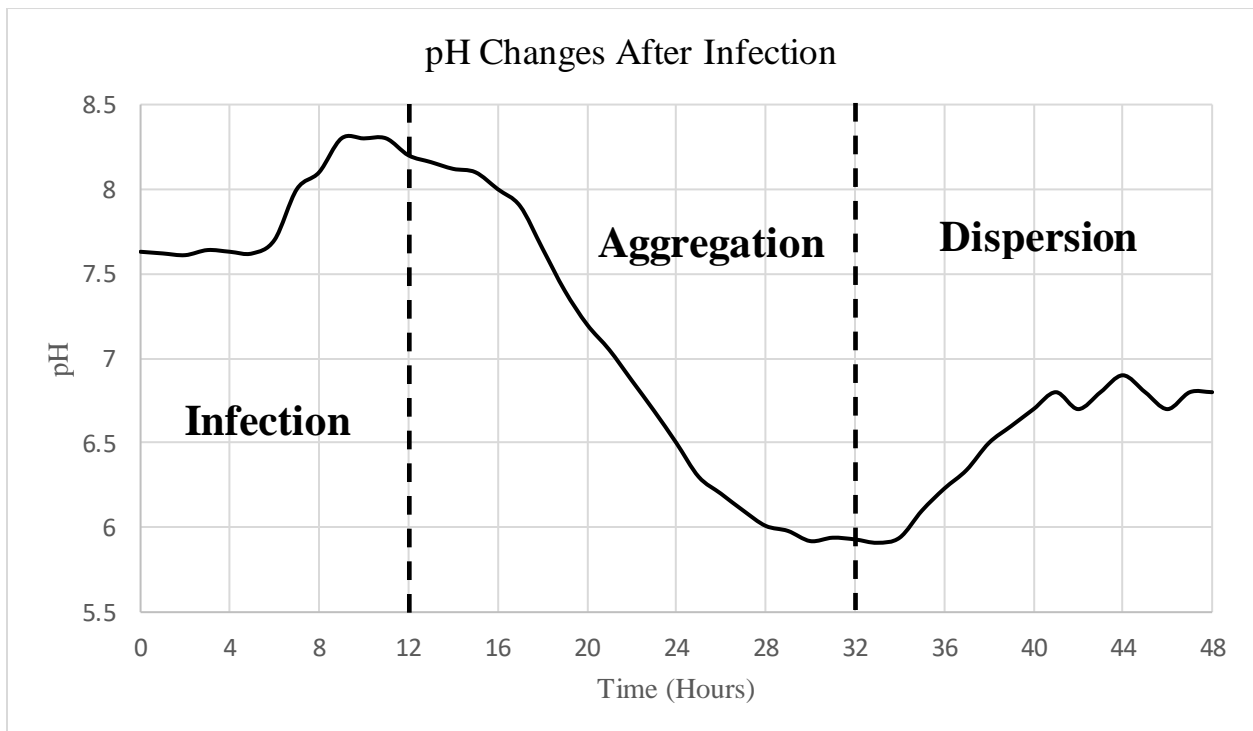
Figure 11. pH changes following infection in the peritoneal cavity

2.1.3 Wound Healing and the pH changes

The skin surface exhibits an acidic pH milieu during normal conditions, and this acidic pH varies from 4 to 6 depending on the age and anatomical location and acts as the human body's first line of defense.

Injuries or microbial infections in wounds disrupt the normal acidic milieu of the skin, and a shift toward alkaline milieu indicates bacterial colonization. A high pH has been reported to support overgrowth of "Candida albicans", a pathogenic yeast that grows on the skin surface [29]. "Staphylococcus aureus" is another common pathogen that contaminates a wound, thus resulting in delayed healing in the presence of an alkaline pH [30]. Therapeutic interventions can be devised by monitoring changes in pH during the wound healing process, and such interventions will assist in the elimination of bacterial contamination, which is a potential cofactor that retards the wound healing process [31]. The pH, if the infection does develop, can vary anywhere between 7.15 and can be as high as 8.9 [32].

Not only is pH a method to monitor the wound and to identify the possibility of infections. By controlling the pH to be in a certain range, the wound healing process can be accelerated and controlled to allow for a healthy recovery. The pH changes observed during the wound healing process can be seen in figure 12.
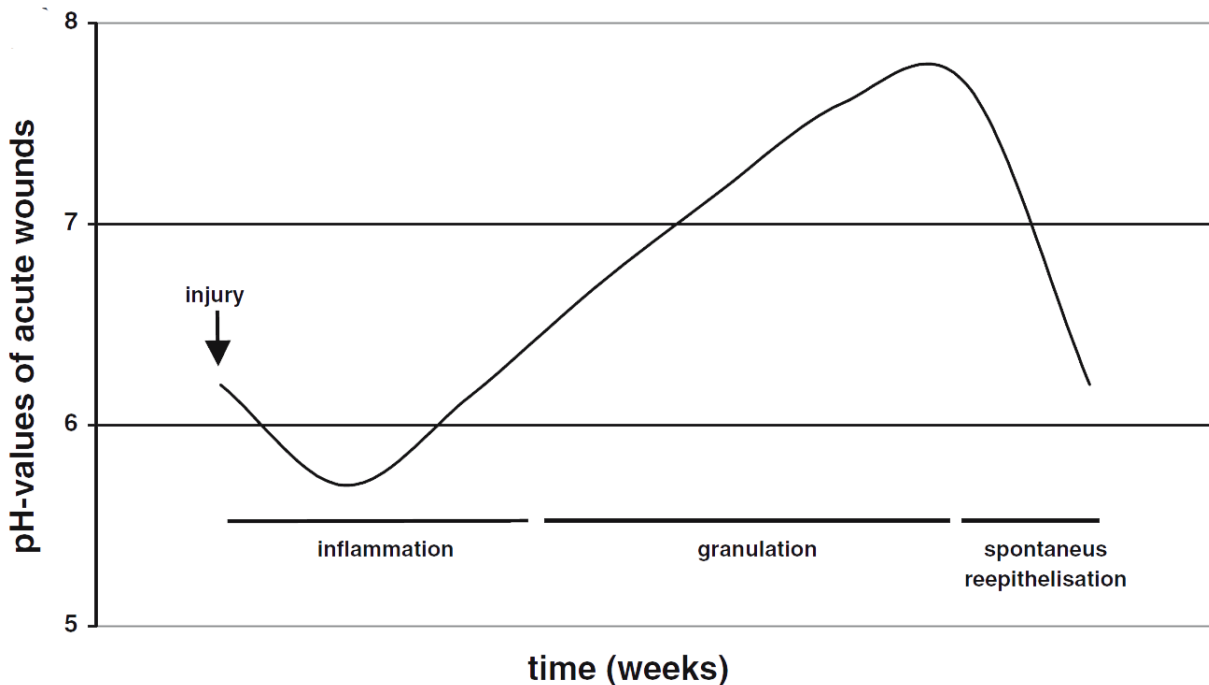
Figure 12. pH changes at the wound site following the surgical incision [31]

2.1.4 Other Medical Applications

It is to be noted that there are other applications, where a pH biosensor may be utilized for implantable medical devices that are not within the scope previously identified. pH sensors can be used to detect ischemia. This has been briefly addressed in the anastomotic leakage section. Ischemia is a restriction in blood supply to tissues, causing a shortage of oxygen and glucose needed for cellular metabolism (to keep tissue alive). If ischemia does develop the tissues move from aerobic metabolism to anaerobic causing a release of lactic acid which causes a local drop in pH [33]. pH biosensors can be utilized across different fields of medicine to identify and detect ischemia at its onset [34-35].

Another area is to utilize the pH biosensors on fetal scalp electrodes. Internal cardiac monitoring with a scalp lead is used to identify fetuses at risk for serious complications from hypoxia during labor. Labor represents a unique stress on the fetus in utero. Uterine contractions reduce the flow of maternal blood to the placenta, in some cases uncovering a deficit in placental capacity [36]. One of the critical parameters that need to be assessed during labor is the amount of blood reaching the fetus. This is performed by taking a blood sample from the fetus's scalp and taken to the lab for testing (with pH being one of the main factors being tested). pH monitoring allows the healthcare provider to identify respiratory acidosis, metabolic acidosis and mixed acidosis.

2.2 Design Constraints and Requirements

It is essential to identify the design constraints and requirements to identify the correct path to follow, technology to adopt or technology to develop. The requirements that will be outlined in this section will be either extracted from literature, abiding by regulatory boards and medical standards, or limited to utilizing the resources available.

The first constraint is **size**. The biochip platform consists of multiple parts that will all be assembled into a package that is 1cm x 2cm. This includes the biosensors, the electronics, the antenna, the insulating

packaging, etc. All of the biosensors will be placed on a unified surface that will allow the sensors to be exposed to biological fluid. The max area that the sensors were allowed to occupy was 500μm x 500μm. We do not prefer that the sensors occupy a much smaller surface area. In terms of the sensors thickness, we specified that the max thickness should be 300μm.

The second constraint is in terms of the pH biosensor **sensitivity**. By analyzing literature and determining the minimum pH change that is an indication of a complication or a disease, we see that a change of 0.1 pH in the body pH is a strong indication [37]. This is because the human body is very good at regulating the pH of the body. We also explore other applications such as the fetal scalp electrode, and we determined that a pH change of 0.1 pH is also a major indicator of whether the fetus would survive or not. Based on this information it was clear that the pH biosensor has to indicate a change of 0.1 pH. However, we are aiming to detect pH changes as small 0.01pH and thus this has been identified as the minimum change the pH biosensor needs to detect. In addition, it is important to identify the pH range that the pH sensor needs to be able to detect. Based on the analysis of the majority of abdominal surgeries and the pH ranges of the complications it has been identified that the sensors need to be operable in the pH range between 2-9 pH.

There is a very important note to identify when determining how the sensor should be sensing pH. The fact of the matter is that human bodies have large variances between them and a pH that could be considered normal for one individual might be fatal to another. This could be related to a variety of factors such as age, gender, life-style, medical background, etc. Which brings up an important question; should the biosensor aim to detect an absolute pH value and relate this value to a complication? To help address this issue several examples would be demonstrated. For example, if the pH biosensor is placed in the peritoneal following a gastric bypass surgery and the sensor reads a pH value of 2.5. This is probably a strong indication of a gastric leakage. Now let us look at a more controversial example where identifying the complication could be more difficult. In a case where for example we has a reading of pH that is 7.8 pH, which is above the normal peritoneal pH observed for most patients (7.60-7.64). What does this number indicate? Could this

be a case of bile fluid (pH of 7.50 to 8.05) leaking or could this be a case of bacteria developing in the peritoneum which we demonstrated earlier could make the pH rise to 7.8 in the peritoneal cavity.

Several scenarios were analyzed, and the following has been concluded. Detecting an absolute pH value, no matter how accurate that pH reading is, would not be sufficient to identify if a complication is developing. This is due to a number of factors, the first factor being the large variance between the patients. The second factor being as the nature of the surgeries change so does the body response to those surgeries (for example the inflammatory response for open surgery is much stronger than that in laparoscopic surgery). We have also set a requirement that the sensors should require either no **calibration** or one calibration (when the device is first implanted)

Instead of detecting an absolute pH the sensor would need to measure $\Delta pH/\Delta T$. The rate at which the pH changes is what truly determines the kind of complication that the patient might be suffering from. Firstly, it eliminates the variance between patients since the natural pH of the individual peritoneum does not contribute to the changes that will occur due to a complication. Secondly, it means that the biosensor might not need calibration in certain sensing mechanisms. Thirdly, by looking at the rate of which the pH changed, certain complications could be eliminated. For example, a rapid drop in pH is probably not caused by bacterial aggregation, it would probably be caused by a form of leakage. On the other hand, it does have a disadvantage, with the disadvantage being that at the time of implantation, if the patient is already suffering from a complication then the sensor would not be able to detect these complications. In theory this could happen, in the medical practice however, this probably would not happen. This is due to the fact that if a complication such as anastomotic leakage developed during or towards the end of the surgery before the surgeon implanted the device. The complication would be visible to the surgeon and an immediate action would be taken to ensure the safety and the health of the patient. To come to this conclusion several test scenarios were analyzed and discussed with surgeons actively working in the field.

One important analysis that has to be outlined is the difference between diagnostic and theranostic. A diagnostic reading will give an accurate, binary, non-subjective, decision making output. An example of

such sensor would be a pregnancy sensor. **Theranostic,** on the other hand, provides a reading to help guide treatment. An example of such sensor would be a glucose monitor, where the glucose reading would guide the type of treatment that the patient would need (For example, how much insulin the patient would need). All readings provided need to be theranostic readings.

Another factor that needs to be considered is for how long do the sensors need to be actively working? To identify this literature has been examined and it has been shown that the latest complication that could develop as a result of the surgery is four weeks following the surgery with the complication being anastomotic leakage [38]. Based on this information it has been determined that the biosensor needs to be active for at least **29 days** following the surgery.

The fourth factor that needed to be considered is the time between readings i.e. how long does it take for a complication to occur and based on this information this is the minimum time that the sensors needs to be active for in order to be considered detecting in **real-time**. Based on literature analysis, it has been decided that the minimum time required for detection is 5 min. This is based on two complications, the time needed for a systematic change in the pH of the body during labor is 10min [39] and the time need for pH change due to gastric leakage is also 10min for most leaks [40].

The fifth factor has to do with the **power constraint** for the pH sensor. It is highly preferable for the pH biosensor to be a passive sensor (does not require any external power source to produce output signal). So basically if the sensor can extract power from the environment (i.e. use an electrochemical system) it would be preferred over other means of detection. If the sensor is to consume power, the maximum power consumption of the system needs to consume less than 250 mW. Another electrical requirement that we specified is that the sensor needs to have its interface method with the microcontroller through a **contact pad**. This is because the our circuitry platform is built around an electrical interface where all sensors from the class can be connected together using contact pads.

The sixth factor is its **sensitivity in the clinical settings**. In other words, in a 100 patients that would develop anastomotic leakage for example, how many of those patients will the pH biosensor pick up on the reading and correctly identify the complication to be anastomotic leakage. For the device to enter the market according to the FDA and according to Health Canada, out of a 100 cases the device needs to at the very least (to be FDA approved) correctly diagnose 95% of the cases [41-42]. The FDA standard also accounts for false negatives and false positives. A false negative is a test result that indicates a person does not have a disease or condition when the person actually does have it. Correspondingly, a false-positive test result indicates that a person has a specific disease or condition when the person actually does not have it

The seventh factor is the **accuracy** of the sensor. This factor will highly depend on the sensing technology that will be utilized but in general, terms the sensor needs to be accurate as possible. If the sensor technology adopted is to utilize an electrochemical form of sensing several factors need to be considered. The first factor is that the pH is being measured in a biological environment, which means that there is a large abundance of mineral ions (magnesium, calcium, sodium, potassium, etc.) that could interfere with the measurement being collected. There is an international standard adopted by the International Union of Pure and Applied chemistry to determine the accuracy of the sensor known as the potentiometric selectivity coefficient [43].

The eighth factor and one of the most critical to consider is the choice of materials when designing the sensor. The sensor is going to be placed inside the body and thus all the materials and the components utilized in the device need to be **biocompatible**. The biocompatibility of a long-term implantable medical device refers to the ability of the device to perform its intended function, with the desired degree of incorporation in the host, without eliciting any undesirable local or systemic effects in that host. The device has to abide by the ISO 10993 standard [44]. The ISO 10993 set entails a series of standards for evaluating the biocompatibility of medical devices. These documents were preceded by the Tripartite agreement and is a part of the international harmonisation of the safe use evaluation of medical devices. The test accounts for many factors such as cytotoxicity, sensitization, genotoxicity, implantation, hemocompatibility,

degradation and carcinogenicity among several other factors. There is also an important factor to account for in biocompatibility which is the fact that the body could interfere with the functionality of the sensors (This is known as biofouling) [45].

We have set a requirement that all materials used when designing the device to be biocompatible and previously approved by the FDA for medical usage. The reason being that studying and researching new materials to prove its effectiveness in Implantable Medical Devices can be very costly. The ninth factor to consider is **cost**. The biosensor needs to be cost-effective for the platform. The max cost for the device fabrication should not exceed $100 USD assuming the device will be manufactured in a research setting (i.e. not accounting for any economic scale up model).

All of the design and requirements have been summarized in table 2. The pH biosensor designed needs to be able to fall within all the constraints and meet all of the design requirements.

Table 2. pH Biosensor constraints and requirements

Constraint	Description
Max Size	500μm x 500μm x 300μm
pH Sensitivity	±0.01 pH
pH Range	2-9 pH
pH Sensing Variable	$\Delta pH/\Delta T$
Reading Type	Theranostic
Active Life-time	29 Days
Clinical Sensitivity	95%
Accuracy	Variable

Power Constraint	Passive Sensing Preferred (>300mW)
Real Time	>5 min (continuous)
Biocompatible	Abiding by the ISO 10993 Standard/All Materials Need to have been Previously FDA Approved
Sensor's Interface	Contact Pads
Cost	>$100.00 USD

3.0 pH Biosensor Design

In this section, an analysis will be performed to explore what has been done in terms of research and what technology could be adopted for the biosensors. Based on the information collected a new design for the pH sensor will be made to abide by the above-mentioned constraints and requirements.

3.1 BioMEMS, BioSensors and Size

It is important to start the analysis by looking going back to the pH measurement techniques that are used commonly on the market that were outlined earlier. All visual techniques are not viable as the pH biosensor will be implanted inside the body (i.e. remote environment) and thus are not applicable. It may be worthwhile to explore the chemicals used for color indication since the color change is most commonly caused by chemical dissociation at different pK_a's.

The next type of pH sensing mechanism that we outlined before it the utilization of a pH meter. However, the size of pH meter and its electrodes would be a major obstacle to overcome, as most pH meters available on the market are not within the size constraints specified. As a matter of fact, the size constraints identified clearly means that the sensor needs to be microfabricated. The science and technology of operating at the microscale for biological and biomedical applications is called BioMEMS. BioMEMS is an abbreviation for biomedical (or biological) microelectromechanical systems.

It is important as well to identify the different classes of biosensors that can be adopted in BioMEMS. Biosensors are devices that consist of a biological recognition system, called the bioreceptor, and a transducer. The interaction of the analyte with the bioreceptor causes an effect that the transducer can convert into a measurement, such as an electrical signal. The most common bioreceptors used in biosensing are based on antibody–antigen interactions, nucleic acid interactions, enzymatic interactions, cellular interactions, and interactions using biomimetic materials. Common transducer techniques include mechanical detection, electrical detection, and optical detection [46].

32

Optical detection methods are not applicable to what we are trying to achieve and hence will not be considered.

Mechanical detection in bio-MEMS is achieved through micro- and nano-scale cantilevers for stress sensing and mass sensing, or micro- and nano-scale plates or membranes. In stress sensing, the biochemical reaction is performed selectively on one side of the cantilever to cause a change in surface free energy. This results in bending of the cantilever that is measurable either optically (laser reflection into a quadposition detector) or electrically (piezo-resistor at the fixed edge of the cantilever) due to a change in surface stress. In mass sensing, the cantilever vibrates at its resonant frequency as measured electrically or optically. When a biochemical reaction takes place and is captured on the cantilever, the mass of the cantilever changes, as does the resonant frequency. Mass sensing is not as effective in fluids because the minimum detectable mass is much higher in damped mediums, something that is overcome with plates or membranes. The advantage of using cantilever sensors is that there is no need for an optically detectable label on the analyte or bioreceptors [47].

Electrical and electrochemical detection are easily adapted for portability and miniaturization and the most promising for pH sensing. In Amperometric biosensors, an enzyme-catalyzed redox reaction causes a redox electron current that is measured by a working electrode. Amperometric biosensors have been used in bio-MEMS for detection of glucose, galactose, lactose, urea, and cholesterol, as well as for applications in gas detection and DNA hybridization. In potentiometric biosensors, measurements of electric potential at one electrode are made in reference to another electrode. Examples of potentiometric biosensors include ion-sensitive field effect transistors (ISFET), Chemical field-effect transistors (chem-FET), and light-addressable potentiometric sensors (LAPS). In conductometric biosensors, changes in electrical impedance between two electrodes are measured as a result of a biomolecular reaction. Conductive measurements are simple and easy to use because there is no need for a specific reference electrode, and have been used to detect biochemicals, toxins, nucleic acids, and bacterial cells [48].

3.2 ISFET (Ion-Sensitive Field-Effect Transistor)

An ISFET is an ion-sensitive field-effect transistor, that is a field-effect transistor (FET) used for measuring ion concentrations in solution. The ISFET, has been used to measure ions concentrations (H_3O^+) in solutions, causing an interface potential on the gate insulator [49]. Currently, the use of ISFET technology encompasses a wide range of applications in a variety of areas, and those in the biomedical and environmental monitoring areas are particularly noteworthy. In this thesis, the focus will be placed on the basic ISFET design that can be utilized to detect pH. In this section, we will explore the utilization of ISFET as a pH biosensor. The theory behind how it works and its previous utilization In medical technology. We will also explore the utilization of nanowires as a sensing platform for pH The challenges of this approach will also be identified.

3.2.1 ISFET Theory

The ISFET is a type of potentiometric device that operates in a way similar to the way the MOSFET (Metal Oxide Semiconductor Field-Effect Transistor) works. In general, a field-effect transistor (FET) consists of three terminals; the source, drain, and gate. The voltage applied between the source and drain of the FET regulates the current flow in the gate voltage. Specifically, the current-control mechanism is based on the electric field generated by the voltage when it is applied to the gate. The current is also conducted by only one type of carrier (electrons or holes) depending on the type of FET (n-channel or p-channel). A positive voltage applied to the gate causes positive charges (free holes) to be repelled from the region of the substrate under the gate. These positive charges move downwards into the substrate, leaving behind a carrier-depletion region. The depletion region is filled by the bound negative charge associated with the acceptor atoms. These charges are "uncovered" because the neutralizing holes have moved downward into the substrate [50].

The positive gate voltage also pulls negative charges (electrons) from the substrate regions into the channel region. When sufficient electrons are induced under the gate, an induced thin n-channel is in effect created, electrically bridging the source and drain regions. The channel is formed by inverting the substrate surface from p-type to n-type (inversion layer). When a voltage is applied between the drain and source with the created channel, a current flows through this n-channel via the mobile electrons (n-type FET). In the case of a p-type semiconductor, applying a positive gate voltage depletes carriers and reduces the conductance, whereas applying a negative gate voltage leads to an accumulation of carriers and an increase in conductance (the opposite effect occurs in n-type semiconductors). The applied gate voltage generates an electric field which develops in the vertical direction. This field controls the amount of charge in the channel, and thus it determines the conductivity of the channel. The gate voltage applied to accumulate a sufficient number of electrons in the channel for a conducting channel is called the threshold voltage (VTH). Note that VTH for an n-channel (p-channel) FET is positive (negative). With these properties, the FET can be configured as a biosensor by modifying the gate terminal with molecular receptors or ion-selective membranes for the analyte of interest. The binding of a charged biomolecule results in depletion or accumulation of carriers caused by change of electric charges on the gate terminal. A schematic representation comparing a MOSFET and an ISFET can be seen in figure 13.
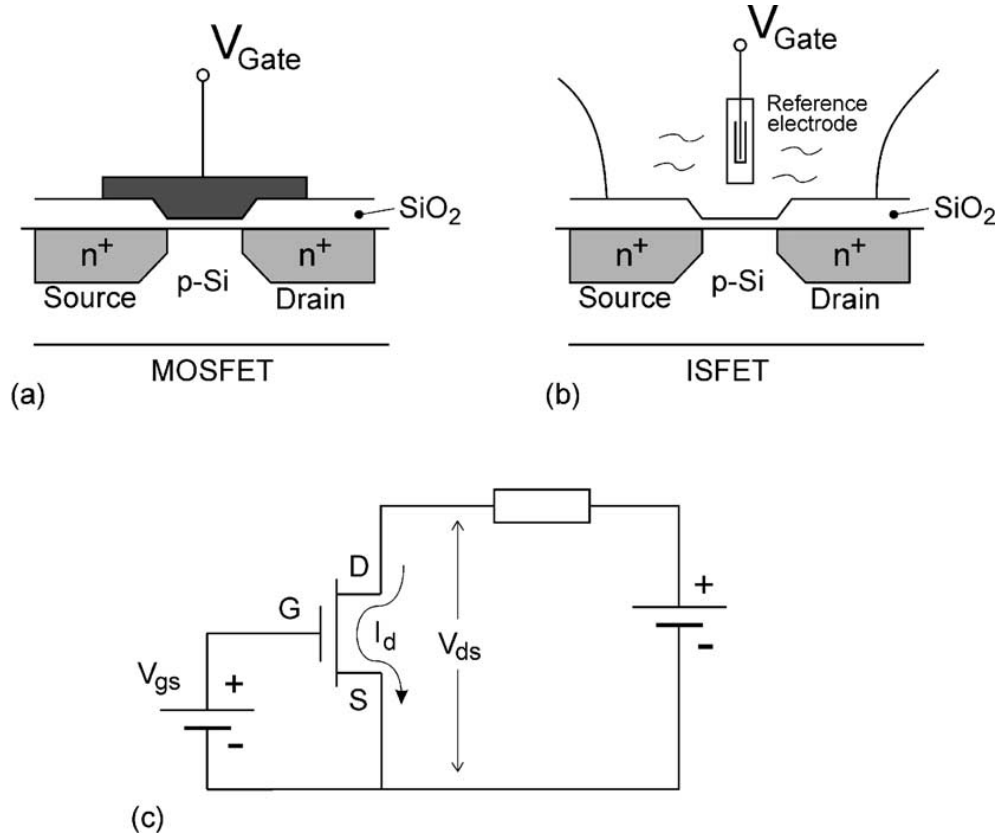
Figure 13. Schematic representation of MOSFET (a), ISFET (b), and electronic diagram (c) [50].

The dependence of the channel conductance on gate voltage makes FETs good candidates for electrical biosensors because the electric field generating from the binding of a charged biomolecule to the gate is analogous to applying a voltage to a gate. In general, the drain current of the FET-type biosensor is defined as follows in equations 6 and 7.

$$I_{Ds} = \frac{1}{2} \times \frac{(\mu C W)}{L}(V_{GS} - T_{TH})^2 \text{ at saturation region } (V_{DS} \geq V_{GS} - V_{TH}) \tag{6}$$

$$I_{Ds} = \frac{1}{2} \times \frac{(\mu C W)}{L}(V_{GS} - T_{TH})V_{DS} - \frac{1}{2}V_{DS}^2 \text{ at triode region } (V_{DS} < V_{GS} - V_{TH}) \tag{7}$$

where μ is the electron mobility in the channel; W and L are the width and the length of the channel, respectively; C is the net gate capacitance per unit area formed by the gate and the channel.

The sensitivity of ISFETs to pH is usually described by the ion-site binding model and the Nernst law. The mechanism responsible for the oxide surface charge can be described by the site-binding model, which describes the equilibrium between the amphoteric SiOH surface sites and the H^+ ions in the solution. The reactions are shown in equations 8 and 9

$$SiOH \leftrightarrow SiO^- + H_b^+ \tag{8}$$

$$SiOH_2^+ \leftrightarrow SiOH + H_B^+ \tag{9}$$

with H_b^+ representing the protons in the bulk of the solution. From these chemical reactions it is clear that an originally neutral surface hydroxyl site can bind a proton from the bulk solution, becoming a positive site as well as donate a proton to the solution, leaving a negative site on the oxide surface. For this reason, it is called an amphoteric site. Amorphous silicon has a high concentration of amphoteric defects, i.e. dangling bonds, already established for bulk a-Si:H [51]. This allows for an increased sensitivity which has been proven experimentally. The theoretical limit according to Nernest equation is 59.2 mV/pH at 298 K. Some reports show nearly Nernstian responses: 54 mV/pH with amorphous silicon ISFETs [52] and 57.3 mV/pH with GaN ISFETs [53]. Supra-Nernstian responses were also reported – 72 mV/pH for hydrogenated diamond ISFET devices [53]. The highest sensitivity has been observed with polycrystalline silicon and a-Si.

3.2.2 ISFET Applications

One distinct merit of the semiconductor-based biosensors like ISFETs, as opposed to optical systems, is their suitability for use in miniaturized measurement systems, thereby allowing its easy integration into the required electronics. In this regard, an ISFET device of small size and low weight might be appropriate for use in a portable monitoring system, i.e., a hand-held drug monitoring system. When it comes to sensitivity and specificity of biosensors, both the fabrication of a nano-scale device and elimination of nonspecific

molecular adsorption would contribute to an improvement in the limit-of-detection (LOD) and selectivity of the biosensor.

Investigators have conducted extensive studies in the electronic analysis of biomolecules by monitoring the variations in the charge density using ISFETs. Currently, various kinds of biorecognition materials for biological analysis such as DNA, proteins, enzymes, and cells are being applied to ISFET measurements owing to the unique electrical and biological properties, thereby elevating the sensitivity and specificity of detection. Among a variety of types of biosensors, one of the most promising approaches and the focus of investigators' concerns is the ISFET-based biosensors and their integration in biological components. In the ISFET system based on different bio-contents for biological analysis, assorted concepts of biosensors like enzyme FETs, Immuno FETs, and DNA FETs that contain layers of immobilized enzymes, antibodies, and DNA strands respectively, have been reported in a large number of documents.

The focus will be placed on the use of the device in devices that interact directly with the human body. We can find an application of ISFETS in its utilization with catheters. Catheter is a thin tube made from medical grade materials serving a broad range of functions. They are medical devices that can be inserted in the body to treat diseases or perform a surgical procedure. By modifying the material or adjusting the way catheters are manufactured, it is possible to tailor catheters for cardiovascular, urological, gastrointestinal, neurovascular, and ophthalmic applications. The pH ISFET chip is very suitable to be built-in in a catheter as has been done by the pacemaker company Cordis in Roden, the Netherlands. The ISFET provided a great advantage where it required no calibration at all after it is released by the manufacturers. This was achieved by incorporating a generating electrode capable of coulometric generation of H^+ or OH^- ions by a specific electrochemical reaction at the electrode. Coulometry was an absolute method of ion generation. Provided that (1) the stoichiometry of the electrode reaction is known, (2) no side reactions occur, and (3) the current efficiency of the electrode reactions is close to 100%, the relation between the number of coulombs applied to the actuator and the amount of generated ions is fixed. Hence, the sensor signal can be adjusted to yield the read-out appropriate to the defined change in concentration by the generated ions [54]. A schematic of

the circuit utilized to detect pH can be seen in figure 14. Based on this information we have identified the applicability and the biocompatibility of the device in the field of implantable medical devices.
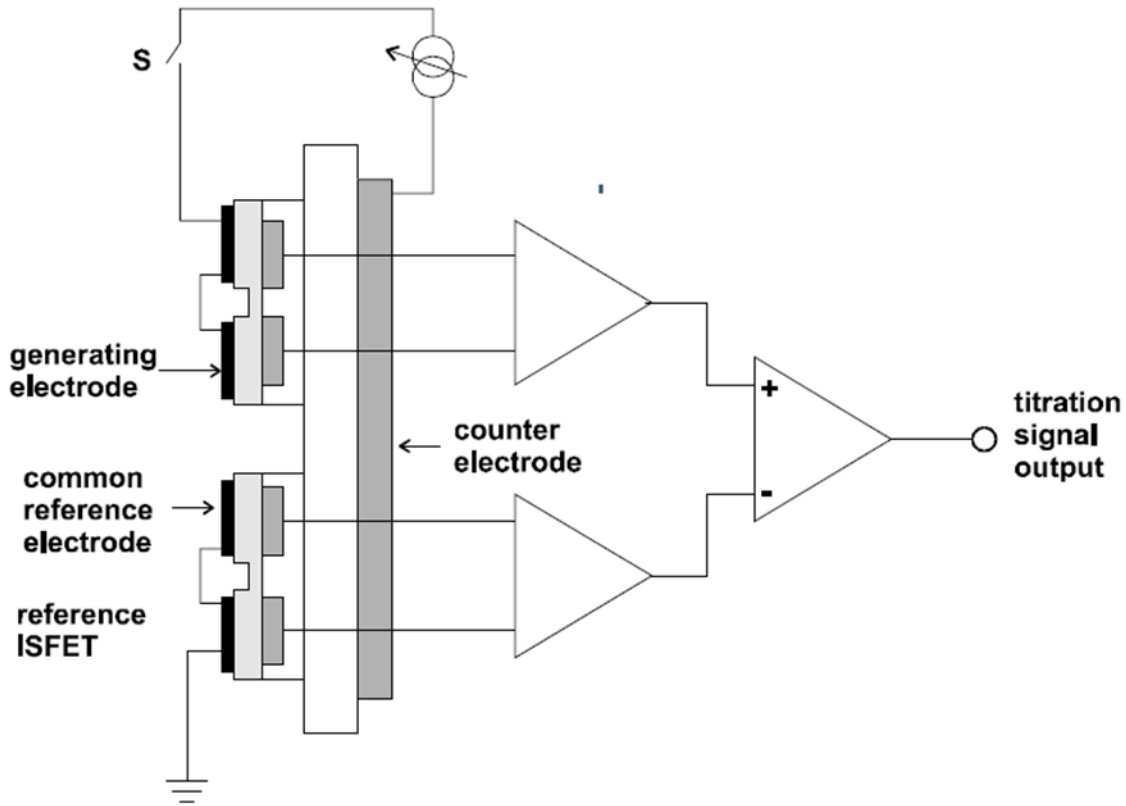
Figure 14. A schematic demonstration of an ISFET that is used on catheters [54].

3.2.3 Nanowire FETs (ISFETS)

The designation 'NanoWire' (NW) can be used to describe an object with a large aspect ratio and a diameter in the range 1–100 nm [54]. A silicon NW (SiNW) solid state FET, whose conductance is modulated by an applied gate, is transformed into a nanosensor by modifying the silicon oxide surface with 3-aminopropyltriethoxysilane (APTES) to provide a surface that can undergo protonation and deprotonation, where changes in the surface charge can chemically gate the SiNW. Linear current (I) versus voltage (V) behavior was observed the SiNW fets, which shows that the SiNW-metal contacts are ohmic, and applied gate voltages produced reproducible and predictable [55].

In figure 15, an illustration of the SiNW device is shown, and the expected signal from the device [56]. Figure 15-A is a Schematic illustrating the conversion of a NWFET into NW nanosensors for pH sensing. The NW is contacted with two electrodes, a source (S) and drain (D), for measuring conductance. Zoom of the APTES-modified SiNW surface illustrating changes in the surface charge state with pH. Figure 15-B graphs the real-time detection of the conductance for an APTES-modified SiNW for pHs from 2 to 9 (The target pH range specified) the pH values are indicated on the conductance plot. (inset, top) Plot of the time-dependent conductance of a SiNW FET as a function of the back-gate voltage. (inset, bottom) Field-emission scanning electron microscopy image of a typical SiNW device. Figure 15-C is a plot of the conductance versus pH; the red points (error bars equal 6 1 SD) are experimental data, and the dashed green line is linear fit through this data. Figure 15-D is the conductance of unmodified SiNW (red) versus pH. The dashed green curve is a plot of the surface charge density for silica as a function of pH [56].
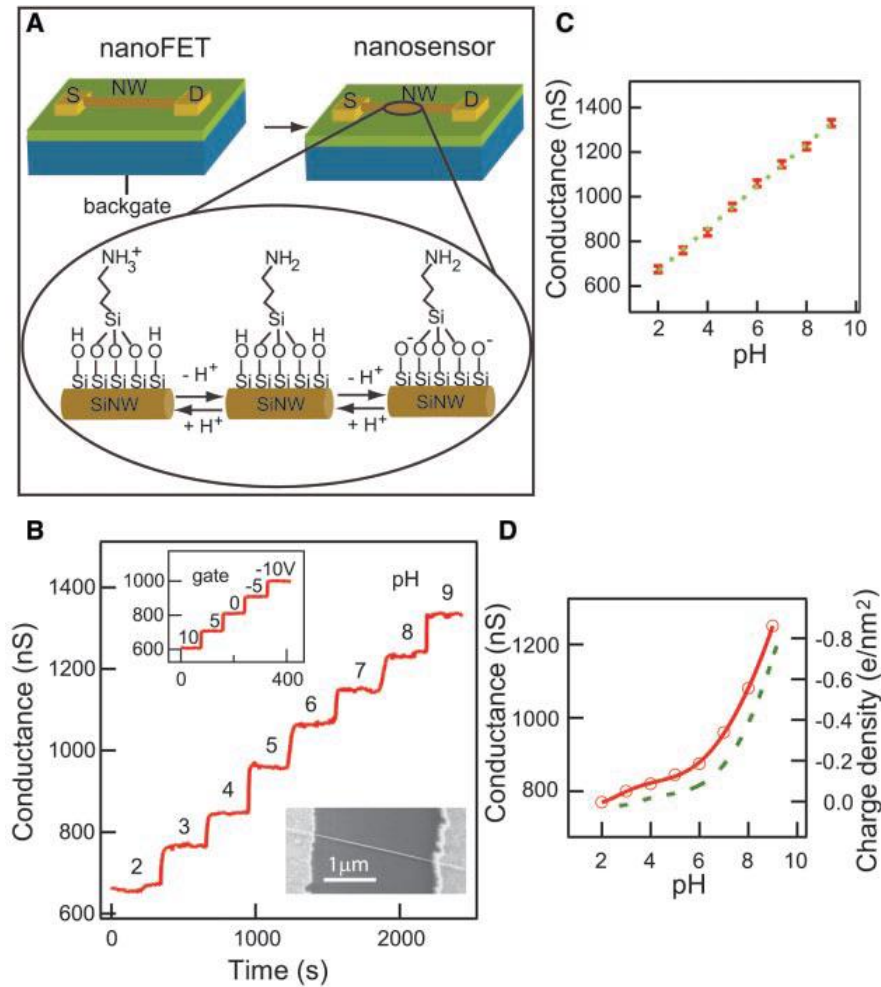
Figure 15. NW nanosensor for pH detection [56].

To fully understand how the technology works it is crucial to analyze what is happening at the surface of the nanowire. Covalently linking APTES to SiNW oxide surface results in a surface terminating in both $-NH_2$ and $-SiOH$ groups which have different dissociation constants, pK_a. At low pH, the $-NH_2$ group is protonated to $-NH_3^+$ and acts as a positive gate, which depletes hole carriers in the p-type SiNW and decreases the conductance. At high pH, $-SiOH$ is deprotonated to $-SiO^-$, which correspondingly causes an increase in conductance. The observed linear response can be attributed to an approximately linear change in the total surface charge density (versus pH) because of the combined acid and base behavior of both surface groups. If the SiNW was unmodified, the conductance measurement would show a nonlinear

pH dependence: The conductance change is small at low pH (2 to 6) but large at high pH range (6 to 9) [56-57].

There are a variety of ways that can be utilized to fabricate SiNW's such as the VLS proves and the template process. For pH sensing, however one of the most optimized fabrication techniques is outlined in figure 16. A Standard (100) SOI wafers (p-type, $15\Omega \cdot cm$) was used as the substrate material. The 100 nm silicon film was thinned to 50 nm, with a 50 nm thick thermal oxide remaining on top to serve as a hard mask. Then active region was formed with conventional lithography and dry etching. Next, Si nanochannel was achieved with e-beam lithography and a 4 nm thick gate oxide was grown at 850 °C . Then, 50 nm thick SiN was deposited by PECVD and patterned to prevent the channel region from the following ion implantation. Arsenic was implanted into the source and drain region and 1000 °C RTA (rapid thermal annealing) for 25 sec was performed to activate the dopants. Using electron beam evaporation and lift-off process, a 250 nm Ag / 20 nm Ti was deposited. Then encapsulation was performed by 2 µm SU-8 over the device so that only the nanochannel region is exposed to liquid environment. Finally, Ag/AgCl pseudo-reference electrodes were fabricated using an electrochemical method where 100 mM KCl solution was dropped on the Ag electrode and was applied at 1 V for 300 seconds [58].
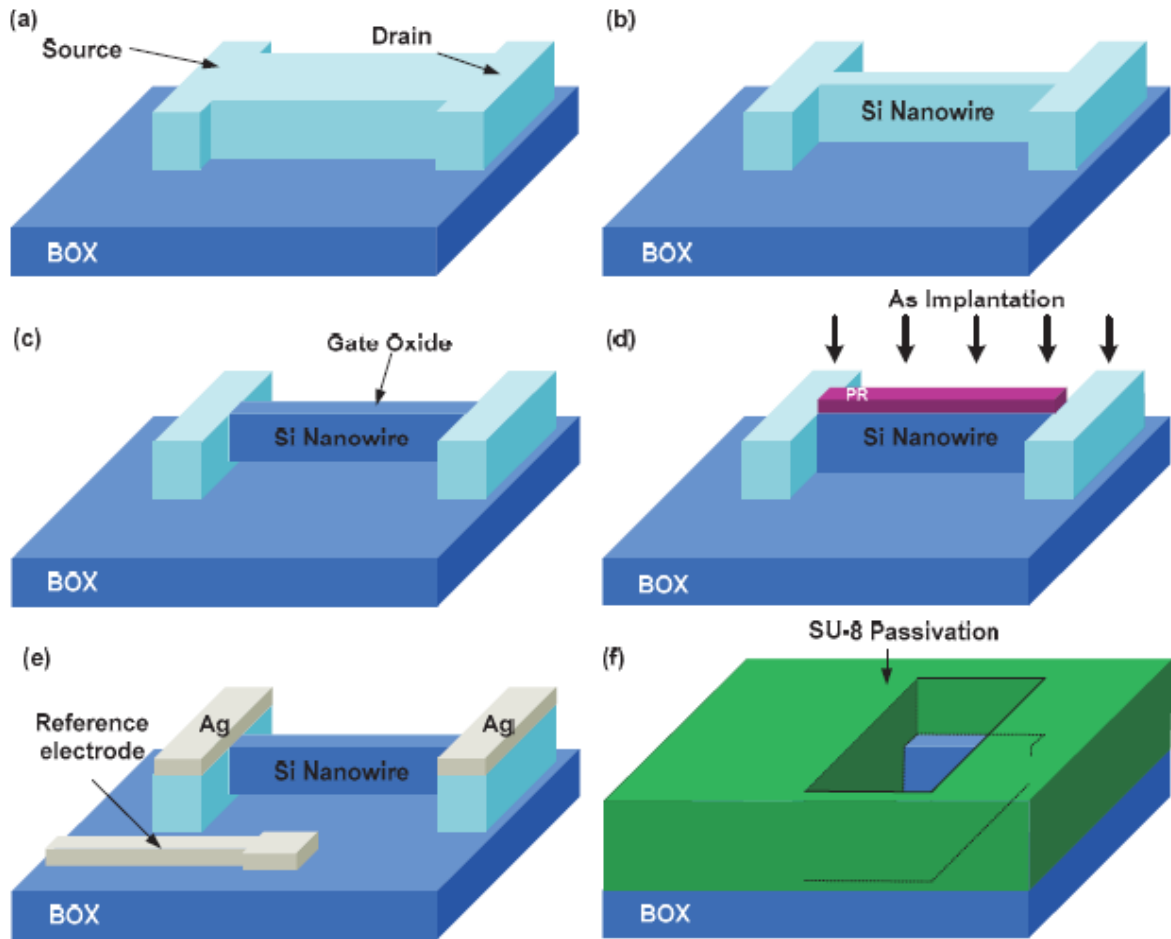
Figure 16. Schematic diagram of Si-NW ISFET fabrication process [58].

3.2.4 ISFET Challenges

An ISFET electrode sensitive to H^+ concentration can be used as a conventional glass electrode to measure the pH of a solution. However, it also requires a reference electrode to operate. If the reference electrode used in contact with the solution is of the AgCl or $HgCl_2$ classical type, it will suffer the same limitations as conventional pH electrodes (junction potential, KCl leak, and glycerol leak in case of gel electrode). A conventional reference electrode can also be bulky and fragile. A too large volume constrained by a classical reference electrode also precludes the miniaturization of the ISFET electrode, a mandatory feature for some biological or in vivo clinical analyses (disposable mini-catheter pH probe). The breakdown of a conventional reference electrode could also make problem in on-line measurements in the pharmaceutical

43

or food industry if highly valuable products are contaminated by electrode debris or toxic chemical compounds at a late production stage and must be discarded for the sake of safety.

For this reason, since more than 40 years many research efforts have been dedicated to on-chip embarked tiny reference field effect transistors (REFET) [49,59]. Their functioning principle, or operating mode, can vary, depending on the electrode producers and are often proprietary and protected by patents. Semi-conductor modified surfaces required for REFET are also not always in thermodynamical equilibrium with the test solution and can be sensitive to aggressive or interfering dissolved species or not well-characterized aging phenomena. This is not a real problem if the electrode can be frequently re-calibrated at regular time interval and is easily maintained during its service life. However, this may be an issue if the electrode has to remain immersed on-line for prolonged period of time, or is inaccessible for particular constraints related to the nature of the measurements itself (geochemical measurements under elevated water pressure in harsh environments or under anoxic or reducing conditions easily disturbed by atmospheric oxygen ingress or pressure changes). A crucial factor for ISFET electrodes, as for conventional glass electrodes, remains thus the reference electrode [60].

In addition, the alkali ion error is an issue that ISFETs have been struggling with for a long time [50]. As we outlined earlier the ionic composition of the peritoneal fluid, the analyte being targeted, has a lot of ions that will build on this error and give false readings.

Another important aspect to consider when looking at the fabrication of ISFET's is the requirement for ion implantation in the fabrication process. Ion implantation is a materials engineering process by which ions of a material are accelerated in an electrical field and impacted into a solid. This process is used to change the physical, chemical, or electrical properties of the solid. The University of Waterloo does not have the equipment to perform this process, and thus the component can not be fabricated in university facilities. It has thus been decided that ISFET's will not be utilized for pH sensing.

3.3 Novel Hydrogel Approaches

In this section, several of the novel approaches seen in research will be outlined alongside some of the concepts that I designed. We will examine first an innovative wound dressing that utilizes a tank circuit to convert the size change of the hydrogel to an electrical signal. Followed by exploring materials that degrade in low pH condition and its utilization in a binary pH circuit. Lastly, a pH sensor utilizes the laminar flow across a microfluidic channel to determine the pH of the fluid flowing through the channel.

3.3.1 Hydrogel-based pH sensor

Hydrogels are cross-linked, three-dimensional polymer networks that have been widely utilized in medical and pharmaceutical applications as well as sanitary products such as wound dressing and diapers as super absorbents [61-62]. Some of the materials swell/de-swell in response to not only the moisture level but also physical and chemical parameters including pH, salinity, temperature, and glucose concentration [63]. Which means that if the hydrogel size changed can be transduced to an electrical signal, it could be used.

MEMS-based sensors that combine passive inductor–capacitor (L–C) resonant tanks with the stimuli-responsive hydrogels for radio-frequency (RF) sensing have been reported [64-65]. This is a very attractive approach for biomedical applications because the passive configuration potentially contributes to making the device low cost and disposable. A major approach to construct the sensors has been to use variable capacitors for the L–C tanks with movable diaphragm electrodes that are actuated by the hydrogels. Since this configuration relies on the deflection of a relatively thin diaphragm against a sealed cavity, there is a potential concern of robustness of the diaphragm and leaks in the cavity seal. In addition, a hydrogel element must be placed outside of the capacitive gap in order to avoid the influence of the variation in electrical properties (e.g., conductivity and dielectric constant) of the liquid to be absorbed. This requirement poses the need for extra structures to hold the hydrogel element, increasing the complexity in the fabrication and construction of the device.

Dr. Takahata from the University of British Columbia devised an approach to detect pH that allows pH to be monitored in wound dressings. He reported a flexible, passive wireless sensor that uses robust variable inductors, eliminating the need for diaphragm/cavity structures in the capacitive approach, with hydrogel elements for biomedical and chemical sensing applications [66]. Figure 17 illustrates the design of the device and its application as a wound dressing.

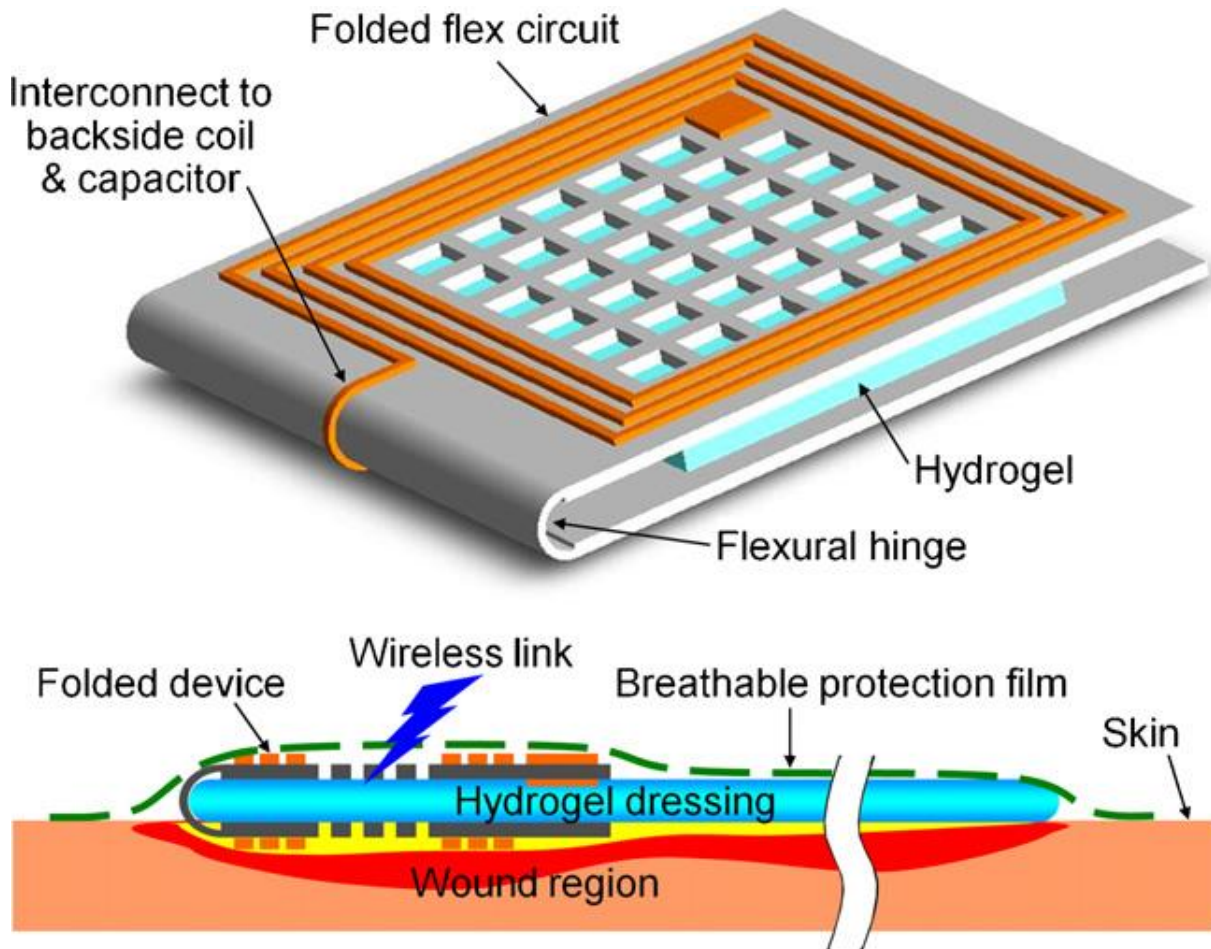Figure 17. The hydrogel-based wireless inductive sensor and its application as a wound dressing [66].

There are several requirements that are not met by this design. First of all the sensor requires specialized equipment to receive the signal other than the one used by current biochip platform. In addition, the sensor size is bigger than the one specified by us. The device does not use contact pads. The sensitivity is not

within the range of ± 0.01 pH. In addition to the complexity of the fabrication and its applicability in terms of integration with the biochip platform.

3.3.2 pH Dependent Degradation

One of the conceptualized design that was very simplistic that was presented, was a method to detect gastric leakage. The method depends on the fact that some polymers can degrade at low pH or the fact that some materials corrode under acidic conditions [67-68]. The basic premise of the device is to connect the power source of the device to the transceiver circuit with a circuit breaker being a polymer that degrades in low pH environments wither due to corrosion or due to polymers degrading in low pH environment. When the polymers degrade and the mix of gastric juice and peritoneal fluid come in contact with the two probes of the circuit, the circuit would reconnect, establishing a connection between the power source, another circuit and the transceiver module. A simple illustration is shown in figure 18 with the grey box representing the pH degradable material. There is a large abundance of materials that degrade in low pH condition that are biocompatible as they are used in oral drug delivery and targeted drug delivery that can be used for this application [69-70].
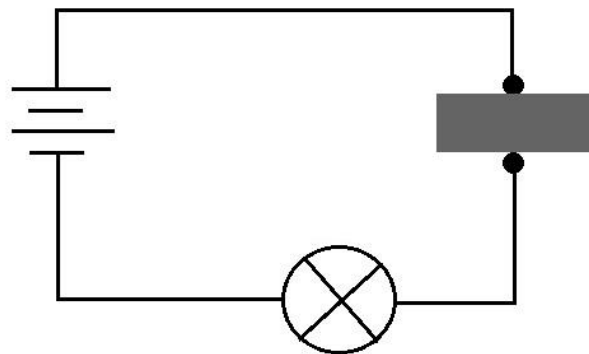

Figure 18. A simplistic schematic of a circuit utilizing the pH degradation properties of materials.

Although this circuit provides a very simplistic signal of whether the pH dropped to the acidic medium or not, it can be used to activate certain components of the device only when a suspected leakage happens. The simplistic nature of this design and its applicability allowed us to utilize this design on the biochip platform.

3.3.3 Time Based Circuit to Measure pH using micro-fluidic channels

This is one of the novel approaches that was conceptualized to be used that would allow pH measurement utilizing the fact that some hydrogels change in size when the pH environment changes. This design has been patented by NERv Technology Inc. [71]. The design utilizes the fact that the follow of fluid across a microfluidic channel is laminar and thus can be calculated and modelled accurately give the fact that the biological environment of the peritoneum is well known. A schematic illustrating the design can be seen in Figure 19.

The basic concept behind the idea is that several microfluidic channels will be setup. The microfluidic channels will be pre-programmed to open up after pre-specified time intervals. This will allow fluid to enter the channel. A circuit has been setup similar to the one shown in Figure 18 at the channel opening. Basically, it registers the time when the fluid first enters the channel. The channel is then blocked with a porous hydrogel that is fully blocking the channel and that has a predetermined thickness. If the polymer is pH sensitive it would react to the pH of the solution and the polymer can be synthesized to shrink under a variety of pH condition and the rate of shrinking can also be pH dependent [72]. The hydrogel would then shrink allowing the fluid to flow from around the gel. The peritoneal fluid would then come in contact with another contact pod. The time between when the fluid came in contact with contact pads at the beginning of the micro channel and the time when the fluid flowed around the first hydrogel can be calculated. The time it took can then be compared to computer simulation or tested models to identify the pH that would correlate with the flow speed of the biological fluid. An example, of a COMSOL model of the fluid flow can be examined in Figure 20 under normal flow conditions.
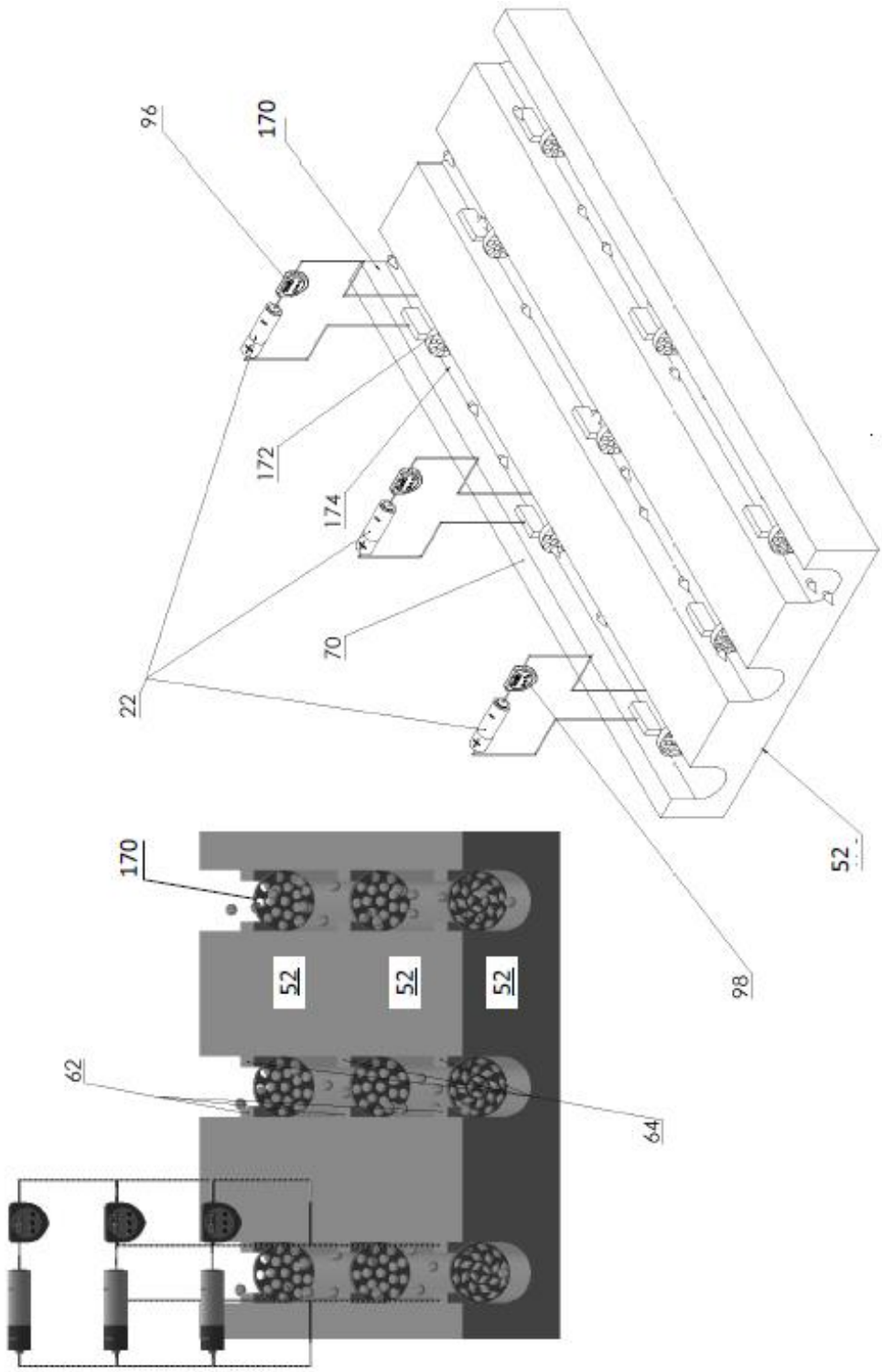
Figure 19. NERv proprietary design for microfluidic analysis [71].
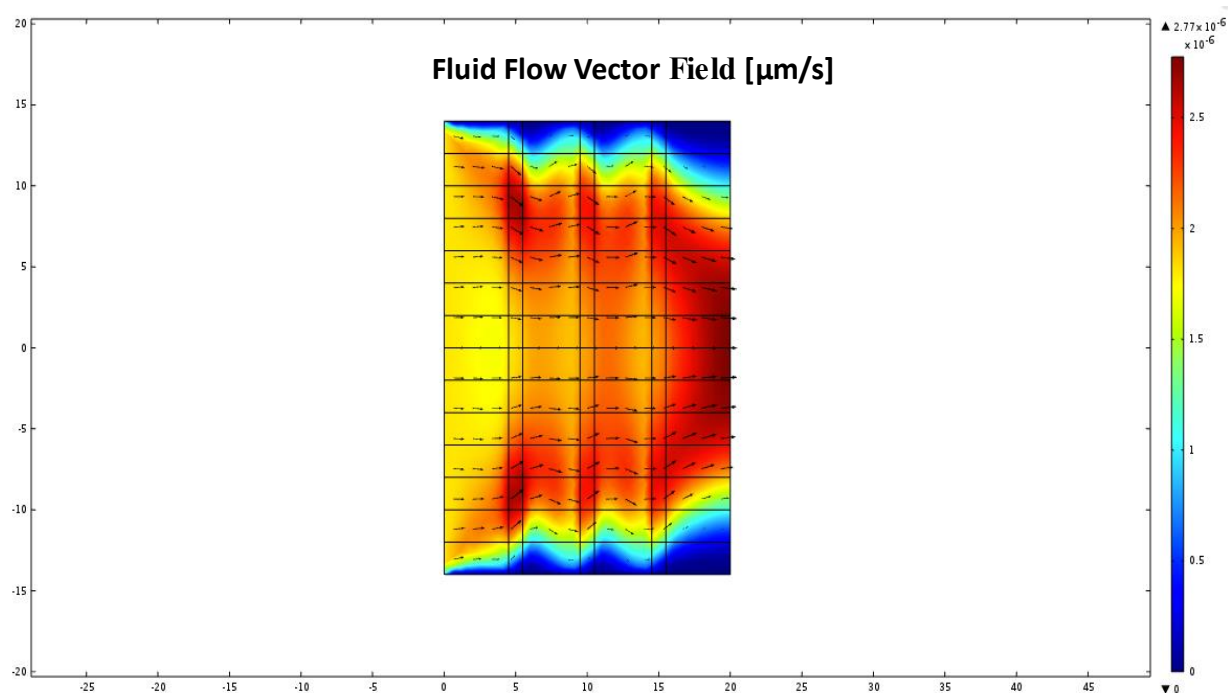
Figure 20. COMSOL model of peritoneal fluid flow across the microfluidic channel

This system has the advantage of being tailorable to pH as well to other biological parameters that can be studied. In addition, the system is simple and does not require many fabrication steps. However, it suffers from the fact that it is not real-time and fluid samples needs to be analyzed periodically. Furthermore, this system is a one-time use (disposable). So once it has been used it cannot be utilized again. In addition to the fact that it requires a new electronic system that is different from the one adopted by our platform currently.

3.4 Electrochemical Nanoparticle Coated pH Sensing Electrodes

In the research literature, there have been seven mechanisms that have been outlined to explain the working principle of electrochemical pH sensors [73-74]. Based on these transduction mechanisms, different configurations of pH sensors were developed. I will just briefly outline the methods that we are most interested in. The first method is H_3O^+ ion exchange in a membrane rich in hydroxyl groups (–OH). It is

the mechanism for conventional glass electrodes. The second method involves a redox equilibrium involving a solid-phase material and H_3O^+ ions, whose hydrogen content can be changed by applying an electrical current, such as conductive polymer-based electrodes. The third method involves changing of the surface potential of a solid-state material due to the pH change of the contacting solution, based on the site dissociation and double-layer models at the solid–liquid interface. Such theory was applied in transistor-based pH sensors. The last is to utilzie variation of electrical properties (such as resistivity) of a material with changes in the pH of the solution.

3.4.1 Potentiometric pH sensing

A typical potentiometric sensor has a two-electrode structure, one electrode being the sensing electrode and the other, the reference electrode with Ag/AgCl is the most commonly used reference electrode in micro-scale pH sensors [75-76]. When both electrodes contact the solution, the electrical potential difference between them is measured to determine the H_3O^+ concentration in solution. Typical potentiometric sensors utilize a three-electrode system. The first electrode is the sensing electrode the second electrode is the counter electrode, and the last electrode is the reference electrode, which is typically a Ag/AgCl electrode. For potentiometric sensors, two possible mechanisms for pH sensing were observed: redox reactions and ion-selective permeation. First, if the material on the sensing electrode has redox reactions with $[H_3O^+]$. Then a potential difference is generated by the free energy change as reversible chemical reactions approaching their equilibrium conditions. Second, if the sensing material acts as an ion-selective membrane, the concentration gradient of ions across the membrane also generates a potential difference. For both cases, the potential can be quantitatively determined by the Nernst equation (Eqn. 4). A simplistic schematic can be seen in Figure 21 describing the general idea behind the potentiometric sensor.
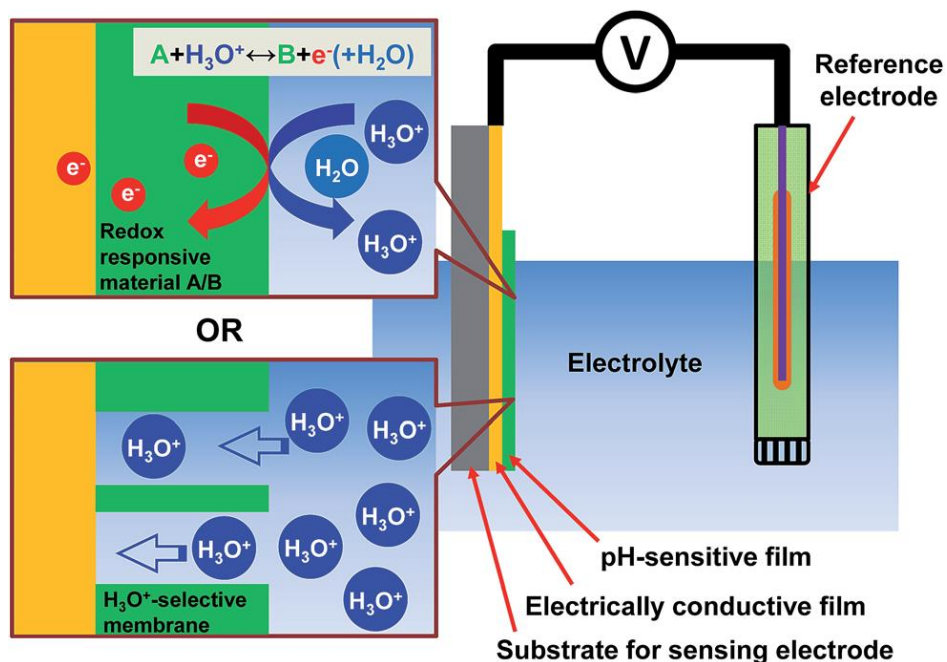
Figure 21. Schematic of a potentiometric pH sensor and its sensing mechanism

The potentiometric configuration is simple when compared to other sensor structures. It only requires two electrodes and no power supply is needed for its operation. Thus, the dimensions of potentiometric sensors can be reduced to the size set forward by the constraints. The potential difference between the sensing and reference electrodes is normally hundreds of millivolts, which can be easily read out by our circuitry. In addition the reported sensitivity and accuracy are in the expected range 0.01 pH [77-78]. The average Nernstian potential reported is 54mV/pH although it is highly dependent on the electrode pairing and the coating material that will be utilized. The methodology covers the expected pH range and is continuous, and the electrodes could interface with the rest of the platform using contact pads. The fabrication process for such technology will also not be very expensive. Several examples of the possible electrodes are listed in Table 3 [77]. This will be the pH sensing method that will be further explored and applied in this research work. Due to the advantages listed above this is the method that will be utilized and explored for our application of pH sensing in Implantable medical devices to detect post-operative complications.

Table 3. pH Electrode pairs for potentiometric pH sensing [77].

Sensitive material	Substrate	Response time, s	Slope mVpH^{-1}	Life span	pH range	-log ($K^{pot}_{H,M}$)
Bulk α and β-PbO$_2$ film	Bulk ceramic electrode	pH <7; 1 pH >7; 30	α; 64.8 β; 57.8	30 d	1.5–12.5	Na$^+$; 12.31 K$^+$; 12.29 Li$^+$; 12.21 Ca^{2+}; 12.58
Bulk IrOx–TiO2	Bulk titanium electrode	120	69.9	–	1–13	Na$^+$; 11.80 K$^+$; 9.66 Li; 11.10
Bulk α and β-PbO$_2$ film	Bulk aluminum electrode	–	α; 57.96 β; 57.80	–	1–12	–
Bulk TiO$_2$ layer	Indium tin oxide (ITO) electrode	40	58.73	–	1–11	–
Bulk SnO$_2$ membrane	Indium tin oxide (ITO) electrode	–	89.17	–	2–12	–
Bulk IrO$_x$ film	Needle-type electrode	5	62	60 d	2–12	–
Bulk CeO$_2$ Film	Screen printed electrode (SPE)	30	51	4 d	5.5–13.2	–
Bulk RuO$_2$ film	Silicon wafer	1	55.64	–	1–13	Na$^+$; 4.43 K$^+$; 5.38
Bulk Gallium nitride (GaN)	Light addressable potentiom- etric sensor (LAPS)	5	52.29	–	2–12	–
Bulk silane derivatives	Coated electrode	3	55	–	–	Na$^+$; 13 K$^+$; 11
Bulk polypyrrole (PPy) films	Bulk electrode	100	54.67	34 d	2–12	–
Fe$_2$O$_3$/carb-on-epoxy composite	Bulk electrode	15	39.7	8 m	1.7–12.2	–
NPs β-PbO$_2$ coat	Thin film microsensor	pH <7; <20 pH >7; <60	84	4 m	0.25–13	Na$^+$; 10.40 K$^+$; 10.50 Li$^+$; 10.47 Ca^{2+}; 11.69

4.0 Fabrication and Material Analysis

In this section, we will start overviewing the fabrication process. Including looking over the fabrication process required to fabricate the electrodes. Experimental setting and setup. Material analysis of the different components that will be used across the design process.

4.1 Substrate

The frequently used term substrate in microelectronics means a flat macroscopic object on which microfabrication processes take place. The most common substrate utilized in microfabrication processes is Silicon [79]. However, to determine the most suitable substrate for this application it is important to look over the requirements.

First of all, the substrate has to be biocompatible. Secondly, the substrate has to be an electrical insulator to isolate the sensing, counter and reference electrodes. In addition, by looking over the application of placing the device on biological tissue it became clear that the substrate must be semi-flexible to allow adherence to a platform that will be placed on non-flat human tissue. The substrate should also be able to withstand harsh chemical and biological conditions. Taking all of these factors into account, Silicon fails to meet several of the requirements. Silicon is a semiconductor, so it can still conduct even if the electrical resistivity is still higher than what is observed in conductors. It is important to note here that Silicon surface can be modified to be an insulator by applying (or growing) a nitride or an oxide layer to the silicon surface. Silicon is also very fragile and could break into several fragments under very little pressure. On the other hand, silicon is biocompatible by itself and in all of its other forms including silicon oxide and silicon nitride. It is important to note however that silicon is considered a second level irritant under FDA regulation and thus can't be used in large amounts for Implantable devices [80-81].

Looking into the literature and the options available two options were identified. The first option being Titanium coated with an oxide layer (TiO_2) [82-83]. Titanium is biocompatible and is the most used

material to be utilized for implants and its oxide is also biocompatible [84]. Titanium isn't very flexible. The second option was polyimide (a polymer of imide monomers). Polyimide materials are lightweight, flexible, resistant to heat, chemicals and biological attacks [85]. Polyimide resin is an acting insulating and passivation layer in the manufacture of digital semiconductor and MEMS chips. The polyimide layers have good mechanical elongation and tensile strength, which also helps the adhesion between the polyimide layers or between polyimide layer and deposited metal layer. The minimum interaction between the gold film and the polyimide film, coupled with high temperature stability of the polyimide film, results in a system that provides reliable insulation when subjected to various types of environmental stresses [85]. Polyimide is also well researched as it is commonly used in a variety of MEMS applications [86-87]. Polyimide is also biocompatible and utilized in applications such as lens drug delievery and skin grafts [88-89]. Lastly, polyimide is a polymer that has no effect on the RF signal produced by the antenna.

For the experiments performed in the sections hereafter, two substrates were utilized. The first substrate was silicon oxide and the second substrate was polyimide. Both wafers were 5-inch wafers. To prepare the Silicon oxide the substrate is first cleaned thoroughly with water, isopropylalcohol (IPA) and acetone for 5 minutes to remove any traces of organic materials. This is then followed by nitrogen blow drying the substrate until no fluid remains on the substrate. For the Silicon oxide wafer the surface was cleaned using oxygen plasma for 60 sec (RF ~13.56 MHz) using the parameters shown in Figure 22. Oxygen plasma refers to any plasma treatment performed while introducing oxygen to the plasma chamber. Oxygen is often used to clean surfaces prior to bonding, deposition or surface treatment [90]. This oxygen plasma cleaning step is utilized to clean the surface of the wafer from any organic material that may have deposited onto the surface of the electrode. For the oxygen plasma cleaning step the Phantom II RIE was used. Polyimide wafers required only water cleaning and nitrogen drying to prepare the wafers.
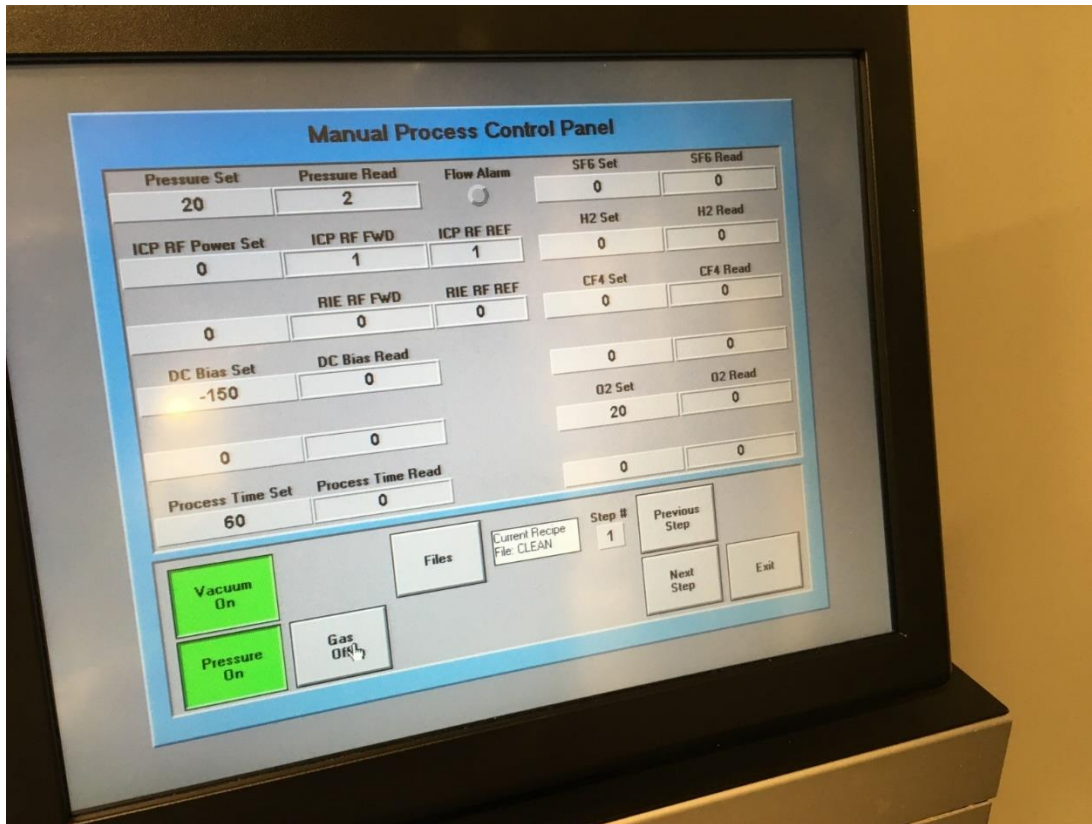
Figure 22. Phantom II RIE setting used for the oxygen plasma cleaning

4.2 Photolithography

Photolithography is a process used in microfabrication to pattern parts of a thin film or the bulk of a substrate. It uses light to transfer a geometric pattern from a photomask to a light-sensitive chemical "photoresist", or simply "resist," on the substrate. A series of chemical treatments then either engraves the exposure pattern into, or enables deposition of a new material in the desired pattern upon, the material underneath the photo resist [79]. Given the size constraint set forward by us there is no need to go beyond photolithography (ex. E-beam lithography) for the patterning as the electrodes could be fabricated at sizes that are above the minimum resolution for photolithography ($\sim 0.5 \mu m$).

To begin the photolithography process it is important to identify the path that will be utilized for depositing the electrodes and the comparison is between two techniques. The first option is to use etching (wet or dry) and the second option is to use lift-off. To illustrate the difference between both methods a graphic

representation of the different steps can be seen in figure 23. Since both of these methods have their advantages and disadvantages both of the methods will be tested in the fabrication of the pH sensor [91-92]. It is to be noted however that for bottom contact electrode which is what is being fabricated in these experiments it is recommended to use the etching method. For top contact, lift-off is usually the recommended method [91]. From this point forward in the thesis I will mainly focus on the lift-off method and the steps presented will be done in the order of how they should be performed if lift-off is the main technique that is going to be utilized. If there are different steps that were followed for the etching method they will be mentioned and clearly outlined.
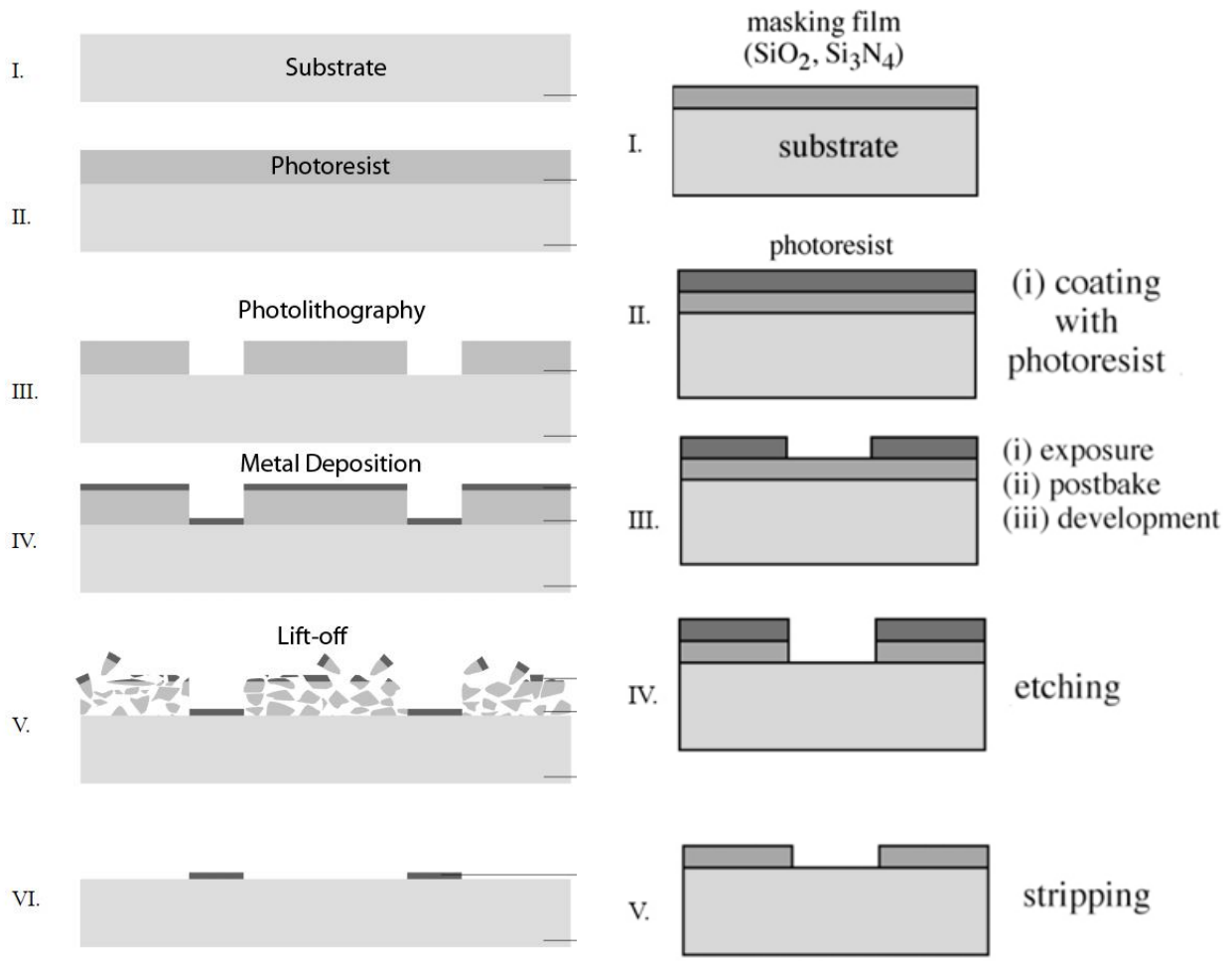

Figure 23. Left: A demonstration of the lift-off process; Right: Demonstration of the etching process.

To perform photolithography, a photomask had to be designed. A photomask is an opaque plate with holes or transparencies that allow light to shine through in a defined pattern. The mask had to allow testing of different electrode structures, configurations, and setups. To maximize the potentiometric signal sensitivity and stability, the highest surface area of interaction between the electrodes has to be maximized as well. The most common design that is used to maximize the surface area of interaction is that of interdigitated electrodes [93]. An image of the designed electrode pair can be seen in Figure 24.
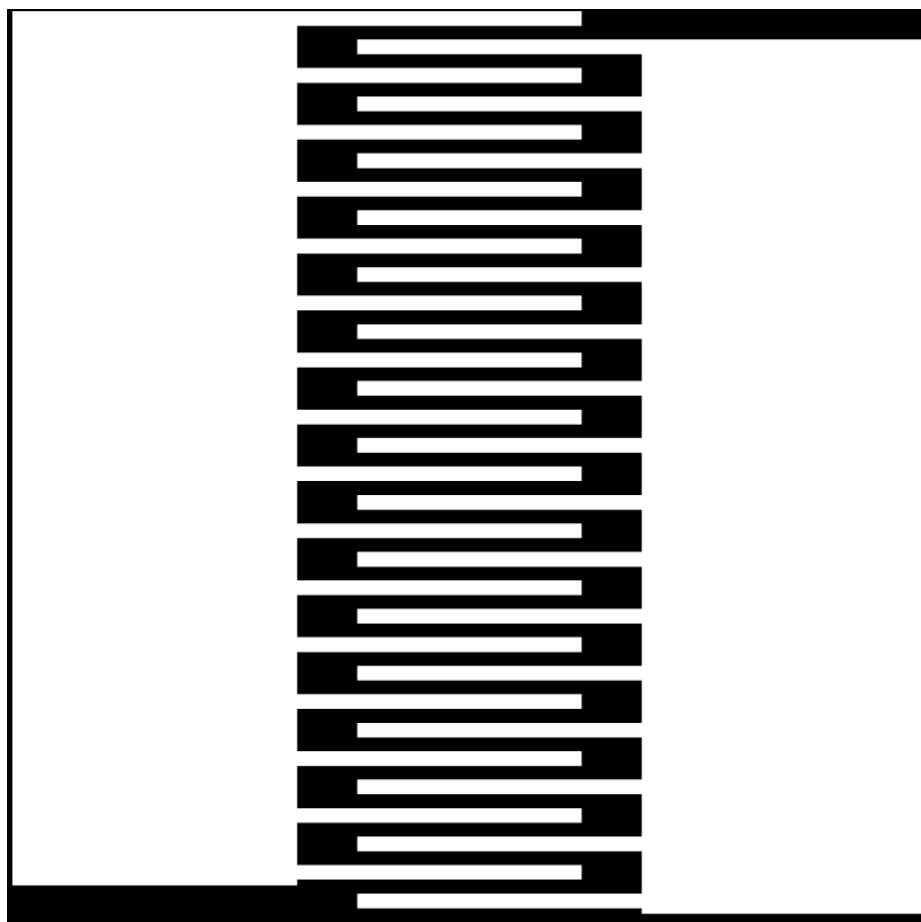
Figure 24. Interdigitated Electrodes used for pH sensing as designed on the photomask.

Different Designs were made to test several factors such as the effect of surface area, the effect of the distance between the electrodes, do the number of digits influence the signal, the optimum electrode dimensions. The electrodes have been designed to have contact pads that would allow for wire bonding and electrical testing. The minimum size of the pads designed was $100 \mu m$ x $100 \mu m$ as per the recommended

58

pad dimension set forward by us. The electrode contact pads allows probing of the electrodes, and it allows bonding of the electrical components to the electrodes. The smallest electrode digit had a minimum width of 3 μm and a minimum length of $9\mu m$.

The mask was also designed to incorporate several other electrode designs, two electrode systems, and three electrode systems. In addition, a design was made to allow measurement of the growth of the coating that will be placed onto the electrodes, NERv logo was also placed onto the mask. A portion of the mask that was designed is shown in figure 25; the dark areas are opaque.

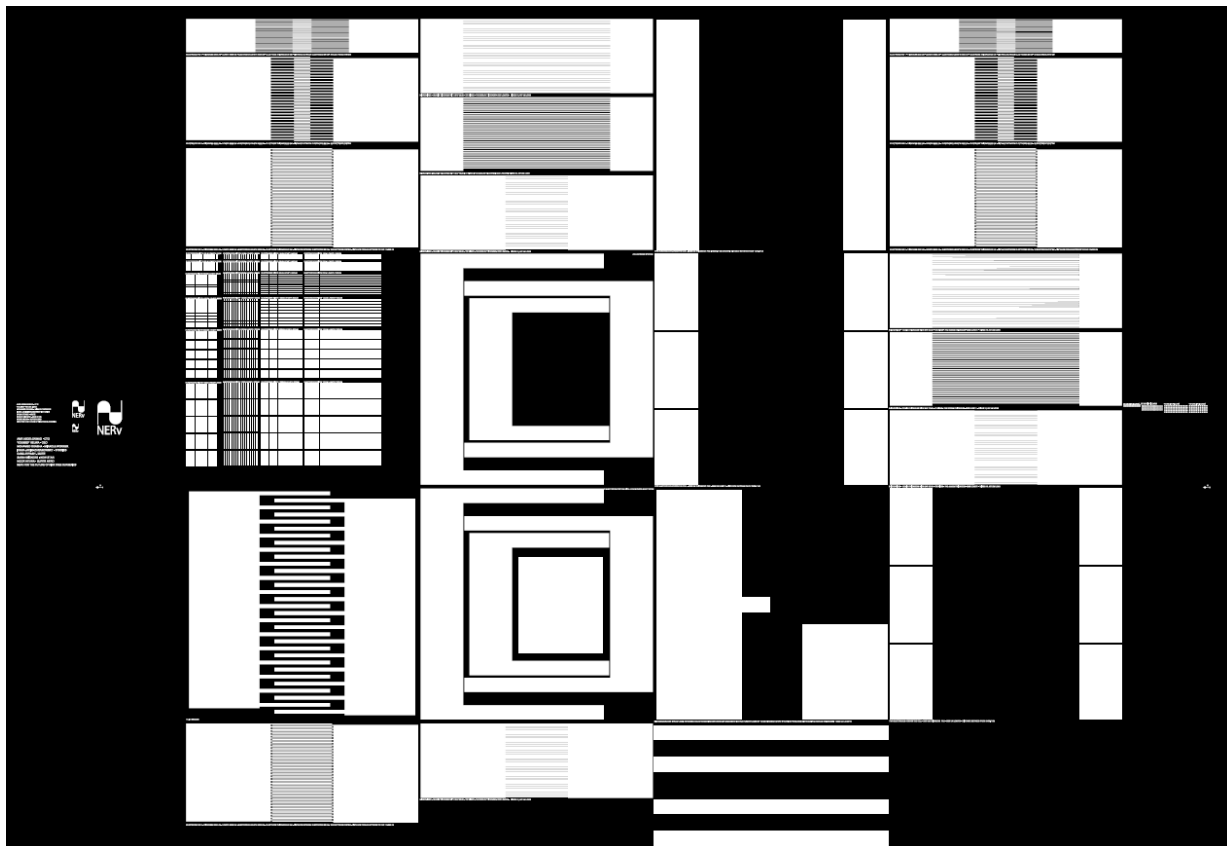Figure 25. A portion of the mask design that was used in the photolithography steps.

After designing the mask, it was sent out for printing. The mask was printed with a dark field polarity and with Right Reading Chrome Down (RRCD) parity. The next step was to apply the photoresist to the substrate. Photoresist is a light-sensitive material used in photolithography to form a patterned coating on

a surface. Photoresist can be either positive or negative. A positive resist is a type of photoresist in which the portion of the photoresist that is exposed to light becomes soluble to the photoresist developer. The unexposed portion of the photoresist remains insoluble to the photoresist developer. A negative photoresist is a type of photoresist in which the portion of the photoresist that is exposed to light becomes insoluble to the photoresist developer. The unexposed portion of the photoresist is dissolved by the photoresist developer [79]. Looking back to Figure 23, if the intention is to use lift-off as the final step, then positive photoresist should be used and if the final step is to do etching; then negative photoresist should be used.

The positive resist that was used in this experiment was AZ 3312 [94]. The photoresist was spun with the following parameters for optimal performance: 500 rpm for 10s followed by 3000 for 30s and then 500rpm for 10s again. One important thing to note is that for the photoresist to adhere to the silicon oxide surface the surface needs to be coated with hexamethyldisilazane (HMDS) by spin coating the chemical at 500 rpm for 10 sec. HMDS is used as an adhesion promoter for photoresist. The expected result following this step is demonstrated in Figure 26. It is important to note that based on the data sheet for AZ 3312 the expected thickness of the photoresist following deposition is ~2.5μm [94].

For the negative phototresist AZ NLOF 5510 was used [95]. The photoresist was spun with the following parameters for optimal performance: 500 rpm for 10s followed by 3000 for 30s and then 500rpm for 10s again (the same parameters as the positive photoresist). The expected thickness of the photoresist layer following spinning is ~1.0μm [95]. Both the positive and the negative photoresist were softbaked at 90°C for 60s following the photoresist coating step.
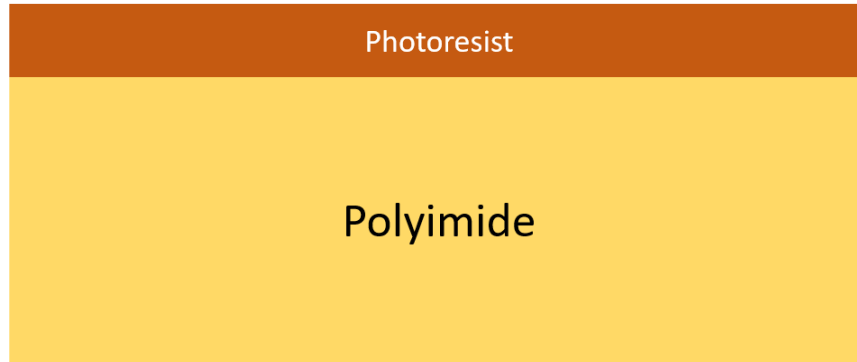
Figure 26. Spin Coating the Photoresist onto the substrate

The next step is perform the photolithography step by exposing the photoresist through the mask. The "Karl suss MA6 mask aligner" was used to align the mask and expose the wafer. The machine supports two different light sources that operate at different spectral lines 436nm (g-line) and 365 nm (i-line). Both of these spectral lines were tested with no difference observed between them in the result as the critical dimension is much larger than the minimum resolution. For optimal exposure results the following parameters were used: the alignment gap was set to be $2.5 \mu m$, the i-line was used, the contact method is soft contact and the exposure time is 8s. Figure 27 illustrates the exposure of the positive photoresist to pattern it.
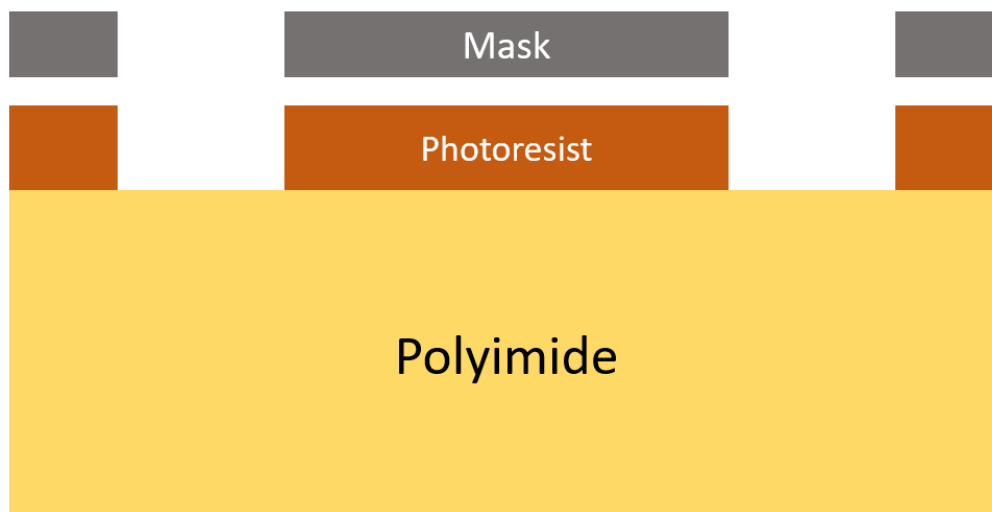
Figure 27. Patterning of the positive photoresist layer through the mask

The sample was then placed in the developer solution following exposure. The developer used in these experiments, for both the positive and negative photoresists, is the AZ 300 MIF developer [96]. The wafer is submerged into the developer until the pattern is clearly visible (~40s). It is important to note that if you are using the negative photoresist, then the sample needs to be hard baked for 90s at 110ºC. The reason the photoresist is not baked in the lift-off procedure is because it will eventually be stripped and thus it is preferable if the layer is soft and easy to strip. Some of the results obtained following the photolithography steps can be observed in Figure 28.

Figure 28. Results obtained following the photolithography steps.

4.3 Electrode Deposition

The next step is to deposit the electrodes. Electron beam evaporation was chosen as the depositing method for the electrodes. Since it permits direct transfer of energy to the source during hea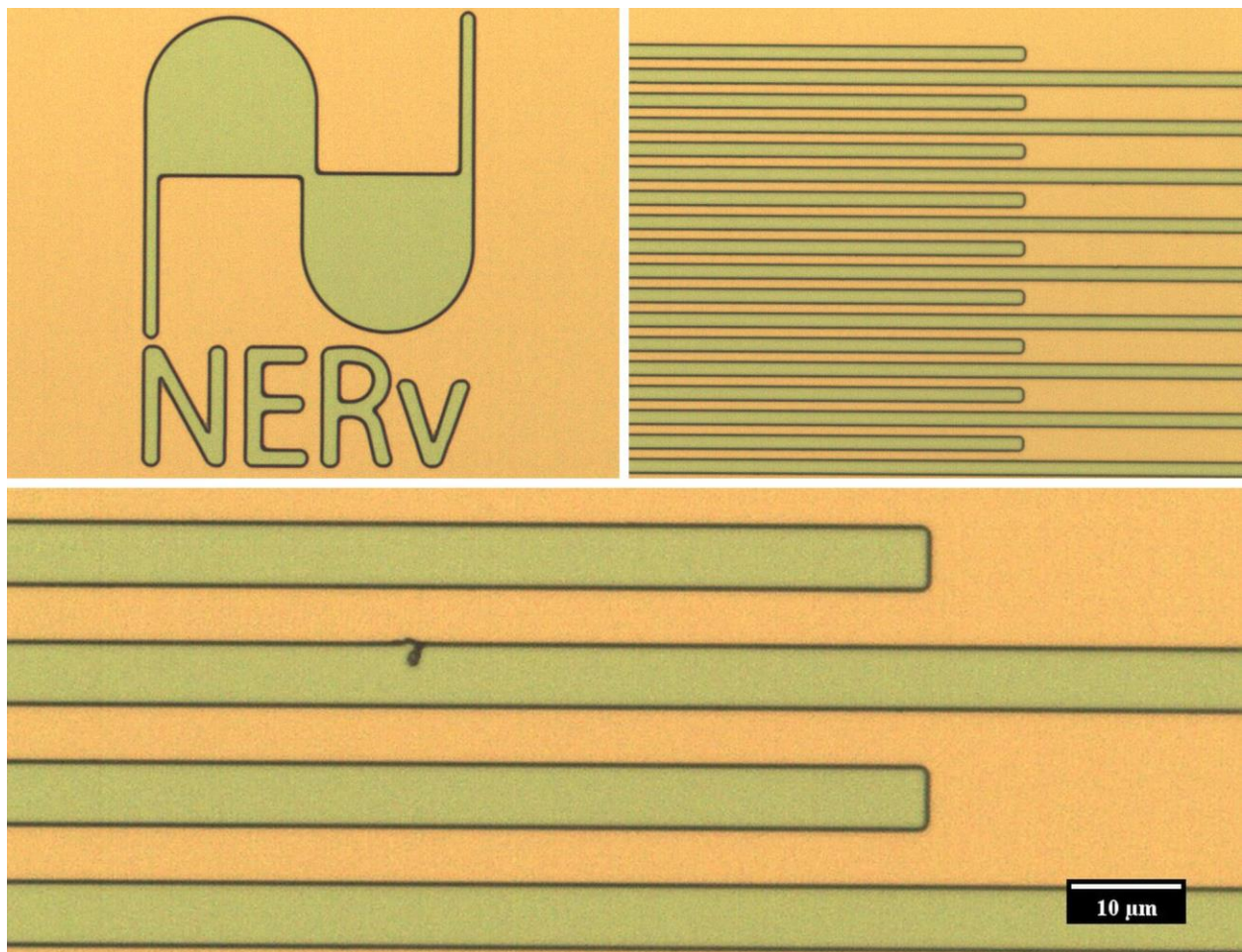ting and very efficient in depositing pure evaporated material to the substrate. In addition, deposition rate in this process can be as low as 1 nm per minute to as high as few micrometers per minute. The material utilization efficiency is high relative to other methods, and the process offers structural and morphological control of films [97].

It is important to determine what material should be utilized for the active electrode. The electrode material should be biocompatible, chemically inert, with good adhesion properties. The electrode material should also be electrically conductive and a material that can be evaporated using e-beam. Based on the analysis that was done for the substrate materials it has identified that Titanium and Gold are the most suitable electrode materials. Gold has the advantage of being completely inert; its disadvantage, however, is that it could be costly given the price requirement that was specified earlier. Titanium, on the other hand, has the advantage of being biocompatible and cost efficient. However its disadvantage is that the oxide layer that would form on the surface of the electrodes could influence the readings [98]. Both materials will be tested and utilized in the experiments.

One experimental conclusion that was observed had to do with the adhesive properties of gold and titanium to both the silicon oxide and the polyimide substrate. Both metals do not properly adhere to the substrate without a transient layer. The transient layer chosen was Chromium as it greatly improves the adhesion properties and it is a bio-compatible material that can be deposited accurately using e-beam. The optimum thickness of the electrodes has been set to be 120nm. This was an experimental conclusion as electrodes that had a thickness that is smaller than 70nm would easily get damaged during probing or under minimal mechanical stress. The layers were designed such that if titanium is being deposited, then 35nm of chromium would be deposited first, followed by 85nm of titanium. While if gold is being deposited then 100nm of chromium would be deposited first followed by 20 nm of gold (this will also decrease the cost of deposition.

The deposition parameters was as follows: The source was first set to be Cr, the rate of deposition was set to be 0.1nm/s, the pressure during deposition was 1×10^{-6}atm. This was then followed by a second deposition of gold or titanium at the same rate and under the same pressure conditions. Figure 29 illustrates the result following this fabrication step when titanium is the metal being deposited.
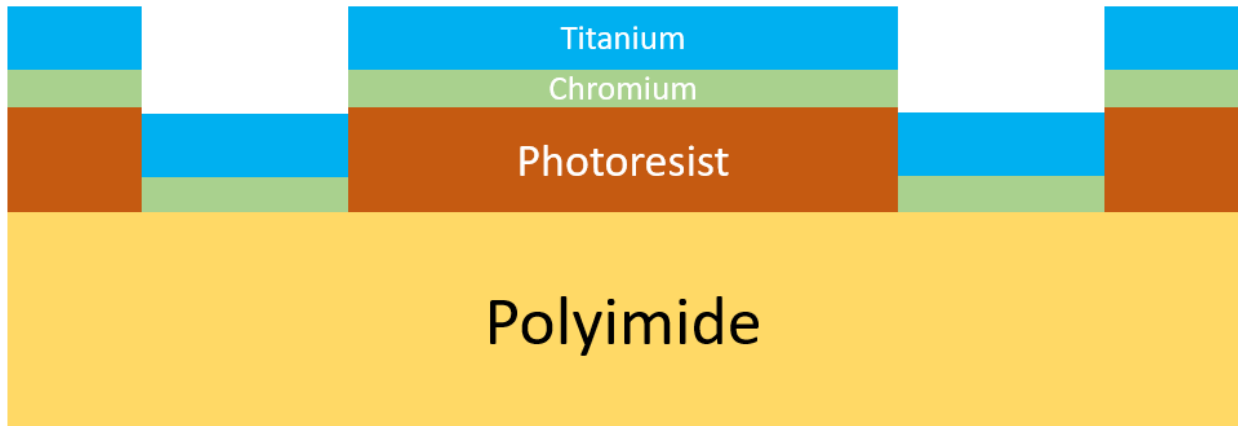

Figure 29. Deposition of the Electrode meals

When performing etching the steps and the ordering is different. To begin with the deposition step is performed before the lithography step. So the materials in order starting from the substrate is polyimide, followed by chromium and then titanium (or gold) and finally the sacrificial photoresist layer. Another deposition step would then be performed to deposit a hard mask (chromium), the purpose of the chromium hard mask is to protect the different components during the wet etching process. Photolithography is then performed to pattern the sacrificial layer. The wafer is then submerged in a titanium etching solution (3% HF), and then the wafer is submerged inside chromium etching solution.

Following the e-beam deposition the electrodes are then ready for lift-off. To perform the lift-off the wafer is dipped into a stripper solution (AZ Kwik Strip has been used)[99]. The wafer is submerged in the solution for 24 hours. This step will be done for both the positive and the negative photoresists. Following that step the wafer is then cleaned for three cycles using acetone and IPA, followed by a 5 min rinse in water. The wafer is then examined. An illustration of the final design is shown in Figure 30. The results obtained from

the fabrication of the electrodes are further shown in Figure 31. Figure 32 shows the wafer following titanium deposition on a silicon oxide substrate
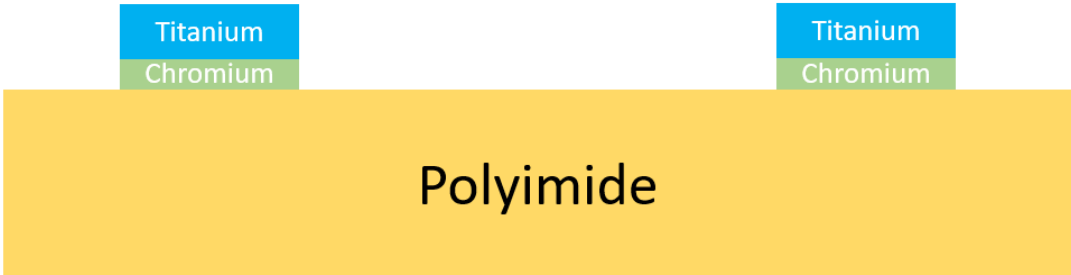
Figure 30. Electrodes after E-beam Deposition illustration
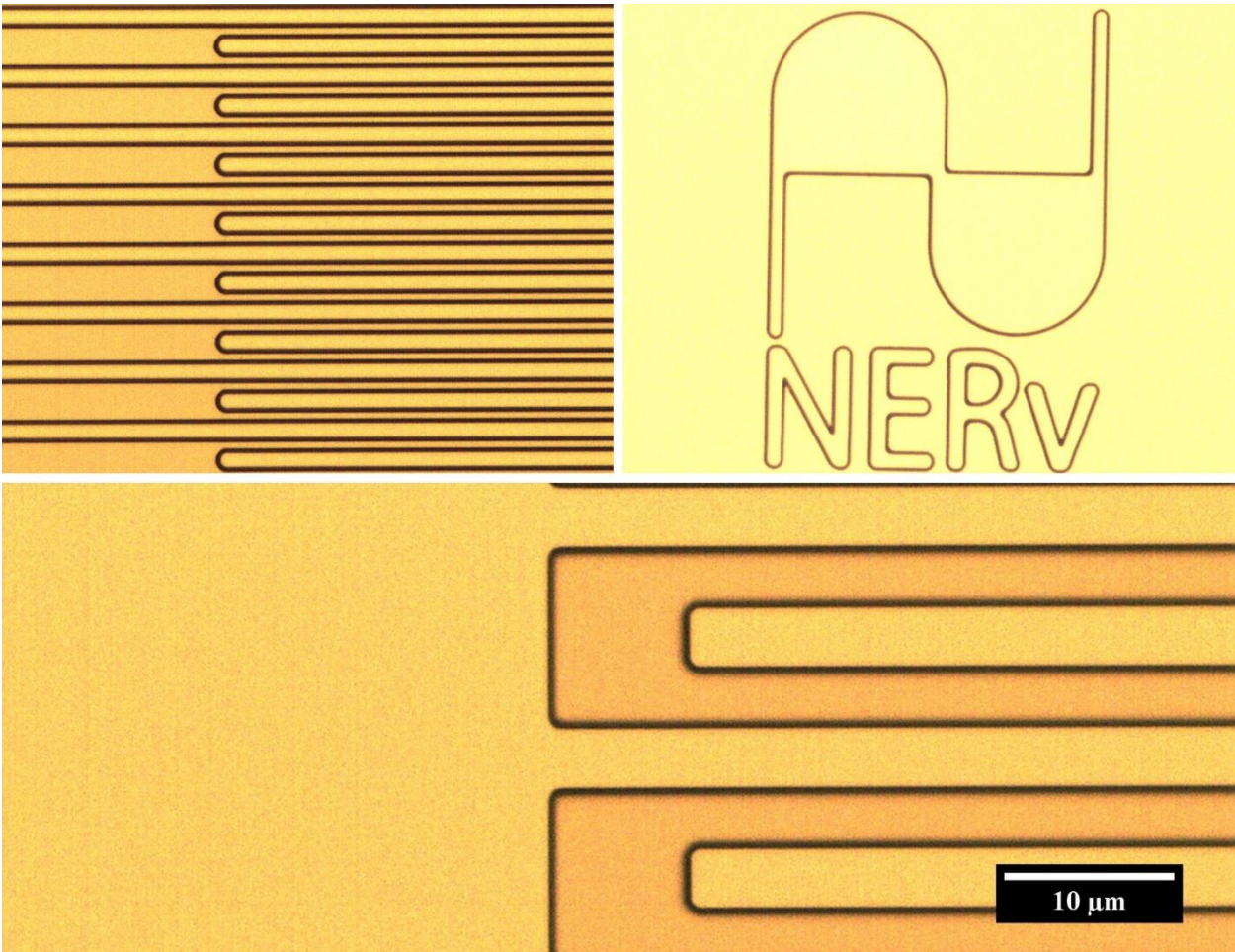
Figure 31. Electrodes after E-beam Deposition
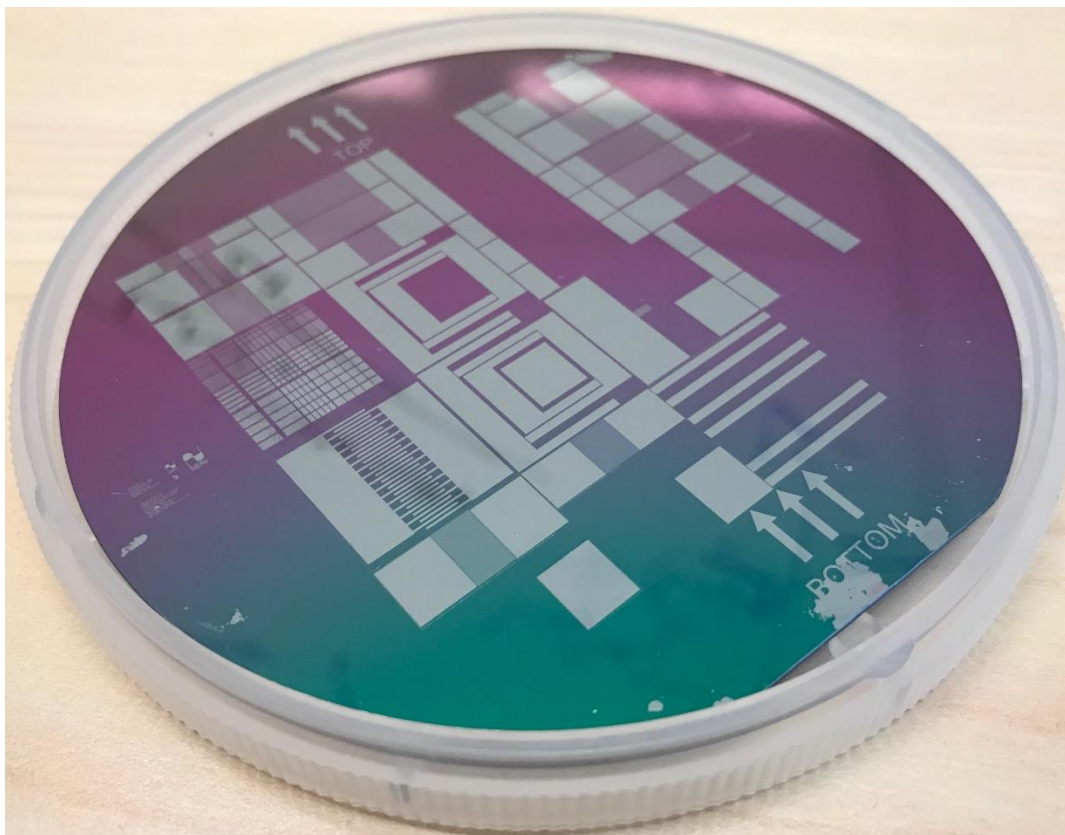
Figure 32. Silicon oxide wafer following electrode deposition of titanium

4.4 Active Layer
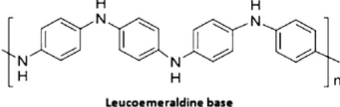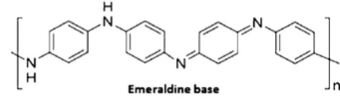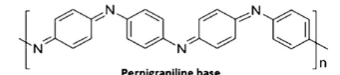
The next aspect of the fabrication of the potentiometric sensor is to deposit an active layer onto the electrode. The main requirement for the active layer is that it has to be biocompatible, conductive and capable of showing Nernstian changes in voltage as the pH changes. Two main polymers have been identified and chosen through literature were Polyurethane (PU) and Polyaniline (PANI) [100-101]. By comparing both polymers, PANI offered one great advantage with that advantage being that PANI can be electro-polymerized onto the electrodes. This means that the contact pads that were initially designed to probe the sample for data is now also suitable to directly grow the pH sensitive polymer directly onto the electrodes.

Polyaniline (PANI) was also chosen as the active material for the electrodes as it displays super-Nernstian potential, it is a biocompatible material, it can be made to be porous increasing the surface area of the active electrode, its properties can be easily controlled by changing the condition for polymerizing the material and most importantly is it is a conductive polymer. At different pH values, the PANI will be protonated or deprotonated. This will lead to a change in charge density at the interface of the PANI film/solution. Polyaniline can be produced through the anodic or chemical oxidation of aniline monomer. The electrochemical polymerization of aniline may be represented with a general stoichiometry shown in equation 10 in which electrons are extracted from aniline by the anode during electrolysis.

$$\text{n } C_6H_5\text{—}NH_2 = \text{—}(C_6H_4\text{—}NH)_n\text{—} + 2nH^+ + 2ne \qquad (10)$$

PANI can take different forms with different properties, which depends on the oxidation state of the polymer. The oxidative polymerization of aniline in an acid produces the protonated, partially oxidized form of the polymer, which has been shown to be the most conductive form of the polymer (Emeraldine). A table summarizing the different forms of PANI and their properties is shown in Table 4. The next step is to actively grow the active emeraldine PANI layer onto the active electrode of the device while making sure that it does not come in contact with the counter electrode.

Table 4. Different Forms of PANI and their properties

	Oxidation States	Color	Conductive	Other info	Structure
Leucoemeraldine	fully reduced form	Transparent	Non-conductive	Can be formed by the reduction of ES. This can be transformed to EB (blue non-conducting Emeraldine by the addition of an alkali).	Leucoemeraldine base
Emeraldine	partially-oxidized	Emeraldine Base-Blue	EB- Non-conductive	Only conducting form of PANI is Emeraldine Salt and is obtained by the doping or protonation of the emeraldine base EB -doping/protonation	Emeraldine base
		Emeraldine Salt-Green	ES- Conductive		
Pernigraniline	Fully oxidized	Dark blue	Non-conductive	Formed by further oxidation of the PANI-ES to a fully oxidized dark blue pernigraniline salt.	Pernigraniline base

Polyaniline was deposited by using either potentiodynamic (sweeping the potential) or potentiostatic (constant potential) techniques. Cyclic potential deposition produces films with better morphology, conductivity, and structural integrity [102]. Polyaniline was first polymerized at the macro level on gold electrodes. This was done utilizing cyclic voltammetry (CV). To electro-polymerize the emeraldine form of PANI using CV the polymerization process has to be performed in an bronsted acidic medium. To begin the polymerization process, an aniline solution is prepared containing 0.1M aniline and 0.5M sulfuric acid (H_2SO_4). Nitrogen is then bubbled through the solution for three hours. The monomer solution has now been prepared. For the potentiostat CV setting the cycles are set to sweep between -0.1V and 8V at a rate of 50mV/s with a Ag/AgCl reference electrode and a Platinum counter electrode. Polyaniline then is observed to be growing onto the gold electrode at the macro level. Figure 33 showcases the CV curves that outline PANI growth and it shows PANI growing on gold electrodes. Deep green Emeraldine can be seen on the surface of gold indicating emeraldine base. Looking at the cyclic voltammogram curves, we observe three redox couples. The first redox couple (A) corresponds to the transition of Leucoemeraldine Base to Emeraldine Base. The second redox couple (B) corresponds to degradation of Impurities. The third redox couple (C) corresponds to the Emeraldine Salto to Pernigraniline Base transition.
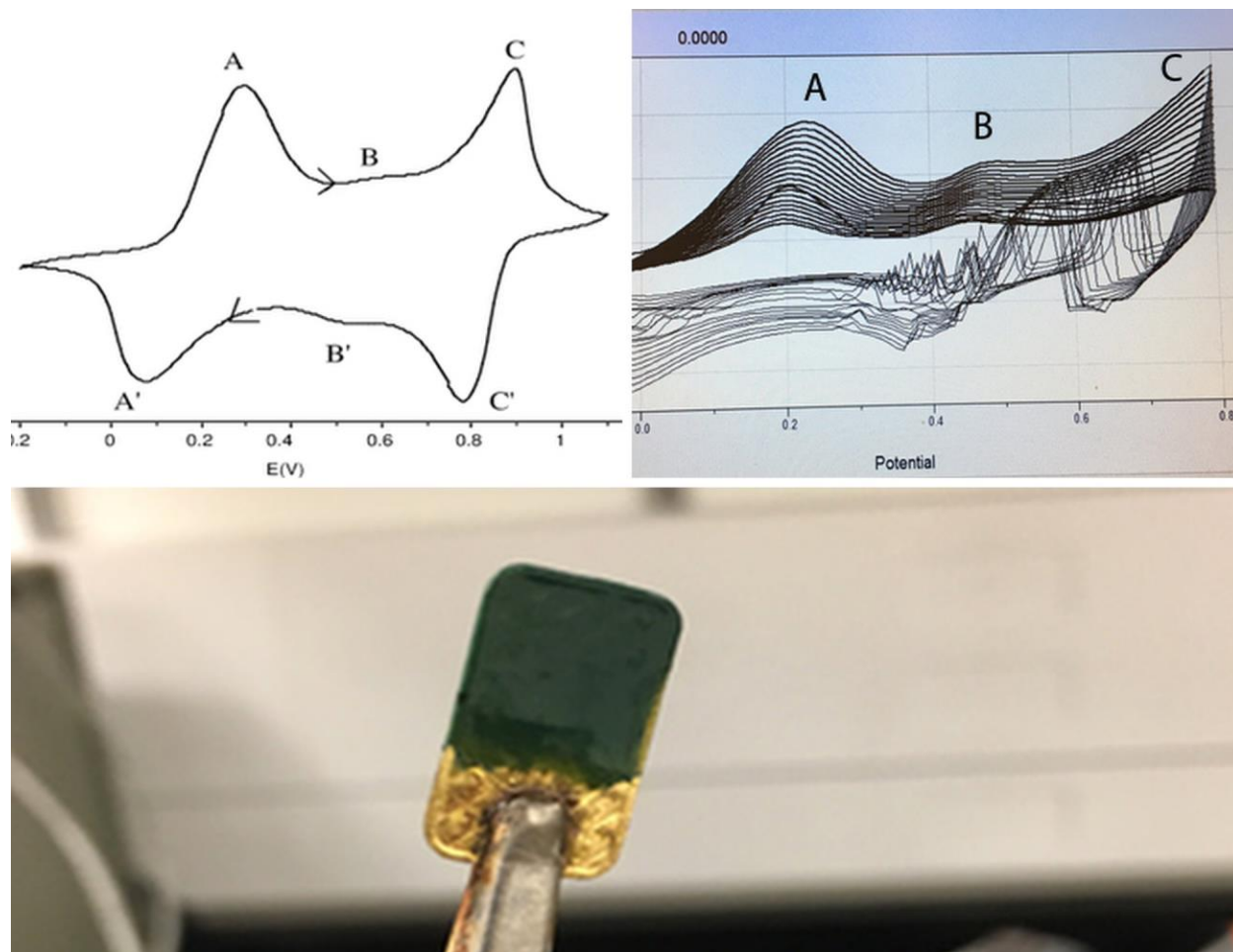
Figure 33. PANI CV grow and growth on macro electrode.

It was observed that by controlling the number of cycles (sweeps), the thickness of the polyaniline layer could be controlled. Based on the electro-polymerization method applied at the macro scale the technique was applied on the interdigitated electrodes. It is to be noted though that the rate of the growth of PANI has to be monitored and controlled since if the PANI does come in contact with the counter electrode the system will no longer work as the circuit would short (PANI is conductive). An illustration of the result is shown in Figure 34 and some of the results obtained are shown in Figure 35.

Figure 34. PANI electropolymerized onto the active electrode.
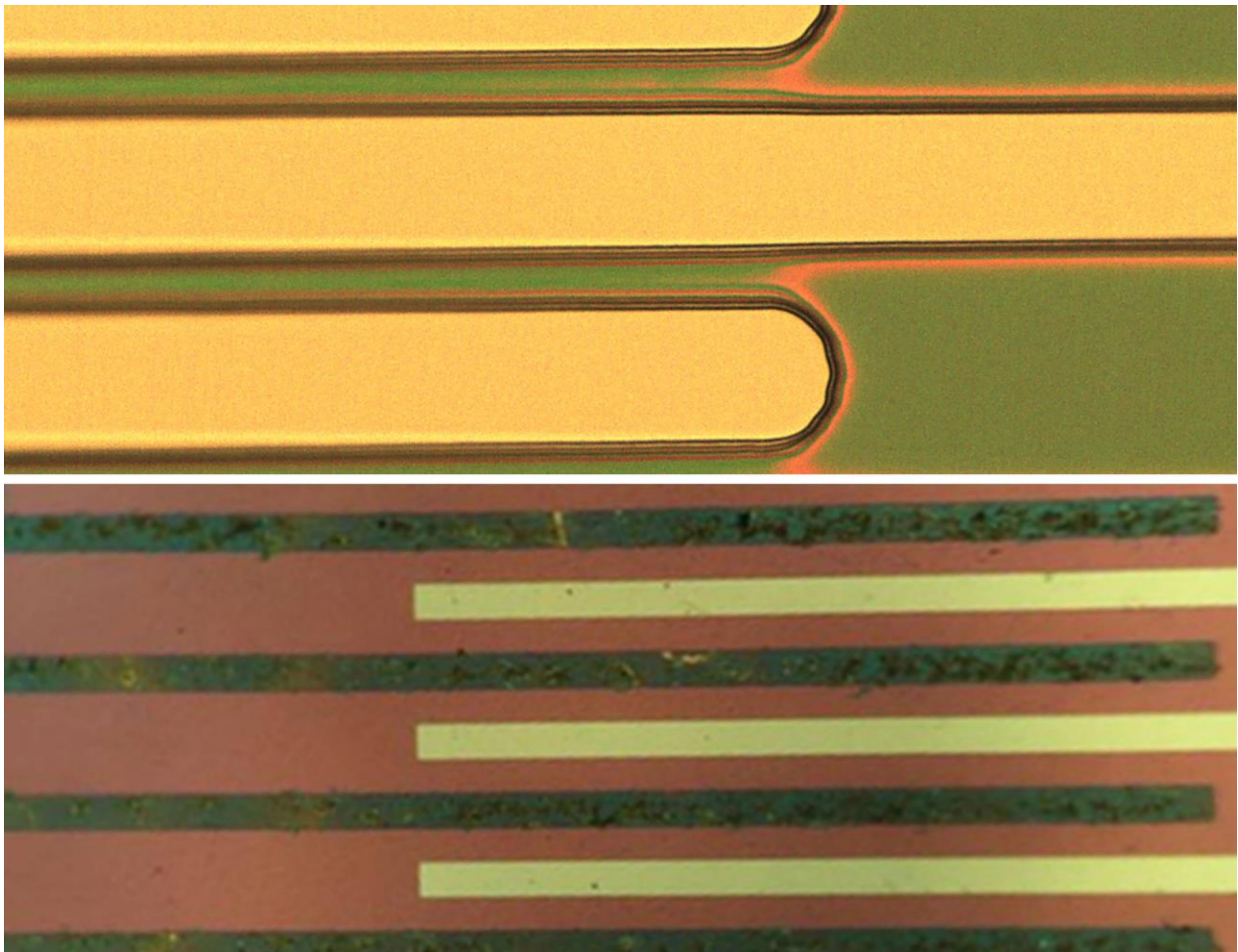
Figure 35. PANI polymerized onto the active electrode

When using the three electrode system for sensing it important to fabricate the reference electrode. Again following similar steps as those used to deposit the active and the counter electrodes an electrode made of silver is deposited (120nm) onto the polyimide substrate. To apply a layer of AgCl on top of the Ag electrode, the chip is dipped in a solution containing concentrated KCL solution (100mM). Then a voltage of 1V is applied to the electrode for 300 seconds creating a 20nm layer of AgCl on top of the electrode [103].

5.0 Results and Conclusion

In this section, we will overview some of the testing that was performed and the results obtained. Conclusions will be provided based on the results. Finally, future steps will be outlined for the project and the means of integration would be explained.

5.1 Results

The sensor pads were wire bonded to our sensing system to test the effectiveness of the pH sensor. To perform the tests, however, we wanted the pH solutions that were being tested to resemble the fluids that were naturally occurring inside the body. A simulated set of bodily fluids was made to represent peritoneal fluid and gastric juice [104]. Peritoneal fluid was simulated according to Table 5 and gastric juice was simulated according to Table 6.

Table 5. Composition of Simulated Peritoneal Fluid

REAGENT	1 L OF SIMULATED PERITONEAL FLUID
SODIUM CHLORIDE	8.035 g
SODIUM BICARBONATE	0.355 g
POTASSIUM CHLORIDE	0.225 g
POTASSIUM PHOSPHATE DIBASIC TRIHYDRATE	0.231 g
MAGNESIUM CHLORIDE HEXAHYDRATE	0.311 g
1 M HYDROCHLORIC ACID	39 mL
CALCIUM CHLORIDE	0.292 g
SODIUM SULFATE	0.072 g
TRIS(HYDROXYMETHYL) AMINOMETHANE	6.118 g
PH	7.4

Table 6. Composition of Simulated Gastric Juice

REAGENT	1 L OF SIMULATED GASTRIC JUICE
SODIUM TAUROCHOLATE (MM)	80 μM
LECITHIN (MM)	20 μM
SODIUM CHLORIDE	8.035 g
SODIUM BICARBONATE	0.355 g
POTASSIUM CHLORIDE	0.225 g
POTASSIUM PHOSPHATE DIBASIC TRIHYDRATE	0.231 g
PEPSIN (MG/ML)	0.1 mg/mL
SODIUM CHLORIDE (MM)	34.2 mM
HYDROCHLORIC ACID	0.08 M
PH	1.45

After simulating both biological fluids, the next step is to test the system using the peritoneal fluid. Then the gastric juice is titrated into the solution for testing in the range between pH 2 and pH 7.5. For all pH's in the alkali region above 7.5 pH a potassium hydroxide was titrated into the solution to test the different pH. The results of the experiment are shown in figure 36. The main things to notice is that the Nernstian potential shown is 67mV/pH, which is slightly below the Nernstian response seen in the literature (74 mV/pH) [76-79]. However, the most important factor to consider is whether this system would allow measurements of pH changes that are on the order of 0.01 pH. To determine the answer to this question the electrical team had to determine the minimum resolution that could be detected using the platform. Based on the data provided it was determined that the circuit can analyze changes in voltage on the range of 0.05 mV. The pH system was tested in tandem with the circuitry system and changes in pH of $\pm$0.005pH were measurable!
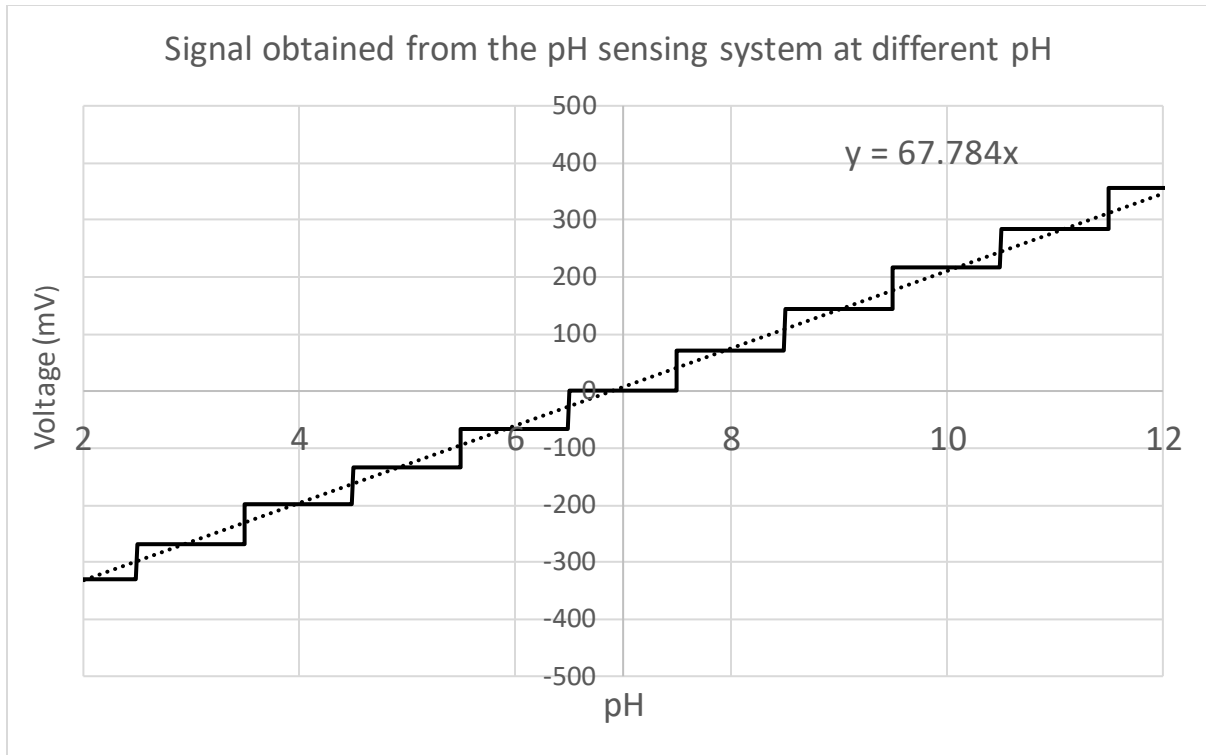
Figure 36. Signal obtained from the pH sensing system at different pH

The next thing to test was the lifetime of the sensor, i.e. does it remain active for the four weeks period in which the patient could develop post operative complications. To perform this test, five pH sensors were fabricated and then PANI was polymerized onto the electrodes at five different time points with a week difference between them. What was observed was interesting. When the sensors were placed in air in between tests, the polymer on the sensor would dry up causing the active material to stop working two weeks following the initial polymerization. However, the peritoneum is covered in peritoneal fluid. This means that the PANI will not dry. An environment was simulated similar to that found in the peritoneum by first simulating the biological fluid and then a mannequin was used to model the fluid build-up inside the peritoneum. This setup can be observed in figure 37. The results showed the sensor could remain active for weeks following the surgery while still maintaining the sensitivity of the electrodes.
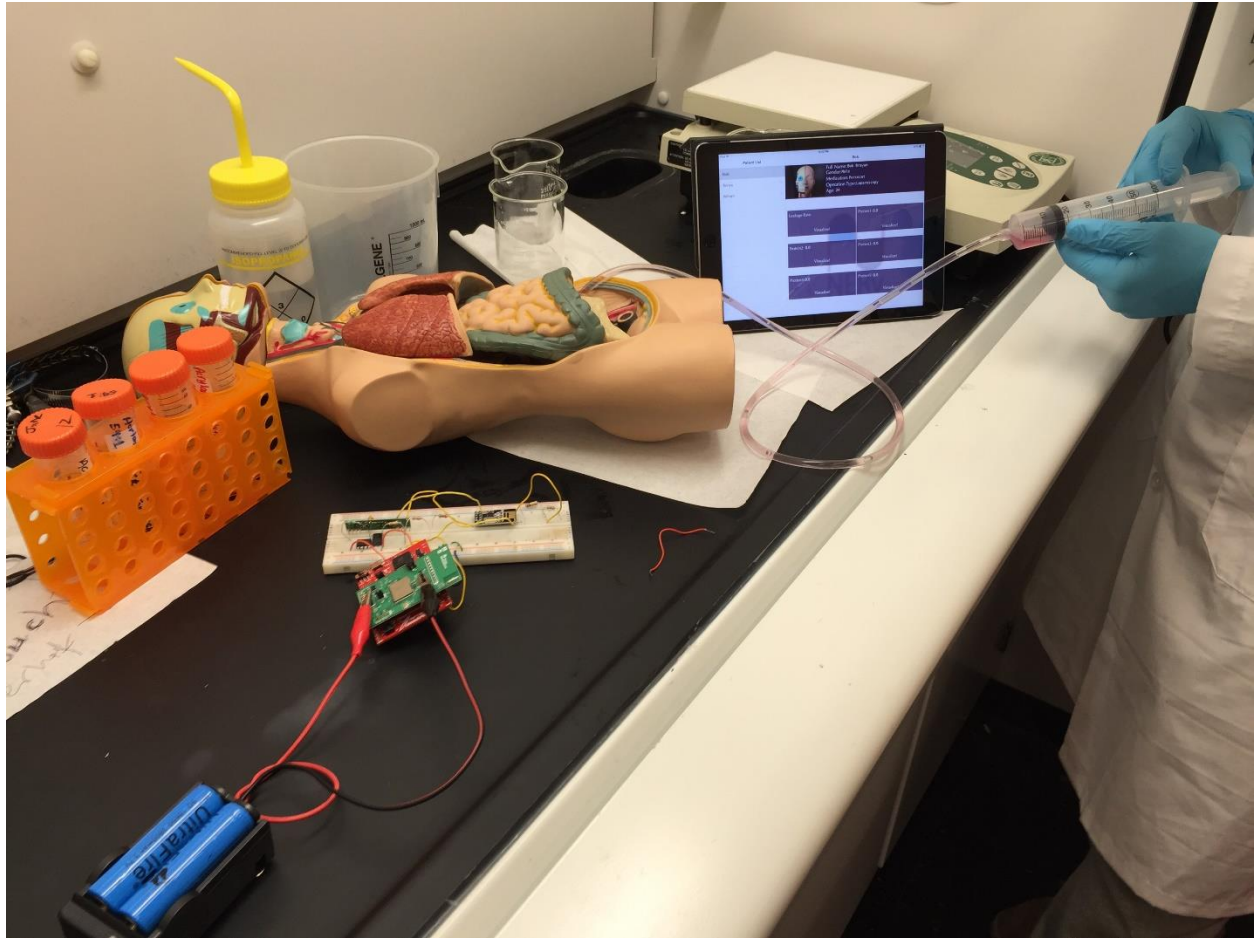
Figure 37. The setup used to test the pH sensor

Looking back at the previously outlined requirements it is clear that almost all of the requirements and constraints have been met and achieved. The sensor has been fabricated on an area of 200μm x 200 μm x 200nm and it has been fabricated on this scale in the research medium. The sensor could be further militarized to cover an area of 100 μm x 100 μm. This means that we can afford to utilize multiple pH sensors and collect multiple arrays of data. This demonstrates that even if one pair of electrodes do fail for any reason we can afford to incorporate at least three more sensors to collect data from and compare the date obtained to omit outliers.

The electrode pair systems utilize contact pads allowing probing of the electrodes. All of the materials utilized have been identified to be biocompatible and have been utilized in a variety of medical application.

The sensors are passive and utilize almost no power other than that utilized by our electronic system. An engineering model has been devised based on the different designs proposed the research work done. This design is shown in Figure 38.
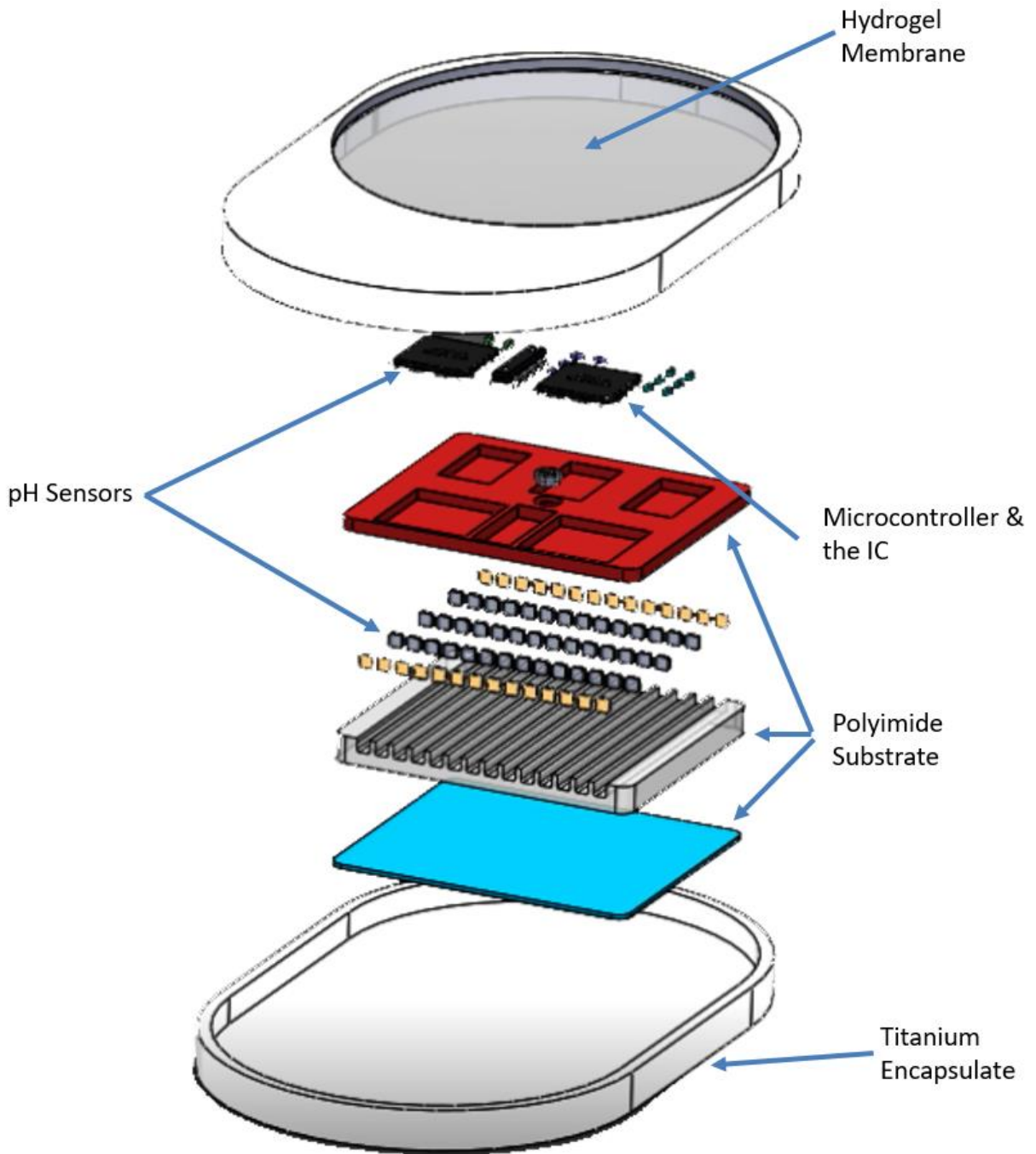
Figure 38. Proposed Design for our Biochip

5.2 Conclusion

In conclusion, a correlation has been identified between a number of post-operative complications and pH changes inside the body. It has been identified that monitoring pH changes of the peritoneal in real time would allow early intervention to help save the patient. Electrochemical pH monitoring systems were determined to be the best method of monitoring pH changes. An electrode system capable of monitoring changes in pH was fabricated. The system fabricated is capable of monitoring pH in real-time for implantable medical devices. All material utilized are FDA approved and have been used in different fields of medicine. The electrodes were deposited using e-beam deposition and patterned using photolithography. Reference electrodes were deposited and modified chemically to be Ag/AgCl electrodes. The active layer of PANI was electropolymerized onto the active electrode. The system of electrodes demonstrated a Nernstian potential capable of detecting variations in pH for up to five weeks that is stable and the pH system has a resolution of 0.05pH.

References

[1]   E. Sadot and H. Spivak, "Weight Loss After Laparoscopic Band-to-Bypass Revision Compared With Primary Gastric Bypass", Surgical Laparoscopy, Endoscopy & Percutaneous Techniques, vol. 25, no. 3, pp. 258-261, 2015.

[2]   T. Jakobson, J. Karjagin, L. Vipp, M. Padar, A. Parik, L. Starkopf, H. Kern, O. Tammik and J. Starkopf, "Postoperative complications and mortality after major gastrointestinal surgery", Medicina, vol. 50, no. 2, pp. 111-117, 2014.

[3]   N. Hirst, J. Tiernan, P. Millner and D. Jayne, "Systematic review of methods to predict and detect anastomotic leakage in colorectal surgery", Colorectal Disease, vol. 16, no. 2, pp. 95-109, 2014.

[4]   P. Jestin, L. Påhlman and U. Gunnarsson, "Risk factors for anastomotic leakage after rectal cancer surgery: a case-control study", Colorectal Disease, vol. 10, no. 7, pp. 715-721, 2008.

[5]   A. Rickert, F. Willeke, P. Kienle and S. Post, "Management and outcome of anastomotic leakage after colonic surgery", Colorectal Disease, vol. 12, no. 10, pp. e216-e223, 2009.

[6]   G. Brisinda, S. Vanella, F. Cadeddu and P. Mazzeo, "Colonic Anastomotic Leak: Risk Factors, Diagnosis, and Treatment", Journal of the American College of Surgeons, vol. 208, no. 6, pp. 1152-1153, 2009.

[7]   M. Lipska, I. Bissett, B. Parry and A. Merrie, "Anastomotic leakage after lower gastrointestinal anastomosis: men are at a higher risk", ANZ Journal of Surgery, vol. 76, no. 7, pp. 579-585, 2006.

[8]   C. Bertelsen, A. Andreasen, T. JÃ¸rgensen and H. Harling, "Anastomotic leakage after anterior resection for rectal cancer: risk factors", Colorectal Disease, vol. 12, no. 1, pp. 37-43, 2010.

[9]   N. Hyman, "Managing anastomotic leaks from intestinal anastomoses", The Surgeon, vol. 7, no. 1, pp. 31-35, 2009.

[10]   M. den Dulk, S. Noter, E. Hendriks, M. Brouwers, C. van der Vlies, R. Oostenbroek, A. Menon, W. Steup and C. van de Velde, "Improved diagnosis and treatment of anastomotic leakage after colorectal surgery", European Journal of Surgical Oncology (EJSO), vol. 35, no. 4, pp. 420-426, 2009.

[11]   B. Piraino, "Peritoneal infections", Advances in Renal Replacement Therapy, vol. 7, no. 4, pp. 280-288, 2000.

[12]   R. Sawyer, M. Spengler, R. Adams and T. Pruett, "The Peritoneal Environment During Infection", Annals of Surgery, vol. 213, no. 3, pp. 253-260, 1991.

[13]   P. Jain, "Spontaneous bacterial peritonitis: Few additional points", World Journal of Gastroenterology, vol. 15, no. 45, p. 5754, 2009.

[14]   D. Margolis, J. Berlin and B. Strom, "Which venous leg ulcers will heal with limb compression bandages?", The American Journal of Medicine, vol. 109, no. 1, pp. 15-19, 2000.

[15]   T. Dargaville, B. Farrugia, J. Broadbent, S. Pace, Z. Upton and N. Voelcker, "Sensors and imaging for wound healing: A review", Biosensors and Bioelectronics, vol. 41, pp. 30-42, 2013.

[16]   G. Galeotti, "Dilatometrische Untersuchungen bei einigen synthetischen Prozessen", Zeitschrift für Physikalische Chemie, vol. 80, no. 1, 1912.

[17]   W. Haynes, T. Bruno and D. Lide, CRC handbook of chemistry and physics. [Boca Raton, Florida]: CRC Press, 2015.

[18]   The accuracy of determination of the pH of river waters. Stevenage/Medmenham/Swindon: WRC, 1984.

[19]   R. Reis, A. Costa and B. Conde, "Pleural adenosine deaminase in the diagnostic workup of tuberculous pleural effusion", Revista Portuguesa de Pneumologia (English Edition), vol. 20, no. 4, pp. 228-229, 2014.

[20]   V. Khutoryanskiy, "Supramolecular materials: Longer and safer gastric residence", Nature Materials, vol. 14, no. 10, pp. 963-964, 2015.

[21]   H. Jacobsen, B. Nergard, B. Leifsson, S. Frederiksen, E. Agajahni, M. Ekelund, J. Hedenbro and H. Gislason, "Management of suspected anastomotic leak after bariatric laparoscopic Roux-en-y gastric bypass", British Journal of Surgery, vol. 101, no. 4, pp. 417-423, 2014.

[22]   J. Zhou, T. Tun, S. Hong, J. Mercer-Chalmers, M. Laabei, A. Young and A. Jenkins, "Development of a prototype wound dressing technology which can detect and report colonization by pathogenic bacteria", Biosensors and Bioelectronics, vol. 30, no. 1, pp. 67-72, 2011.

[23]   J. Zhou, A. Loftus, G. Mulley and A. Jenkins, "A Thin Film Detection/Response System for Pathogenic Bacteria", Journal of the American Chemical Society, vol. 132, no. 18, pp. 6566-6570, 2010.

[24]   M. Aguirre and M. Collins, "Lactic acid bacteria and human clinical infection", Journal of Applied Bacteriology, vol. 75, no. 2, pp. 95-107, 1993.

[25]   H. Simmen, H. Battaglia, P. Giovanoli and J. Blaser, "Analysis of pH, pO2 and pCO2 in drainage fluid allows for rapid detection of infectious complications during the follow-up period after abdominal surgery", Infection, vol. 22, no. 6, pp. 386-389, 1994.

[26]   R. SAWYER, M. SPENGLER, R. ADAMS and T. PRUETT, "The Peritoneal Environment During Infection", Annals of Surgery, vol. 213, no. 3, pp. 253-260, 1991.

[27]   S. Rasilainen, M. Juhani and L. Kalevi, "Microbial colonization of open abdomen in critically ill surgical patients", World Journal of Emergency Surgery, vol. 10, no. 1, 2015.

[28]   A. Baothman, F. Md and N. Reddy, "Study of mannheims peritonitis index in patients with peritonitis", International Surgery Journal, pp. 746-750, 2016.

[29]   B. Runeman, J. Faergemann, O. Larkö, "Experimental Candida albicans Lesions in Healthy Humans: Dependence on Skin pH", Acta Dermato-Venereologica, vol. 80, no. 6, pp. 421-424, 2000.

[30]   K. Aykut, Y. Çetinkol, G. Albayrak and M. Güzeloğlu, "Bacterial Colonization In Venous Ulcers And The Effect Of Antibiotic Therapy On Wound Healing", The Journal of Tepecik Education and Research Hospital, vol. 22, no. 2, pp. 107-110, 2012.

[31]   M. Khan, U. Ansari and M. Ali, "Real-time wound management through integrated pH sensors: a review", Sensor Review, vol. 35, no. 2, pp. 183-189, 2015.

[32]   G. Hämmerle and R. Strohal, "Efficacy and cost-effectiveness of octenidine wound gel in the treatment of chronic venous leg ulcers in comparison to modern wound dressings", International Wound Journal, vol. 13, no. 2, pp. 182-188, 2014.

[33]   A. Jabre, Y. Bao and E. Spatz, "Brain pH monitoring during ischemia", Surgical Neurology, vol. 54, no. 1, pp. 55-58, 2000.

[34]   S. Love, "Oxidative Stress in Brain Ischemia", Brain Pathology, vol. 9, no. 1, pp. 119-131, 2006.

[35]   C. Loeb, "Transient Ischemic Attack, Protracted Transient Ischemic Attack, and Completed Stroke", European Neurology, vol. 22, no. 1, pp. 68-73, 2008.

[36]   A. Ghosh and R. Tipton, "Fetal Scalp Electrodes", The Lancet, vol. 307, no. 7968, p. 1075, 1976.

[37]   J. Kellum, "Determinants of blood pH in health and disease", Critical Care, vol. 4, no. 1, p. 6, 2000.

[38]   D. Rebuck, S. Haywood, K. McDermott, K. Perry and R. Nadler, "What is the long-term relevance of clinically detected postoperative anastomotic urine leakage after robotic-assisted laparoscopic prostatectomy?", BJU International, p. no-no, 2011.

[39]   C. Rørbye, A. Perslev and C. Nickelsen, "Lactate versus pH levels in fetal scalp blood during labor – using the Lactate Scout System", The Journal of Maternal-Fetal & Neonatal Medicine, vol. 29, no. 8, pp. 1200-1204, 2015.

[40]   D. DeArmond, A. Carswell, C. Louden, J. Simmons, J. Bayer, N. Das and S. Johnson, "Diagnosis of anastomotic leak: Electrolyte detection versus barium fluoroscopy", Journal of Surgical Research, vol. 182, no. 2, pp. 192-197, 2013.

[41]   J. Jin, "FDA Authorization of Medical Devices", JAMA, vol. 311, no. 4, p. 435, 2014.

[42]   J. Yusko, "Medical Device Safety: The Regulation of Medical Devices for Public Health and Safety", Health Physics, vol. 82, no. 5, p. 749, 2002.

[43]   "Potentiometric Selectivity Coefficients of Ion-Selective Electrodes", Chemistry International -- Newsmagazine for IUPAC, vol. 24, no. 6, 2002.

[44]   "Use of International Standard ISO-10993, Biological Evaluation of Medical Devices

[45]   J. Harding and M. Reynolds, "Combating medical device fouling", Trends in Biotechnology, vol. 32, no. 3, pp. 140-146, 2014.

[46]   Handbook of biosensors and biochips. Chichester [u.a.]: Wiley, 2007.

[47]   R. Bashir, "BioMEMS: state-of-the-art in detection, opportunities and prospects", Advanced Drug Delivery Reviews, vol. 56, no. 11, pp. 1565-1586, 2004.

[48]   S. Badilescu and M. Packirisamy, BioMEMS. Boca Raton: Taylor & Francis/CRC Press, 2011.

[49]   P. Bergveld, "Thirty years of ISFETOLOGY", Sensors and Actuators B: Chemical, vol. 88, no. 1, pp. 1-20, 2003.

[50]   C. Lee, S. Kim and M. Kim, "Ion-Sensitive Field-Effect Transistor for Biological Sensing", Sensors, vol. 9, no. 9, pp. 7111-7131, 2009.

[51]   S. MARTINOIA, G. MASSOBRIO and L. LORENZELLI, "Modeling ISFET microsensor and ISFET-based microsystems: a review", Sensors and Actuators B: Chemical, vol. 105, no. 1, pp. 14-27, 2005.

[52]   D. Kim, Y. Kim, J. Amsden, B. Panilaitis, D. Kaplan, F. Omenetto, M. Zakin and J. Rogers, "Erratum: "Silicon electronics on silk as a path to bioresorbable, implantable devices" [Appl. Phys. Lett. 95, 133701 (2009)]", Applied Physics Letters, vol. 95, no. 26, p. 269902, 2009.

[53]   S. Olibet, E. Vallat-Sauvain and C. Ballif, "Model for a-Si:H/c-Si interface recombination based on the amphoteric nature of silicon dangling bonds", Physical Review B, vol. 76, no. 3, 2007.

[54]   C. Jagadish, Nanowires. Bristol: Inst. of Physics Publ., 2010.

[55]   Y. Huang and C. Lieber, "Integrated Nanoscale Electronics and Optoelectronics: Exploring Nanoscale Science and Technology Through Semiconductor Nanowires", ChemInform, vol. 36, no. 26, 2005.

[56]   Y. Cui, "Nanowire Nanosensors for Highly Sensitive and Selective Detection of Biological and Chemical Species", Science, vol. 293, no. 5533, pp. 1289-1292, 2001.

[57]   Y. Chen, X. Wang, S. Erramilli, P. Mohanty and A. Kalinowski, "Silicon-based nanoelectronic field-effect pH sensor with local gate control", Applied Physics Letters, vol. 89, no. 22, p. 223512, 2006.

[58]   S. Kim, T. Rim, K. Kim, U. Lee, E. Baek, H. Lee, C. Baek, M. Meyyappan, M. Deen and J. Lee, "Silicon nanowire ion sensitive field effect transistor with integrated Ag/AgCl electrode: pH sensing and noise characteristics", The Analyst, vol. 136, no. 23, p. 5012, 2011.

[59]   M. Schöning and A. Poghossian, "Recent advances in biologically sensitive field-effect transistors (BioFETs)", The Analyst, vol. 127, no. 9, pp. 1137-1151, 2002.

[60]   K. Muhieddine, M. Ullah, B. Pal, P. Burn and E. Namdas, "Field-Effect Transistors: All Solution-Processed, Hybrid Light Emitting Field-Effect Transistors (Adv. Mater. 37/2014)", Advanced Materials, vol. 26, no. 37, pp. 6409-6409, 2014.

[61]   I. Khimji, E. Kelly, Y. Helwa, M. Hoang and J. Liu, 'Visual optical biosensors based on DNA-functionalized polyacrylamide hydrogels', Methods, vol. 64, no. 3, pp. 292-298, 2013.

[62]   Y. Helwa, N. Dave and J. Liu, 'Electrostatically directed liposome adsorption, internalization and fusion on hydrogel microparticles', Soft Matter, vol. 9, no. 26, p. 6151, 2013.

[63]   R. Liu, Qing Yu and D. Beebe, "Fabrication and characterization of hydrogel-based microvalves", Journal of Microelectromechanical Systems, vol. 11, no. 1, pp. 45-53, 2002.

[64]   G. Gerlach, M. Guenther, J. Sorber, G. Suchaneck, K. Arndt and A. Richter, "Chemical and pH sensors based on the swelling behavior of hydrogels", Sensors and Actuators B: Chemical, vol. 111-112, pp. 555-561, 2005.

[65]   N. Sheppard, R. Tucker and S. Salehi-Had, "Design of a conductimetric pH microsensor based on reversibly swelling hydrogels", Sensors and Actuators B: Chemical, vol. 10, no. 2, pp. 73-77, 1993.

[66]   V. Sridhar and K. Takahata, "A hydrogel-based passive wireless sensor using a flex-circuit inductive transducer", Sensors and Actuators A: Physical, vol. 155, no. 1, pp. 58-65, 2009.

[67]   V. Garripelli, J. Kim, R. Namgung, W. Kim, M. Repka and S. Jo, "A novel thermosensitive polymer with pH-dependent degradation for drug delivery", Acta Biomaterialia, vol. 6, no. 2, pp. 477-485, 2010.

[68]   C. Ruan, K. Zeng and C. Grimes, "A mass-sensitive pH sensor based on a stimuli-responsive polymer", Analytica Chimica Acta, vol. 497, no. 1-2, pp. 123-131, 2003.

[69]   H. Wang, Y. Helwa and G. Rempel, 'Preparation of polyacrylamide based microgels with different charges for drug encapsulation', European Polymer Journal, vol. 49, no. 6, pp. 1479-1486, 2013.

[70]   G. Tiwari, R. Tiwari, P. Wal, A. Wal and A. Rai, "Primary and novel approaches for colon targeted drug delivery – A review", International Journal of Drug Delivery, vol. 2, no. 1, pp. 1-11, 2010.

[71]   Nerv Technology Inc., "System, method, and device for detecting postoperative complications", WO 2016142844 A1, 2017.

[72]   Y. Helwa, N. Dave, R. Froidevaux, A. Samadi and J. Liu, 'Aptamer-Functionalized Hydrogel Microparticles for Fast Visual Detection of Mercury(II) and Adenosine', ACS Appl. Mater. Interfaces, vol. 4, no. 4, pp. 2228-2233, 2012.

[73]   P. Gou, N. Kraut, I. Feigel, H. Bai, G. Morgan, Y. Chen, Y. Tang, K. Bocan, J. Stachel, L. Berger, M. Mickle, E. Sejdić and A. Star, "Carbon Nanotube Chemiresistor for Wireless pH Sensing", Scientific Reports, vol. 4, no. 1, 2014.

[74]   Y. Qin, H. Kwon, M. Howlader and M. Deen, "Microfabricated electrochemical pH and free chlorine sensors for water quality monitoring: recent advances and research challenges", RSC Adv., vol. 5, no. 85, pp. 69086-69109, 2015.

[75]   S. Safari, P. Selvaganapathy and M. Deen, "Microfluidic Reference Electrode with Free-Diffusion Liquid Junction", Journal of the Electrochemical Society, vol. 160, no. 10, pp. B177-B183, 2013.

[76]   S. Safari, P. Selvaganapathy, A. Derardja and M. Deen, "Electrochemical growth of high-aspect ratio nanostructured silver chloride on silver and its application to miniaturized reference electrodes", Nanotechnology, vol. 22, no. 31, p. 315601, 2011.

[77]   H. Arida, "Novel pH microsensor based on a thin film gold electrode modified with lead dioxide nanoparticles", Microchimica Acta, vol. 182, no. 1-2, pp. 149-156, 2014.

[78]   W. Gao and J. Song, "Polyaniline Film Based Amperometric pH Sensor Using A Novel Electrochemical Measurement System", Electroanalysis, vol. 21, no. 8, pp. 973-978, 2009.

[79]   M. Gad-el-Hak, The MEMS handbook. Boca Raton: CRC Taylor & Francis, 2006.

[80]   D. Kim, Y. Kim, J. Amsden, B. Panilaitis, D. Kaplan, F. Omenetto, M. Zakin and J. Rogers, "Silicon electronics on silk as a path to bioresorbable, implantable devices", Applied Physics Letters, vol. 95, no. 13, p. 133701, 2009.

[81]   Saddow, Stephen E. Silicon Carbide Biotechnology. Waltham, MA: Elsevier

[82]   B. Zhang, L. Lei, J. Yang, X. Guo and G. Zhang, "Fatigue properties of titanium alloy thin foils for MEMS applications", Materials Letters, vol. 89, pp. 302-304, 2012.

[83]   V. Chidambaram, X. Ling and C. Bangtao, "Titanium-Based Getter Solution for Wafer-Level MEMS Vacuum Packaging", Journal of Electronic Materials, vol. 42, no. 3, pp. 485-491, 2012.

[84]   D. Hill, Design engineering of biomaterials for medical devices. Chichester: Wiley, 1998.

[85]   D. Liaw, K. Wang, Y. Huang, K. Lee, J. Lai and C. Ha, "Advanced polyimide materials: Syntheses, physical properties and applications", Progress in Polymer Science, vol. 37, no. 7, pp. 907-974, 2012.

[86]   S. Xiao, L. Che, X. Li and Y. Wang, "A novel fabrication process of MEMS devices on polyimide flexible substrates", Microelectronic Engineering, vol. 85, no. 2, pp. 452-457, 2008.

[87]   C. Shearwood, M. Harradine, T. Birch and J. Stevens, "Applications of polyimide membranes to MEMS technology", Microelectronic Engineering, vol. 30, no. 1-4, pp. 547-550, 1996.

[88]   K. Carter, J. Hedrick, R. Richter, P. Furuta, D. Mecerreyes and R. Jérôme, "Nanoporous Polyimide Films from Polyimide-Aliphatic Polyester or Polyimide-Aliphatic Polycarbonate Copolymers", MRS Proceedings, vol. 431, 1996.

[89]   R. Kilaru, Z. Celik-Butler, D. Butler and I. Gonenli, "NiCr MEMS Tactile Sensors Embedded in Polyimide Toward Smart Skin", Journal of Microelectromechanical Systems, vol. 22, no. 2, pp. 349-355, 2013.

[90]   R. Wise, "Advanced plasma etch technologies for nanopatterning", Journal of Micro/Nanolithography, MEMS, and MOEMS, vol. 12, no. 4, p. 041311, 2013.

[91]   T. Choi and D. Hess, "Chemical Etching and Patterning of Copper, Silver, and Gold Films at Low Temperatures", ECS Journal of Solid State Science and Technology, vol. 4, no. 1, pp. N3084-N3093, 2014.

[92]   T. Choi and D. Hess, "Chemical Etching and Patterning of Copper, Silver, and Gold Films at Low Temperatures", ECS Journal of Solid State Science and Technology, vol. 4, no. 1, pp. N3084-N3093, 2014.

[93]   S. Schaur and B. Jakoby, "A numerically efficient method of modeling interdigitated electrodes for capacitive film sensing", Procedia Engineering, vol. 25, pp. 431-434, 2011.

[94]   "AZ 3300 Series", Imicromaterials.com, 2017. [Online]. Available: http://www.imicromaterials.com/index.php/products/ig-line-photoresists/az-3300-series. [Accessed: 14-Jul- 2017].

[95]   "AZ nLoF 5510", Imicromaterials.com, 2017. [Online]. Available: http://www.imicromaterials.com/index.php/products/ig-line-photoresists/az-nlof-5510. [Accessed: 14- Jul-2017].

[96]   "300MIF Specs", Imicromaterials.com, 2017. [Online]. Available: http://www.imicromaterials.com/index.php/Products/Developers/300MIF-specs. [Accessed: 14- Jul-2017].

[97]   T. Michely, M. Kalff and G. Comsa, "The Effect of Deposition Method on Growth Morphology - Comparison of Molecular Beam Epitaxy, Ion Beam Assisted Deposition and Sputter Deposition", MRS Proceedings, vol. 528, 1998.

[98]   A. Lupu, D. Compagnone, S. Orlanducci, M. Terranova, V. Magearu and G. Palleschi, "Titanium Carbide Thin-Film Electrodes: Characterization and Evaluation as Working Electrodes", Electroanalysis, vol. 16, no. 20, pp. 1704-1710, 2004.

[99]   D. MicroChemicals, "Photoresist Processing - Ancillaries - Remover/Stripper", Photoresists.eu, 2017. [Online]. Available: http://www.photoresists.eu/photoresist_1232.html. [Accessed: 18- Jul- 2017].

[100]   K. Il Joung, H. Jung Yoon, H. Nam and K. Paeng, "Development of pH sensor based on aromatic polyurethane matrix", Microchemical Journal, vol. 68, no. 2-3, pp. 115-120, 2001.

[101] N. Ferrer-Anglada, M. Kaempgen and S. Roth, "Transparent and flexible carbon nanotube/polypyrrole and carbon nanotube/polyaniline pH sensors", physica status solidi (b), vol. 243, no. 13, pp. 3519-3523, 2006.

[102] S. Bhadra, D. Khastgir, N. Singha and J. Lee, "Progress in preparation, processing and applications of polyaniline", Progress in Polymer Science, vol. 34, no. 8, pp. 783-810, 2009.

[103] Y. Yu, J. Zhang, W. Zhang, R. Liu, X. Wu and Z. Zhu, "Universal route to fabricate facile and flexible micro-supercapacitors with gold-coated silver electrodes", RSC Adv., vol. 6, no. 85, pp. 81936-81942, 2016.

[104] R. L. a. M. A. Margareth R. C. Marques, "Simulated Biological Fluids with Possible Application in Dissolution Testing," Faculty of Pharmacy and Pharmaceutical Sciences, University of Alberta, Edmonton, 2011.